HEAT TRANSFER IN THE ROLL GAP DURING HOT ROLLING

by

CRAIG OHRIST HLADY

B. A. Sc., The University of British Columbia, 1991

A THESIS SUBMITTED IN PARTIAL FULFILLMENT OF

THE REQUIREMENTS FOR THE DEGREE OF

MASTER OF APPLIED SCIENCE

in

THE FACULTY OF GRADUATE STUDIES

Department of Metals and Materials Engineering

We accept this thesis as conforming

to the required standard

THE UNIVERSITY OF BRITISH COLUMBIA

January 1994

In presenting this thesis in partial fulfilment of the requirements for an advanced degree at the University of British Columbia, I agree that the Library shall make it freely available for reference and study. I further agree that permission for extensive copying of this thesis for scholarly purposes may be granted by the head of my department or by his or her representatives. It is understood that copying or publication of this thesis for financial gain shall not be allowed without my written permission.

(Signature)

Department of Metals and Materials Engineering.

The University of British Columbia
Vancouver, Canada

Date Jan 28, 1994.

DE-6 (2/88)

ABSTRACT

A series of pilot mill hot-rolling tests involving AA5052, AA5182, and copper samples has been performed. These rolling tests encompassed a range of rolling pressures, rolling speeds, reductions and temperatures. In addition, two types of lubricants were employed in the hot rolling of the aluminum alloy samples. Instantaneous roll-gap heat-transfer coefficients (HTCs) have been calculated from roll-gap surface temperature measurements. These measurements were made from double-intrinsic thermocouples secured on the surface of the samples. Average roll-gap HTCs have been calculated from the bulk temperatures of the samples immediately before and after rolling. The roll-gap HTC was calculated by an implicit, one-dimensional finite-difference technique. The resulting roll-gap HTCs of both the aluminum alloy and the copper samples were compared to those obtained for steel rolling in a previous study. The roll-gap HTC has been proposed to be a function of the harmonic conductivity of the material being rolled and the roll, the ratio of the rolling pressure to the surface flow stress of the material being rolled, and the surface roughnesses of the roll and the material being rolled.

TABLE OF CONTENTS

LIST OF TABLES

LIST OF ILLUSTRATIONS

NOMENCLATURE

a	Radius of heat channel (m)
A	Constant used in steady-state stress constitutive equation
A_a	Apparent contact area (m^2)
A_c	Fractional contact area
A_r	Real contact area (m^2)
c	Radius of button contact spot (m)
C, C_0	General constants (m^{-1})
C'	Inverse of C (m)
C_1	Constant used in Fourier equation
$C_{p,i}$	Specific heat of the material at node i (kJ/kg °C)
C_{ps}	Specific heat of the sample (kJ/kg °C)
C_{pr}	Specific heat of the roll (kJ/kg °C)
d_b	Constant used for Vickers microhardness correlation
ΔE_s	Change of energy of the sample due to rolling (kJ)
f	Fraction of the roll-bite contact time t_c
F	Force (N)
Fo	Fourier number
h, $h(t)$	Heat-transfer coefficient at the sample surface (kW/m^2 °C)
H	Surface hardness of the sample (kg/mm^2)
$H(t)$	Sample thickness in roll bite (m)
H_{avg}	Average thickness of the sample in the roll bite (m)
H_b	Bulk hardness of work piece (kg/mm^2)

H_f	Exit thickness of the sample (m)
H_i	Entry thickness of the sample (m)
H_j	Thickness of the sample at time step j (m)
ΔH	Roll draft, H_i - H_f (m)
k_m	Harmonic mean conductivity (kW/m °C)
k_s	Thermal conductivity of the slab (kW/m °C)
k_r	Thermal conductivity of the roll (kW/m °C)
k_t	Thermal conductivity of the tool (kW/m °C)
k_{wp}	Thermal conductivity of the workpiece (kW/m °C)
L	Projected arc length (m)
m	Interface friction factor
n	Constant used in steady-state constitutive equation
n'	Number of contact spots per unit area (m^{-2})
n_1	Number of samples in population group 1
n_2	Number of samples in population group 2
N	Angular velocity of the roll in rotations per minute
N_r	Number of nodes discretizing the roll surface layer δ
N_s	Number of nodes discretizing the sample half-thickness
P_a	Apparent pressure (kg/mm^2)
P_r	Mean roll pressure (kg/mm^2)
Pe	Peclet number
$\dot{q}_f$	Frictional heat flux (kW/m^2)
$\dot{q}_{f,r}$	Frictional heat flux received by the roll (kW/m^2)
$\dot{q}_{f,s}$	Frictional heat flux received by the strip (kW/m^2)

Q	Activation energy (kJ)
$\dot{Q}_{def}$	Heat generation due to deformation (kW)
$\dot{Q}$	Heat flow (kW)
r	Radial thickness of roll (m)
r_i	Radial position of roll node i (m)
Δr_i	Radial thickness of roll node i
R	Gas constant (J/mole °C)
R_0	Roll radius (m)
R^*	Radius of the roll interior not heated by the sample, $R^*=R_0-\delta$ (m)
S	Spread factor
$(S_p)^2$	Pooled variance
S_1	Standard deviation of population group 1
S_2	Standard deviation of population group 2
t	Time (s)
t_c	Contact time (s)
Δt	Change in time (s)
T	Temperature (°C, K)
T_c	Axial temperature of the roll (°C)
T_f	Bulk temperature of the sample after rolling (°C)
T_i	Bulk temperature of the sample before rolling (°C)
T_i^j	Temperature of node i at time step j (°C)
T_h	Ambient temperature (°C)
T_s	Temperature of the sample (°C)
$T_s(x, t)$	Temperature of the sample at a position x at a time t (°C)
T_r	Temperature of the roll (°C)

ΔT_1	Component of ΔT_c due to Material 1 (°C)
ΔT_2	Component of ΔT_c due to Material 2 (°C)
ΔT_c	Macroscopic difference in temperature between the surface temperatures of two materials (°C)
ΔT_{def}	Increase in the sample temperature due to deformation (°C)
$T_r(x, t)$	Temperature of the roll at a radius r at a time t (°C)
$\Delta T_{r\text{-}s}$	Average difference in the temperature between the sample and roll surfaces in the roll bite (°C)
ΔT_s	Change in the sample temperature due to rolling (°C)
$\tan \phi$	Mean of absolute slope of surface irregularities, $\tan\phi = \sqrt{\tan^2 \phi_t + \tan^2 \phi_{wp}}$
$\tan \phi_t$	Absolute slope of tool surface asperities
$\tan \phi_{wp}$	Absolute slope of workpiece surface asperities
V_s	Half-volume of the sample in the roll bite (m^3)
W	Width of the sample (m)
W_i	Width of the sample before rolling (m)
W_f	Width of the sample after rolling (m)
x	Through thickness direction (m)
Δx_i	Thickness of strip node i (m)
y	Length direction (m)
Y_0	Yield stress in pure tension (kg/mm^2)
z	Transverse direction (m)
Z	Zener-Holloman parameter
α	Constant used in steady-state constitutive equation (MPa^{-1})
α_{eff}	Harmonic thermal diffusivity (m^2/s)

α_r	Thermal diffusivity of the roll (m^2/s)
α_s	Thermal diffusivity of the sample (m^2/s)
β_1	Constant used in Fourier equation
δ	Depth of surface layer undergoing thermal cycle (m)
δ_t	Average asperity height of tool (m)
δ_{wp}	Average asperity height of workpiece (m)
$\delta_{1\%}$	Depth of internal point at which the difference between surface temperature and initial temperature of material is 1 pct. (m)
Δ	Cut-off time in the roll bite for HTC prediction (s)
$\bar{\varepsilon}$	Mean strain
$\bar{\dot{\varepsilon}}$	Mean strain rate (s^{-1})
$\dot{\varepsilon}$	Strain rate (s^{-1})
η	Efficiency of conversion of mechanical work to heat
ϑ	Root mean square of the roughness of the contacting surfaces (m), $\vartheta = \sqrt{\vartheta_t^2 + \vartheta_{wp}^2}$
ϑ_t	Standard deviation of profile height of tool asperities (m)
ϑ_{wp}	Standard deviation of profile height of workpiece asperities (m)
μ	Coefficient of friction
μ_1	Mean of population group 1
μ_2	Mean of population group 2
v_r	Velocity of roll surface (m/s)
v_s	Velocity of sample (m/s)
θ	Angle of rotation of the roll (radians)
θ_c	Non-dimensional temperature
θ_{RB}	Contact angle (radians)

ρ_i	Density of material at node *i* (kg/m^3)
ρ_r	Density of the roll (kg/m^3)
ρ_s	Density of the sample (kg/m^3)
σ	Steady-state flow stress (MPa)
σ_i	Steady-state flow stress of node *i* (MPa)
σ_{ps}	Plane-strain steady-state flow stress (MPa)
$\bar{\sigma}$	Mean steady-state flow stress (MPa)
τ	Frictional shear stress (kg/mm^2)
τ_0	Shear stress (kg/mm^2)
ω	Angular speed of roll (rad/s)

ACKNOWLEDGEMENTS

I would like to express my appreciation to Drs. I. V. Samarasekera, E. B. Hawbolt and J. K. Brimacombe, for the welcome input and support they provided me these past two years.

Financial assistance from NSERC is gratefully aknowledged. I would also like to thank ALCAN Ltd. for supply of materials and advice, and in particular, Dr. David Lloyd deserves special mention for his helpful support of this project.

My gratitude also goes to fellow graduate student Wei Chang Chen; the advice and expertise that he provided helped me greatly.

CHAPTER 1

INTRODUCTION

Modern aluminum hot-rolling practice calls for the achievement of high productivity coupled with the precise control of strip mechanical properties. These twin goals can only be attained through a thorough understanding of the complete hot rolling process. There is also a need for accurate, reliable and quick temperature measurements of the strip during the hot-rolling process. Predictive and adaptive models used on-line can then fully control the hot mill, responding to any situation to maintain quality and production standards.

Of the total heat lost by aluminum strip during the hot-rolling process, three-quarters or more can be lost to the rolls [1]. Thus, accurate characterization of the roll-gap heat-transfer coefficient (HTC) is the single most important component of the knowledge base required for precise prediction and control of the strip temperature during hot rolling.

The importance of the (HTC) has been well realized [2] for steel hot-rolling. In the case of aluminum rolling, however, there have been relatively few studies performed to date which measure the roll-gap HTC [3-6].

Until recently, there have also been difficulties in applying the results of the studies performed in the laboratory to the industrial scale. The studies performed to date have been limited in scope and usefulness because of a lack of fundamental knowledge of the mechanism of the roll-gap HTC. Therefore, there clearly exists a need to gain a

fundamental understanding of the physical basis behind the HTC, and thus also gain the ability to characterize the HTC as a function not only of rolling parameters, but of the thermal and physical properties of the material being rolled as well.

Even though the exact nature of the lubrication condition in the roll gap is not known, there is a general agreement that some type of mixed lubrication condition prevails [7, 8, 9]. This type of lubrication condition is also known as partial elastohydrodynamic lubrication; it describes the situation where the lubricant film between the strip surface and the roll is partly interrupted by surface asperities of the roll and strip coming into direct contact with each other. The asperities of the strip in contact with the roll then undergo deformation during the rolling process.

Figure 1.1 shows a schematic of two surfaces contacting each other only at discrete contact points. As the normal pressure forcing the two surfaces together increases, the asperities deform and the contact area grows. The results of an increased contact area are twofold. Firstly, the greater the contact area, the higher the friction force becomes as the lubrication layer is broken down. Secondly, since the majority of heat is transferred through the contact spots, the flux of heat between the two surfaces increases.

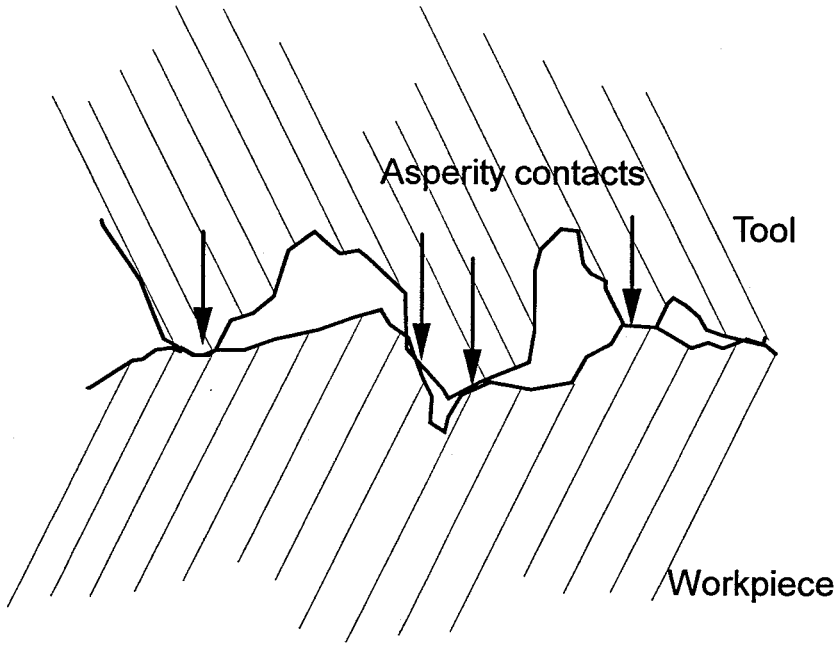

Figure 1.1 Contact between real surfaces (from Samarasekera [2])

The concept that two nominally smooth surfaces are in fact rough on a micro-scale, and therefore, contact each other directly only at discrete spots is the basis of advanced friction theory [10-12]. In addition, this concept has been used in studies characterizing the HTC as a function of the true contact area, ie. the area of two contacting surfaces that are in direct contact [13-17]. However, the potential of this concept as a means of explaining the nature of the roll-gap HTC in industrial rolling was only realized later by Samarasekera [2], who showed indirect evidence that the roll-gap HTC is strongly dependent on the real area of contact. Subsequent studies by Devadas *et al.* [18] and by Chen *et al.* [19] have examined the relationship between the roll-gap HTC and the real area of contact. The objective of this study, then, is to advance research on this subject.

CHAPTER 2

LITERATURE REVIEW

2.1 Previous Estimates of the Roll-Gap Heat-Transfer Coefficient

Research on roll-gap heat transfer during the hot rolling of aluminum has lagged behind that for steel. Thus, only a few estimates for the HTC specific to aluminum hot rolling have been published.

Chen *et al.* [3] reported values of 10 to 50 kW/m² °C for the hot rolling of Al-5 pct. Mg alloy, using Type K thermocouples having a 1.0 mm wire diameter for the temperature measurements. The roll-gap HTC was reported to increase continually along the roll gap. Furthermore, the HTC was found to be constant at any position in the roll gap relative to the entry point in three different tests which were conducted at three different reductions. The studies were conducted with aluminum samples instrumented with four thermocouples. Two thermocouples were placed on the sample surface, one was located 1.8 mm below the surface, and one was placed at the centreline of each aluminum sample. Before rolling experiments were performed, the roll was heated to 70°C. These workers expressed a belief that the HTC depends on a combination of factors such as rolling pressure, the nature of the oxide layer, position of the neutral point and surface roughness; however, no evidence was provided to verify these claims.

Semiatin *et al.* [4] conducted high strain-rate ring upsetting tests of AA2024, an aluminum-copper alloy, from which resulting HTCs were reported to lie between 15 and 20 kW/m² °C. Thermocouples placed at 0.15 mm and 0.91 mm from the die surface

recorded the subsurface die temperatures. Pressures attained during these tests were not reported.

Timothy *et al.* [5] also employed subsurface thermocouples in the laboratory hot rolling of AA5083 to obtain a value of 15 kW/m² °C. These workers noted that the rolled aluminum sample regained a homogenous temperature 30°C lower than the initial rolling temperature approximately 0.5 seconds after leaving the roll bite.

Pietrzyck and Lenard [6] reported HTC's between 18.5 and 21.5 kW/m² °C in the warm rolling (155°C to 210°C) of commercial pure aluminum, using extrinsic thermocouples embedded in the aluminum slab. These workers did not calculate an average roll-bite HTC from the instantaneous response of the surface thermocouples, but from the temperature drop incurred by the sample due to the rolling operation:

$$h = \frac{\left(\rho_s C_{ps} \Delta T_s + \bar{\sigma}\bar{\varepsilon}\right) H_{avg} v_r}{2 \Delta T_{r-s} L} \tag{2.1}$$

where ρ_S is the density of the aluminum, C_{PS} is the heat capacity of the aluminum, ΔT_{avg} is the average temperature drop of the sample due to rolling, and $\bar{\sigma}$, $\bar{\varepsilon}$ and H_{avg} are the average flow stress, mean strain rate and average thickness of the sample, respectively, in the roll gap. The term v_r is the rolling speed, ΔT_{r-S} is the average temperature difference between the sample and strip in the roll bite, and L is the projected arc length.

2.2 Dependence of the Real Contact Area on Pressure

Williamson and Hunt [57] conducted experiments in which a 12-mm diameter steel ball was pressed into indium and aluminum samples with artificially-roughened surfaces. After the deformation of the sample, the surface profile of the deformed area was traced,

and a real contact area was measured. These experiments demonstrated that for local indentations, the real area of contact is proportional to the nominal contact area, independent of pressure. Furthermore, the experiments showed that the persistence of asperities even at high pressures was not attributable to work-hardening mechanisms, friction, or the trapping of fluid within the valleys of the asperities. Evidence was also given which suggested that for solids with homogeneous hardnesses, the real area of contact was equal to one-half the nominal area of contact; and that for solids with hardened surface layers, the real area of contact decreased to 25-35 pct. of the nominal area of contact.

In a related study, Pullen and Williamson [56] conducted experiments in which aluminum samples with artificially-roughened surfaces were pressed by a flat, hardened-steel ram. Before being pressed, the aluminum samples, which were cylindrical in shape, were forced into tight-fitting holes in hardened-steel dies. The placement of the aluminum samples into the steel dies prevented any bulk deformation of the samples as they were pressed by the ram. Thus, surface pressures of up to fifteen times the yield stress of aluminum were attained in the study. From these experiments Pullen and Williamson [56] established that the true area of contact can be characterized as follows:

$$A_c = \frac{\frac{P_a}{H}}{1+\frac{P_a}{H}} \tag{2.2}$$

where P_a is the nominal pressure and H is the surface hardness of the material. The term A_c is the fractional area of metal-metal contact; it is defined as

$$A_c = \frac{A_r}{A_a} \tag{2.3}$$

where A_a is the apparent or bulk area of contact, and A_r is the 'real' area, the area of metal-metal contact. An important result obtained from Equation (2.2) is that, since for an unsupported material the ratio P_a/H can never be greater than unity, the maximum fractional contact area that can be obtained between two surfaces is 0.5. Experimental substantiation of this calculated result is provided by Williamson and Hunt [57].

2.3 Dependence of the HTC on Pressure

2.3.1 Experimental Observations

Semiatin *et al.* [4] noted that, in the absence of bulk deformation, the HTC increases with applied interface pressure, attaining a constant value above a certain pressure. Furthermore, it was postulated that deformation must smooth asperities at the interface, bringing the tool and workpiece into better thermal contact.

Chen *et al.* [3] attempted to relate the measured variation of the HTC along the arc of contact with roll pressure and the change in true area of contact. However, the measured HTC did not compare well with the calculated roll pressure variation.

Samarasekera [2] more comprehensively explained the dependence of the roll-gap HTC at the interface between the workpiece and roll on the fractional area of contact. It was suggested that the HTC dependence on the fractional area of contact accounted for the previously observed variation of the HTC on such parameters as rolling speed, degree of reduction, gauge and lubrication. Experimental verification of the relationship between HTC and real area of contact for the hot rolling of steel was provided by

Devadas *et al.* [18], and by Chen *et al.* [19], who established a linear relationship between the roll-workpiece interface HTC and the roll pressure.

2.3.2 Theoretical Treatment

A small body of research has been published in which the dependence of the HTC between two nominally flat but microscopically rough surfaces on contact pressure has been considered. Cooper *et al.* [13] proposed the relationship

$$\frac{h}{k_{\mathrm{m}}}\frac{\tan\phi}{\vartheta} = 1.45\left(\frac{P_a}{H}\right)^{0.985} \tag{2.4}$$

for heat conduction between the contacting surfaces of a tool and workpiece under pressure in a vacuum, where h is the HTC, P_{a} is the apparent or bulk pressure, and H is the surface hardness of the workpiece. The term k_{m} is defined as the harmonic mean conductivity of the workpiece and tool:

$$k_{\mathrm{m}} = \frac{2k_{\mathrm{t}}k_{\mathrm{wp}}}{k_{\mathrm{t}} + k_{\mathrm{wp}}} \tag{2.5}$$

where k_{t} and k_{wp} are the conductivities of the tool and workpiece, respectively. The terms ϑ and $\tan\phi$ are surface roughness parameters; $\tan\phi$ is the average of the absolute slope of the surface irregularities of the two contacting surfaces,

$$\tan\phi = \sqrt{\tan^2\phi_{\mathrm{t}} + \tan^2\phi_{\mathrm{wp}}} \tag{2.6}$$

and ϑ is the average standard deviation of the profile height of the surface asperities of both surfaces,

$$\vartheta = \sqrt{\vartheta_t^2 + \vartheta_{wp}^2} \tag{2.7}$$

using a theory based on a Gaussian distribution of heights. The apparent pressure P_a acting on the two surfaces is calculated from an applied load F acting on the apparent area of contact A_a of the two surfaces:

$$P_a = \frac{F}{A_a} \tag{2.8}$$

Equation (2.4) was experimentally verified by a small set of tests conducted with P_a/H ratios of less than 0.1. The exponent 0.985 was experimentally derived from these tests.

Fenech *et al.* [16], using a "button model" of two surfaces in contact, proposed that

$$h = \frac{\dfrac{A_c}{1-A_c}}{\dfrac{\delta_1}{k_t} + \dfrac{\delta_2}{k_{wp}} + \dfrac{0.47\sqrt{A_c / n'}}{k_m}} \tag{2.9}$$

neglecting heat transfer outside of direct metal-metal contact; δ_t and δ_{wp} are the average void height for the tool and workpiece surfaces, respectively. The term k_m refers to the harmonic mean conductivities of the tool and workpiece, as before, and n' is the number of contacts per unit area. The term A_c is the fractional area of metal-metal contact, as defined in Equation (2.3). In the button model A_c is defined as the square of the radius of

the button contact spot c divided by the radius of the heat channel a, or $A_c=(c/a)^2$. Figure 2.1 shows how Fenech *et al.* [16] used the button model to simulate actual contact.

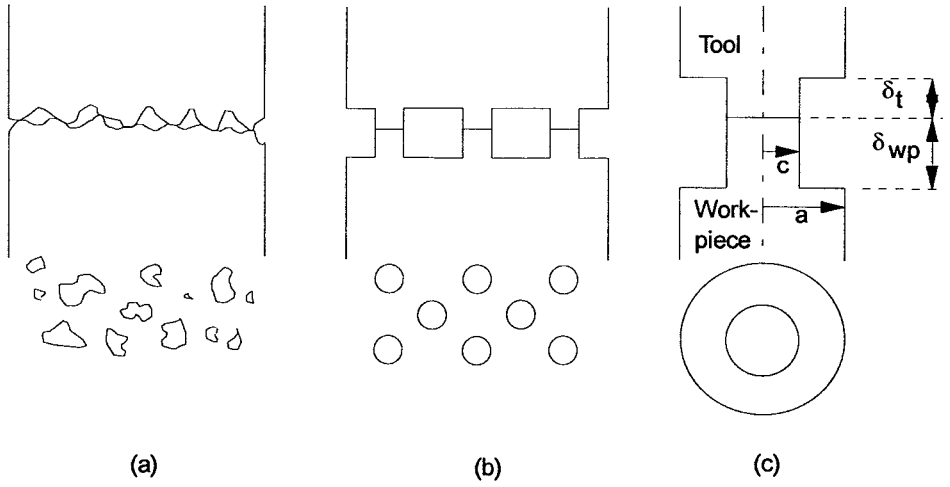

Figure 2.1 Button model for contacting surfaces (from Fenech [16])
(a) Actual contact
(b) Button model
(c) Heat channel for button model

Mikic [17] presented variations of Equation (2.4) to take into account different assumptions of the mode of deformation at the surface, ranging from pure plastic deformation to pure elastic deformation. Considering plastic flow only, Mikic [17] proposed a modification of Equation (2.4):

$$h = 1.13\frac{k_m \tan\phi}{\vartheta}\left(\frac{P_a}{H+P_a}\right)^{0.94} \tag{2.10}$$

As compared to Equation (2.4), the HTC as calculated by Equation (2.10) will be reduced at relatively high pressure-to-surface-hardness ratio, whereas at lower pressures the two equations produce very similar values of h.

Mikic also considered the case involving both plastic and elastic deformation. This case involves a correction factor to the pure plastic deformation case. However, the correction assumes that the elastic displacement of each asperity can be considered independently. This assumption has been shown to become invalid at extremely small P_a/H ratios by Pullen and Williamson [56], who showed that the deformation zones of each asperity overlap and interfere with each other almost immediately under the slightest plastic deformation.

Song and Yovanovich [20] developed an explicit equation relating the HTC to the bulk hardness of the material, rather than the surface microhardness:

$$h_c = \frac{1.13k}{d_b^{0.25}} \left(\frac{P_a}{H_b} \right)^{0.97} \left(\frac{\vartheta}{\tan\phi} \right)^{-0.75} \tag{2.11}$$

where H_b is the bulk hardness of the workpiece, as opposed to the surface hardness, and d_b is a constant used for a Vickers microhardness correlation. This equation was shown to have good agreement with experimental data in the range $10^{-6} \leq P_a/H_c \leq 2.3\text{x}10^{-2}$, where H_c is defined as the contact microhardness, which is related to surface roughness characteristics and Vickers microhardness test results.

Chen [21] applied the work of Fenech [16] to the case of hot rolling of steel, and with some suitable approximations and modifications, established a theoretical linear relationship between the HTC and the apparent pressure:

$$h = \frac{1}{0.47\sqrt{C_0}} \frac{k}{\sqrt{H}} P_a \tag{2.12}$$

where C_0 is a general constant.

2.4 Modelling Heat Transfer in the Roll Gap

There are many mathematical models in the literature which compute the temperature distribution of the workpiece in the roll gap during hot rolling [5, 19, 22-33]. Of these models, many assume that the contact resistance for the flow of heat at the roll-strip interface is negligible [22, 25, 27, 31, 33]. Other models assign a constant HTC throughout the roll gap [5, 23, 26, 28, 29, 30, 32]. However, only Chen *et al.* [19] have related the HTC to rolling pressure.

2.4.1 Model Types and Solving Schemes

Smelser and Thompson [23] modelled hot rolling assuming purely viscous flow and employed a two-dimensional finite-element scheme to solve for forming loads and temperature distribution. Timothy *et al.* [5] also used a 2-D finite element scheme in their analysis, utilizing a general, non-linear code. Lenard and Pietzryck [26], on the other hand, adopted a rigid-plastic finite-element approach to model the rolling process. Dawson [34] used a 2-D finite-element formulation which employs deformation mechanism maps to evaluate different types of constitutive equations.

However, in most studies which examined only temperature distribution in the strip and/or roll, the finite-difference method is most favoured. Both Lahoti *et al.* [25] and Sellars [30] used a two-dimensional finite difference method in their modelling of the rolling process. Tseng [27] also used a two-dimensional finite difference method, but

used a technique known as GFD -- generalized finite difference -- in which the strip is discretized by a non-orthogonal mesh which is compatible with the shape of the roll-strip interface.

However, the most widely-used technique for modelling temperature in the strip during rolling is the one-dimensional, unsteady-state finite-difference formulation. [19, 24, 29, 32, 33] These researchers all agree that heat conduction in the width and length of the strip is insignificant as compared to the heat conduction through the thickness of the strip, ie. in the direction perpendicular to the roll-strip interface.

2.4.2 Surface Temperature Measurement Techniques in the Roll Bite

The most novel roll-gap strip temperature measurement technique reported in the literature was the use of surface temperature transducers by Kannel and Dow [35]. The transducers were made by vapour-deposition of titanium onto a steel roll. However, most researchers employed either surface or subsurface thermocouples embedded either in the roll or the strip, or a combination of the two, in their studies.

Several researchers employed only subsurface thermocouples in their studies. Timothy *et al.* [5] used extrinsic chromel-alumel subsurface thermocouples embedded in an aluminum sample in their heat-transfer study of aluminum hot rolling. They located the thermocouples 1.0 mm below the sample surface, at the quarter-thickness, and at the sample centreline. Semiatin *et al.* [4] utilized subsurface thermocouples in their two-die experiments. The thermocouples were located 0.15 and 0.91 mm from the die surface. Karagiozis and Lenard [36] employed extrinsic chromel-alumel thermocouples having a wire diameter of 1.59 mm located 1.8 mm below the sample surface and at the sample centreline in their study of heat transfer in the hot rolling of steel. In a study of cold rolling, Steindl and Rice [37] also used thermocouples embedded in the sample surface.

They employed 0.127 mm diameter copper-constantan thermocouples located 1.5 mm from the sample surface and at the sample centreline.

There are disadvantages in utilizing subsurface thermocouples for measuring the thermal history of the strip during rolling. Timothy *et al.* [5] noted that the response time of the thermocouples was a finite fraction of the total time the thermocouples spent in the roll gap. In follow-up analyses of the work performed by Karagiozis and Lenard [36], Lenard and Pietrzyk [26] and Pietrzyk *et al.* [38] determined that the response time of the subsurface, extrinsic thermocouples was 0.4 seconds, which was too slow to accurately record temperature changes within the steel samples. Therefore, many researchers have employed surface thermocouples in their studies.

Jeswiet and Rice [39] were concerned with the probability of large temperature gradients in both the strip and roll close to the interface, and therefore used a thermocouple that was embedded in the roll normal to the roll surface. The thermocouple wires were insulated from the roll and each other, and terminated at the roll surface. Therefore, as a strip sample was rolled, a double-intrinsic junction was established at the surface of the sample surface. Devadas *et al.* [18] also used double-intrinsic thermocouples at the surface, but attached them to the sample rather than to the roll. The thermocouples were Type K, having chromel-alumel wires of diameter 0.25 mm. Chen *et al.* [3] also used surface thermocouples as well as subsurface thermocouples in their study of heat-transfer during the hot rolling of aluminum, but employed extrinsic chromel-alumel thermocouples with wire diameters of 1.0 mm.

The response time of small-gauge, intrinsic thermocouples has been shown to be very fast, of the order of one millisecond [18]. Furthermore, the perturbation error of the intrinsic type of thermocouple (that is, the change in the local temperature caused by the presence of the thermocouple) is the lowest of any thermocouple type [40]. And finally,

even severe deformation of the thermocouple wire has been found to have no significant effect on the accuracy of the thermocouple response [41].

2.5 Friction in the Roll Gap

2.5.1 Characterization of Friction in the Roll Gap

Almost no agreement was found in the literature on the nature of frictional behaviour at the roll-strip interface during hot rolling. Tseng *et al.* [31], for example, employed a value of 0.2 for the coefficient of friction in their study of hot rolling of AA5052 alloy. Devadas and Samarasekera [32] employed a coefficient of friction which was dependent on the temperature of the steel strip. Chen *et al.* [42] employed a value of 0.3 to approximate what they termed as 'near sticking friction'.

Dawson [35] states that, even in hot rolling, some type of sliding friction prevails, although no value of the coefficient of friction is offered. Despite this view, other researchers have instead adopted the concept of an interface friction factor, m:

$$m = \frac{\tau}{\tau_0} \tag{2.13}$$

where the frictional shear stress τ is a fraction m of the shear stress τ_0 of the deformed material. The interface friction factor, m, characterizes sticking friction, as opposed to the conventionally-employed coefficient of friction, μ, which characterizes sliding friction:

$$\mu = \frac{\tau}{P} \tag{2.14}$$

where the frictional shear stress is a fraction μ of the normal load *P* being exerted upon the deforming material.

Male *et al.* [43] have shown that employing *m* rather than μ in flow stress calculations for ring compression tests improves the quantitative prediction of the frictional component of the deformation load. Timothy *et al.* [5] set m=0.8 in their analysis, considering that value to be a typical one associated with sticking friction during hot rolling. Semiatin *et al.* [4], also used a friction shear factor in their heat-transfer analysis of ring-upsetting tests.

2.5.2 Distribution of the Frictional Heat

Tseng *et al.* [31] distributed the frictional heat uniformly between the roll and strip. In a more sophisticated approach, Hatta *et al.* [44] recognized that the thermal conductivity of steel decreases with temperature; therefore, in the case of steel hot rolling, since the roll surface is much cooler than the strip surface in the roll gap, the heat conductivity of the rolls is about two times that of the strip. Therefore, Hatta *et al.* [44] distributed the heat generated due to friction more to the roll than to the strip. Wilson *et al.* [24] distributed the frictional heat between the strip and rolls according to a 'heat partition coefficient'. However, no information was provided on how to calculate the value of this coefficient.

2.6. Previous Considerations of Flow Stress Variation Through the Strip

Sheppard and Wright [33] have previously noted that, in the rolling of aluminum slabs, due to the quenching effect of the roll on the surface of the aluminum slab, there is a flow-stress variation in the direction perpendicular to the roll-slab interface. These workers observed the effect of the flow-stress variation on a structural difference between

the surface and centre of the aluminum slab, but did not consider any effect of the flow-stress variation on heat transfer at the interface.

CHAPTER 3

SCOPE AND OBJECTIVES

The thesis of this study is that the roll-gap heat-transfer coefficient can be characterized as a function of the mean rolling pressure and the thermal and physical properties of the material being rolled.

The objectives of this project are three-fold:

Firstly, to experimentally obtain heat-transfer coefficients in the roll gap during the hot rolling of the aluminum alloys AA5052 and AA5182 and to establish a relationship between the roll-gap heat-transfer coefficient and mean rolling pressure.

Secondly, from the aluminum alloy rolling tests, additional copper rolling tests and data from steel rolling tests from a previous study [21], to determine the relationship that exists between the roll-gap heat-transfer coefficient and the thermal and physical properties of the material being rolled.

And thirdly, ultimately to apply the heat-transfer coefficients developed in this study to the prediction and control of the temperature profile of the strip being rolled, in order to control and optimize the mechanical properties of the rolled strip.

CHAPTER 4

EXPERIMENTAL DESIGN AND MEASUREMENTS

4.1 Materials

Two aluminum-magnesium alloys and a commercial-pure copper were examined in this study. The alumunum alloys studied were AA5052 (Al-2 pct. Mg) and AA5182 (Al-4.5 pct. Mg). They were supplied in the form of slices cut perpendicular to the vertical axis of D.C. ingots for this study by the Kingston Research and Development Centre of Alcan Ltd. The copper was provided from storage in-house in an annealed condition.

4.1.1 Homogenization Treatment

Since the aluminum alloys were received in the as-cast condition, they were subjected to a heat treatment in order to homogenize their physical properties. The homogenization treatment for each alloy was as follows. AA5182 samples were heated to 530°C and held at that temperature for one hour. AA5052 samples were heated to 560°C and held at that temperature for two hours. The copper samples did not undergo any homogenization treatment.

4.1.2 Flow Stress Characterization

In order to characterize the steady-state flow stress behaviour of both the aluminum alloys and the copper used in this study, 10 mm dia. x 15 mm long cylindrical samples of the materials were subjected to compression tests. All compression tests were performed

by the Gleeble 1500 at UBC, a thermo-mechanical simulator which relies on resistance heating to elevate and control the temperature of the specimens.

Figure 4.1 shows a schematic diagram of the Gleeble apparatus. Tantalum or carbon foil between the test specimen and the anvil prevented welding of the two together during high temperature tests. A quartz L-strain device was used to measure the length of the test specimen, and a C-strain device measured the diameter of the test specimen. Providing that barrelling of the specimen does not occur to any large degree, the combination of L-strain and C-strain measurements, in addition to the force required for deformation of the specimen (recorded by the load cell), provided the information necessary to construct true stress-true strain data.

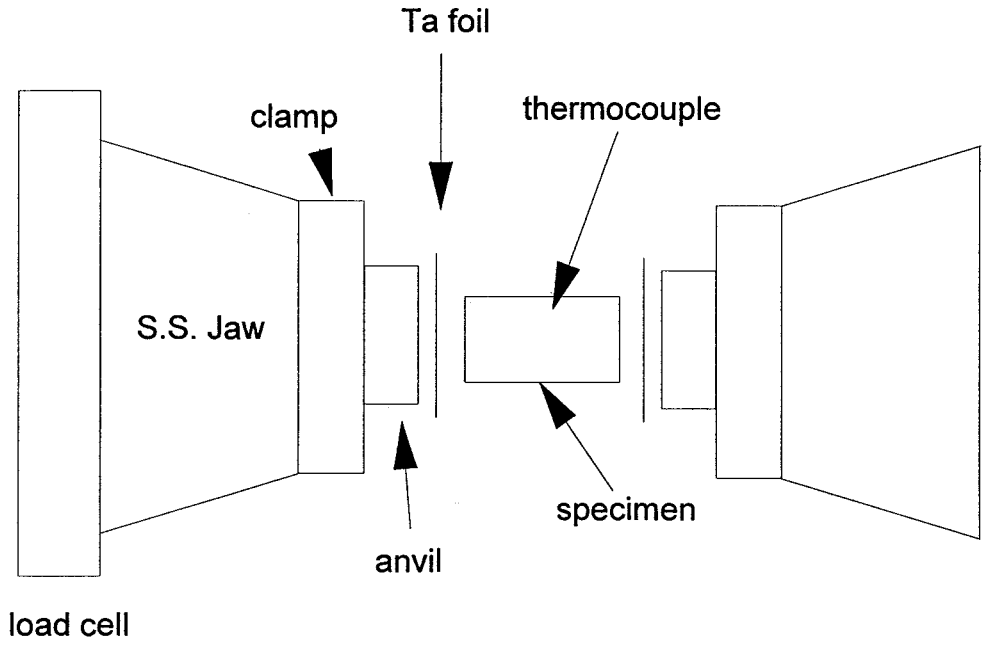

Figure 4.1 Schematic diagram of GLEEBLE apparatus

Prior to the actual deformation, the homogenized aluminum alloy test samples (both AA5052 and AA5182) were heated at 5 °C/s to 530 °C, held at that temperature for

one minute, cooled at 2 °C/s to the deformation temperature, and then held at the deformation temperature for one more minute. This holding time ensured a uniform sample temperature. After deformation, the test samples were allowed to air cool. Each alloy was tested at four different temperatures (300, 375, 430 and 520 °C), and at five different nominal strain rates (0.01, 0.5, 3, 7 and 10 s^{-1}), for a total of twenty tests.

Copper cylindrical test specimens were heated to 700 °C at 10 °C/s in the Gleeble, held at that temperature for one minute, then cooled to the deformation temperature at 5 °C/s, and held at that temperature for one more minute. This ensured a uniform testing temperature. After deformation, the specimens were allowed to air cool. The copper was tested at three different temperatures, 475, 575 and 675 °C, and at each temperature at three different strain rates, 0.1, 1 and 10 s^{-1}, for a total of nine tests. The true stress-true strain data obtained from the compression tests were then fitted to the hyperbolic-sine constitutive equation:

$$Z = \dot{\varepsilon} \exp\left(\frac{Q}{RT}\right) = A \sinh(\alpha\sigma)^n \tag{4.1}$$

In Equation 4.1, Z, the Zener-Holloman parameter, is the temperature-compensated strain rate; $\dot{\varepsilon}$ is the strain rate; Q is the activation energy; R is the gas constant; T is the absolute temperature; σ is the steady-state flow stress and A, α and n are constants. The flow stress for the analysis was taken at a strain of 0.5. At this strain, the experimental flow stresses were in a steady-state regime. The strain rate and sample temperature were calculated over a strain range of 0.2 to 0.5. The equation parameters Q, α , n, and ln (A) were calculated using a method developed by Davies *et al.* [45], which allowed each

parameter to have an unconstrained value. The resulting parameters of the constitutive equation are shown in Table 4.1.

Table 4.1. Constants for constitutive steady-state stress equation

Parameter	AA5182	AA5052	Copper
Q (kJ/mol)	185	189	173.2
α (MPa^{-1})	0.0450	0.0317	0.0729
n	1.818	3.536	1.257
ln (A)	24.48	26.13	18.02

4.2 Test Design

4.2.1 Test Facilities

In order to minimize the transfer time of the sample from the furnace to the roll stand, a square tube furnace was designed to butt against the rolls of the laboratory mill. The rolling mill used in this study is a two-high reversing mill with specifications shown in Table 4.2. The rolling mill was outfitted with a load cell to record the total separating force experienced by the mill during rolling, as well as a lubrication system that delivered lubricant to the top roll of the mill and a guide located at the roll-gap exit to prevent samples from sticking to the top roll and curling upon exit from the roll gap. Figure 4.2 shows a schematic diagram of the rolling mill and furnace.

Table 4.2. UBC pilot mill specifications

Manufacturer	STANAT
Rolling Speed	34.3/68.5 rpm
Roll Diameter	100 mm
Roll Material	Vanadium BB*
Max. Roll Separating Force	200 kN

*A proprietary alloy of VASCO Inc. -- similar to SAE 52100

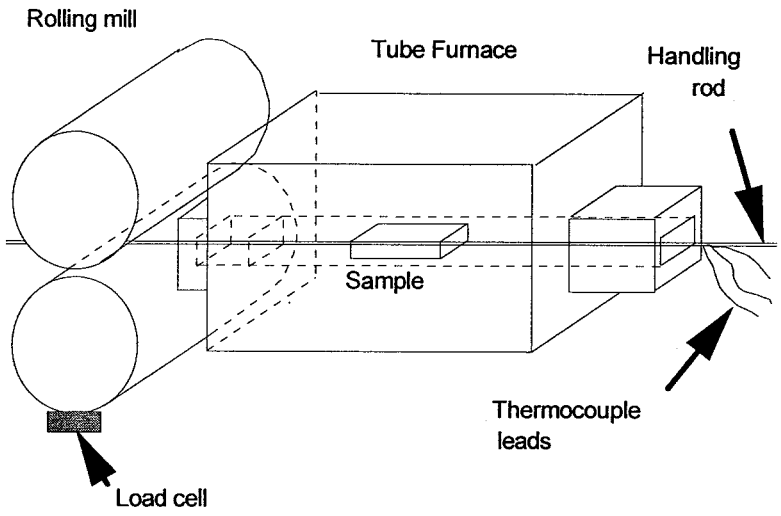

Figure 4.2. Schematic diagram of the UBC pilot rolling mill

The load cell, along with the three thermocouples attached to the instrumented sample, was connected to a COMPAQ portable microcomputer, which was equipped with a DT2805 data acquisition board. During all rolling tests the data acquisition rate was 1500 Hz.

The lubrication system consisted of a one-litre reservoir, attached to the top of the mill, and a brush which spread the lubricant over the surface of the top roll. Lubricant passed from the reservoir to the brush through a polypropylene hose at 200 ml/min during rolling. The bottom roll was lubricated by the excess lubricant that poured off the top roll. A container placed under the bottom roll collected the used lubricant.

The exit guide, attached to the exit table of the rolling mill, formed a channel 10 mm high through which the sample had to pass upon exit from the rolls. This prevented the samples from curling up and therefore prevented the sample surface thermocouples from being in contact with the top roll past the roll exit plane. Figure 4.3 schematically shows the lubrication system and the exit guide.

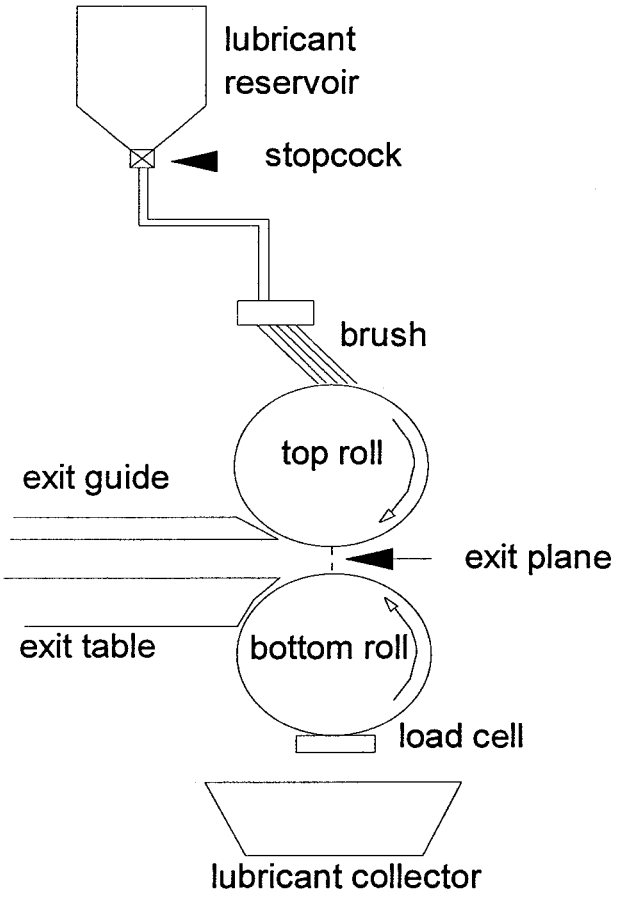

Figure 4.3. Schematic diagram of roll lubrication system

4.2.2 Preparation of Test Samples

4.2.2.1 Aluminum Alloy Samples

Aluminum samples (8.7 mm x 50.8 mm x 127 mm) were machined as shown in Figure 4.4, with the axial direction of the original D.C. ingot shown with a dashed arrow. The width-thickness ratio of the samples was 5.84. Using an empirical spread-prediction equation proposed by Beese [46],

$$S = 0.61\left(\frac{H_i}{W_i}\right)^{1.3} \exp\left\{-0.32\left(\frac{H_i}{\sqrt{R_0 \Delta H}}\right)\right\} \tag{4.2}$$

where H_i is the original thickness of the sample, W_i is the original width of the sample, R_0 is the roll radius, ΔH is the draft, and S, the spread factor, is defined as

$$S = \frac{\ln(W_f / W_i)}{\ln(H_i / H_f)} \tag{4.3}$$

The spread factor was calculated to be 0.0457. This corresponds to a 9.1 pct. deviation from a pure plane strain condition, since when S=0, the strain is plane, and when S=0.5, the strain is distributed equally in the width and length direction. This calculated deviation from pure plane strain was judged to be small enough to not invalidate plane-strain assumptions used in calculations of flow stress.

After a homogenization treatment (see Section 4.1.1 for details) each sample was instrumented with three thermocouples (1.6 mm dia. INCONEL-sheathed Type-K thermocouples having Chromel-Alumel wires 0.25 mm in dia.); two of the thermocouples, S1 and S2, were located on the sample surface and a third, C1, at the centre of the sample, as shown in Figure 4.5. Thermocouples S1 and S2 were inserted into horizontal holes extending halfway into the sample, and the exposed Chromel-Alumel wires were brought to the surface through the vertical holes drilled from the top surface, which intercepted the horizontal holes. The Chromel-Alumel wires were placed on the sample surface approximately one-half millimetre apart to establish a double-intrinsic junction, and fastened to the sample surface by inserting the wires into a shallow

0.6-mm dia. hole drilled into the sample surface, which was subsequently punched shut. Figure 4.6 shows a schematic view of the double-intrinsic junction. The thermocouple holes were drilled oversize so that deformation of the sample would not deform the thermocouple sheathing; uncertainties involving the effect of thermocouple sheath deformation on temperature measurement thus were avoided. For thermocouple C1 the thermocouple wires were spot-welded together to form an extrinsic junction. Electrical resistance checks ensured that the extrinsic junction made contact with the sample.

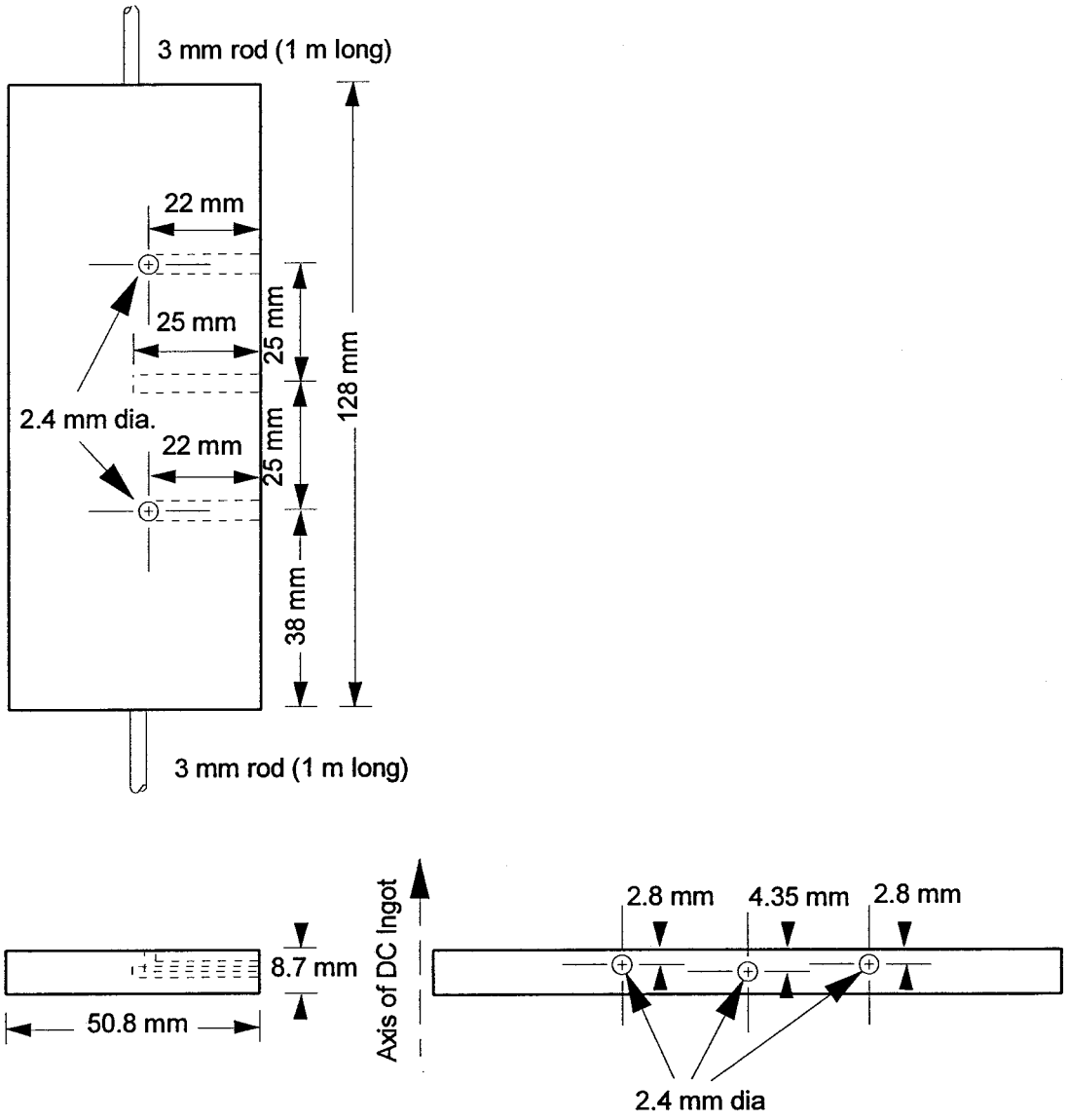

Figure 4.4. Design of aluminum sample

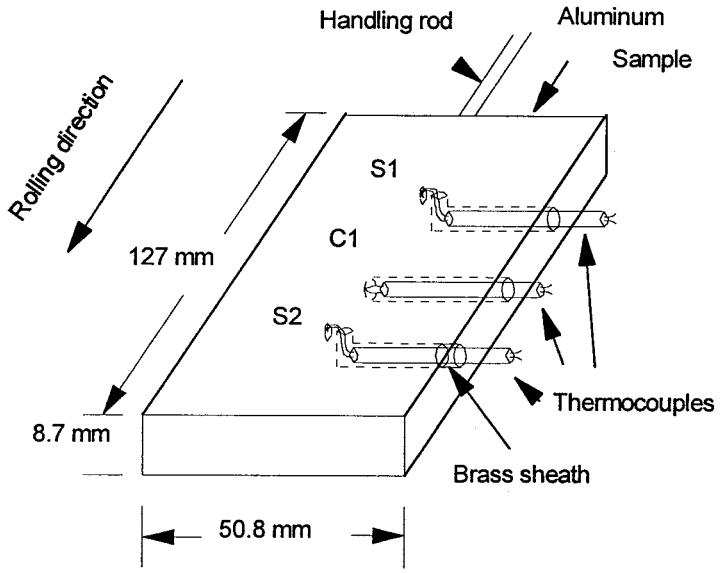

Figure 4.5. Schematic diagram of aluminum test piece

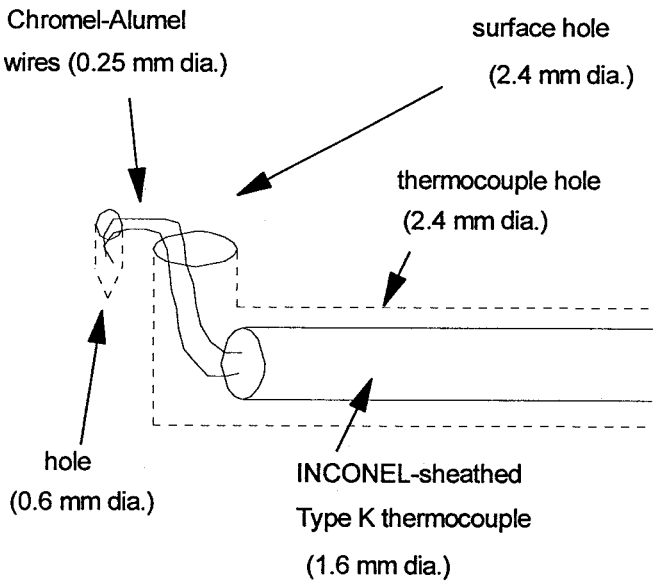

Figure 4.6. Close-up of surface thermocouple

4.2.2.2 Copper Samples

Two copper samples were machined in a manner similar to the aluminum samples, with the omission of the centre thermocouple hole. After machining, the copper samples (6.4 mm x 50.8 mm x 114 mm) were instrumented with two surface thermocouples, as shown in Figure 4.7, using the same procedure that was developed for the aluminum samples.

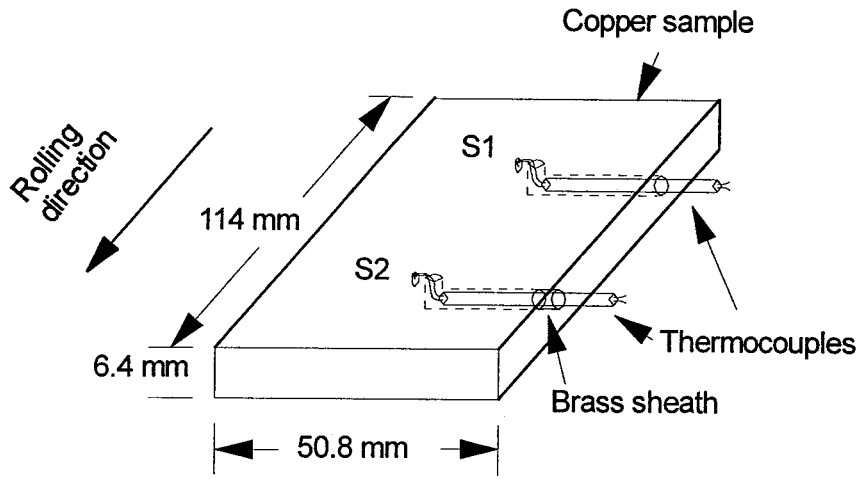

Figure 4.7. Schematic of copper test piece

4.3 Test Procedure

4.3.1 Aluminum Test Schedule

In general, each aluminum sample was rolled three times. Initially the samples were rolled without bulk plastic deformation. This first pass served to flatten the thermocouple wires into the sample, thereby assuring good electrical contact with the sample and establishing the double-intrinsic junction at the surface. The samples were then returned to the furnace and reheated prior to being rerolled. For the second pass, the roll gap was narrowed so that a nominal bulk deformation of twenty percent was

achieved. The samples were then returned to the furnace a second time and reheated. The sample was then rolled once more, this time by a nominal reduction of ten percent. During the passes involving deformation, the rolls were continually lubricated by one of two oil (5 pct.) - water emulsions. These emulsions were prepared from two industrial rolling oils provided by Alcan Inc. using an ultrasound mixing probe. During the majority of the aluminum rolling tests, the rolls were lubricated with a viscous, low-friction lubricant, designated as Lubricant 'A'. During the remainder of the aluminum rolling tests, the rolls were lubricated with a less-viscous, higher-friction lubricant, designated as Lubricant 'B'. Table 4.3 presents the conditions of the aluminum tests.

Table 4.3. Conditions Employed in Aluminum Rolling Tests

Test ID	Material	Initial thickness (mm)	Initial Temp. (°C)	Reduction (pct.)	Rolling Speed (m/s)	Strain Rate (s^{-1})	Mean Pressure (kg/mm^2)
AL10	5182	7.04	470	5.1	0.358	5.21	14.26
AL12	5052	8.70	515	19.8	0.358	9.83	10.41
AL13	5052	7.01	510	11.2	0.180	3.93	10.09
AL15*	5052	8.70	520	20.1	0.358	9.92	10.35
AL16	5052	6.99	510	10.9	0.358	7.74	8.81
AL18	5182	8.70	505	19.8	0.358	9.83	13.80
AL19	5182	7.01	500	10.1	0.180	3.70	12.45
AL21	5052	8.70	415	18.9	0.358	9.56	13.50
AL22	5052	7.09	505	11.8	0.358	8.03	9.49
AL24	5182	8.70	375	20.1	0.358	9.92	19.89
AL27	5182	8.70	320	19.2	0.358	9.65	21.51
AL28	5182	7.06	320	9.3	0.358	7.05	22.7
AL30	5052	8.70	320	20.3	0.358	9.99	16.46
AL31	5052	6.96	320	10.9	0.358	7.76	17.27
AL33	5052	8.70	370	20.1	0.358	9.92	14.75
AL34*	5052	6.99	320	10.5	0.358	7.58	16.59
AL37*	5182	6.99	320	10.2	0.358	7.46	20.79
AL39†	5182	8.70	300	8.4	0.358	6.01	22.57

*These tests were performed with Lubricant 'B'. All other tests were performed with Lubricant 'A' (except test AL39)
†This test was performed without lubrication.

4.3.2 Copper Test Schedule

Each of the two copper samples was rolled three times in a similar manner as the aluminum samples (see 4.3.1). Table 4.4 presents the conditions of the copper tests.

Table 4.4. Conditions Employed in Copper Rolling Tests

Test ID	Initial thickness (mm)	Initial Temp. (°C)	Reduction (pct.)	Rolling Speed (m/s)	Strain Rate (s^{-1})	Mean Pressure (kg/mm^2)
CU4	6.35	700	13.2	0.358	9.05	11.20
CU5	5.51	700	12.4	0.358	9.38	10.45
CU7	6.35	650	13.6	0.358	9.21	11.10
CU8	5.49	650	11.6	0.358	9.04	11.64

4.4 Thermal Response

4.4.1 Thermal Response of Aluminum Samples

Figures 4.8-4.12 show the thermal response of some of the aluminum tests. Figure 4.8 shows the thermal response of the three thermocouples during Test AL13, as well as the output of the load cell. For this test, the output of all the thermocouples was exceptionally smooth. The surface thermocouples showed good reproducibility. The temperature of each thermocouple decreased extremely rapidly from 505°C as the sample surface was quenched by the roll to 300°C. As the sample at the thermocouple location exited from the rolls, the sample surface temperature then quickly reheated to approximately 425°. The temperature at the sample centre decreased smoothly from 505°C to 425°C. The thermocouple response indicates that the sample temperature

became essentially homogeneous approximately 200 milliseconds after the rolling operation was complete.

In general, the apparent oscillation of the roll load is due to the electrical interference from the 60 Hz A.C. power supply with the low-voltage (on the order of two to three millivolts) signal of the load cell. The output signal from the load cell during this test, however, exhibited greater noise than usual, possibly due to the power source.

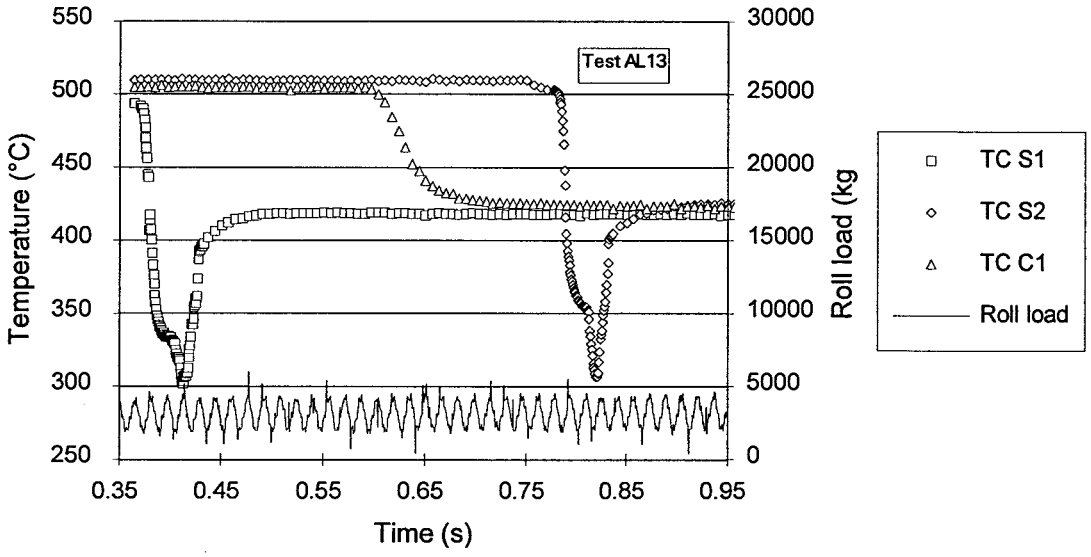

Figure 4.8. Thermocouple and load response for Test AL13

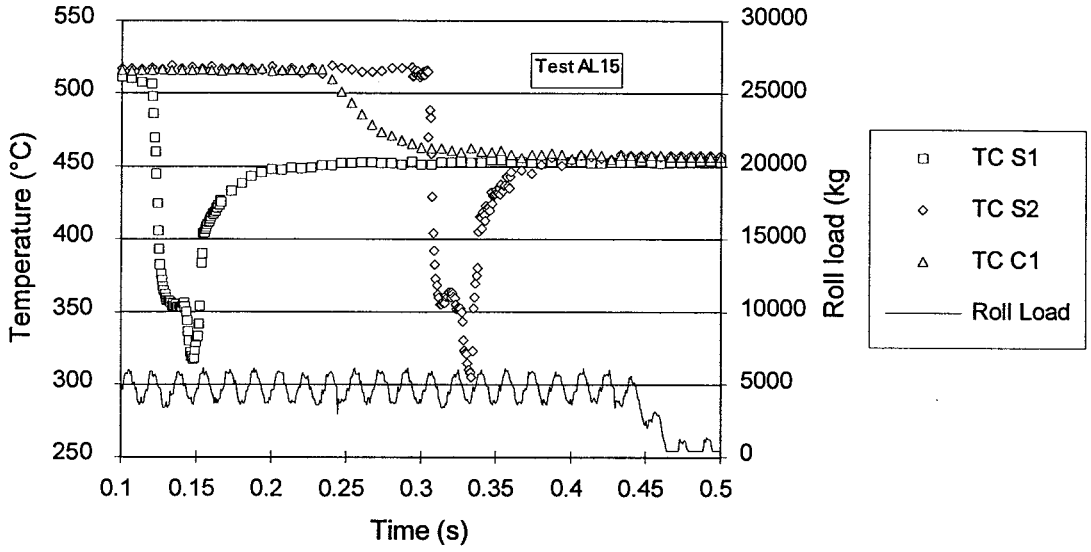

Figure 4.9. Thermocouple and load response for Test AL15

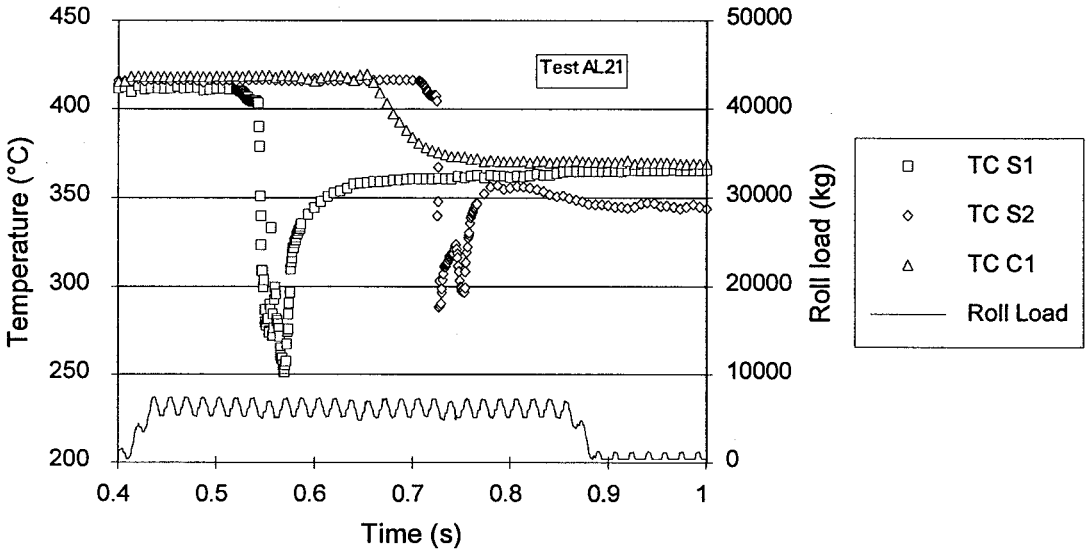

Figure 4.10. Thermocouple and load response for Test AL21

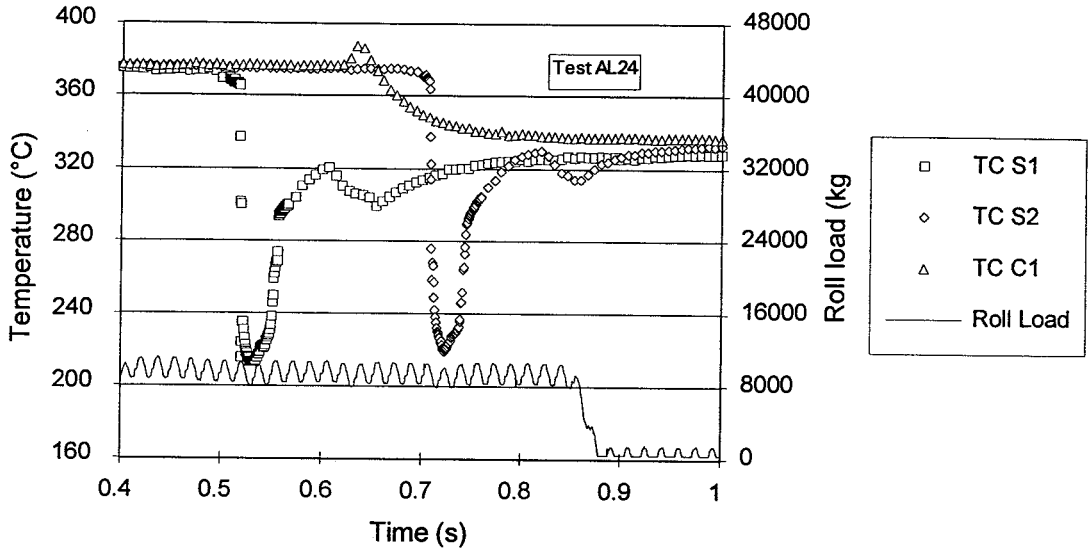

Figure 4.11. Thermocouple and load response for Test AL24

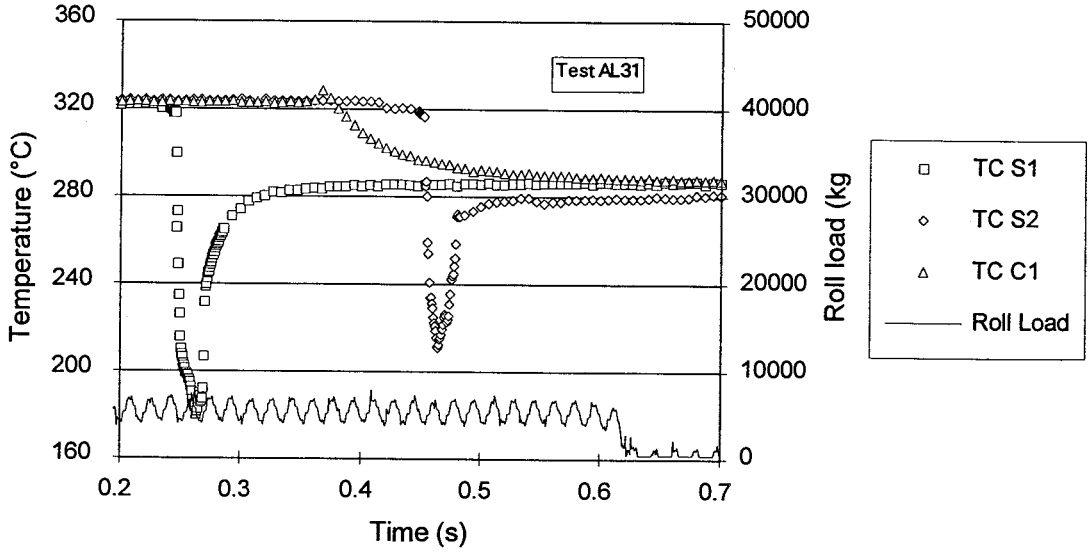

Figure 4.12. Thermocouple and load response for Test AL31

Figure 4.9 shows another test, Test AL15, in which the reproducibility of the two surface thermocouples is quite good, despite a small amount of noise in the output of

thermocouple S2. Figure 4.10, on the other hand, shows an instance (Test AL21) where both thermocouples appear to have failed. TC S1 exhibited a questionable response while in the roll bite, but seemed to recover after exiting the roll gap. TC S2, on the other hand, failed completely, sensing very erratic temperatures both in the roll bite and upon exit from the rolls. The reason for the erratic output of the thermocouples during this test is unknown.

Figure 4.11 shows the results of Test AL24. The initial rolling temperature of the aluminum sample during this test was much lower than for Tests AL13, AL15, or AL21. Due to the higher flow stress of the aluminum sample during this low-temperature test, the roll load is seen to be significantly higher. Furthermore, the centreline thermocouple TC C1 exhibits an initial temperature rise before decreasing to the lower, post-rolling temperature. This temperature is due to the bulk heat of deformation, and is most apparent at tests involving lower temperatures. The reason for this is that the temperature increase due to deformation is dependent on the flow stress of the aluminum sample, which is significantly higher at low rolling temperatures than at high temperatures.

4.4.2 Thermal and Load Response of Copper Samples

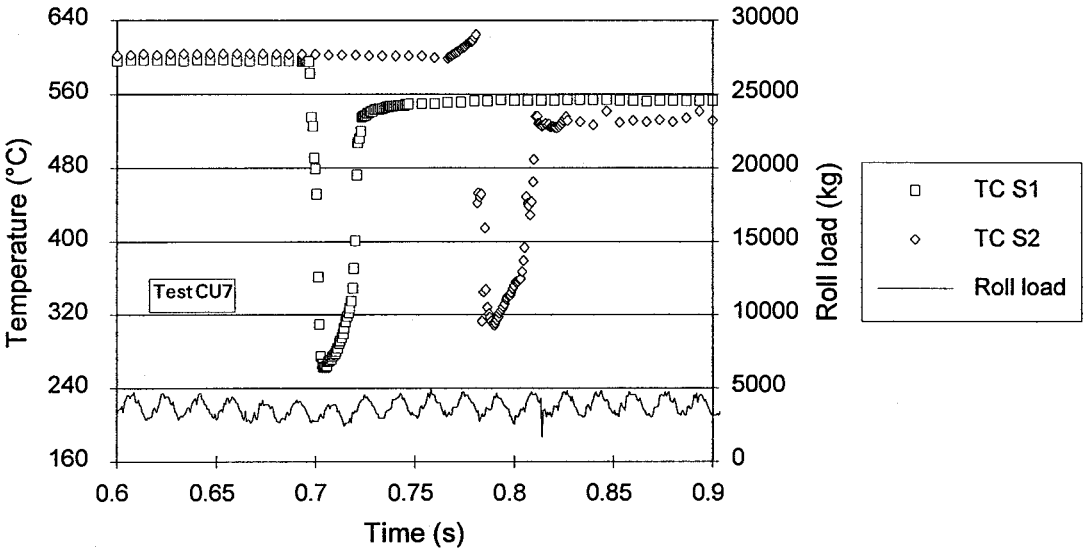

Figure 4.13. Thermocouple and load response for Test CU7

Figure 4.13 shows the thermocouple and load output for Test CU7. The copper samples did not contain centreline thermocouples. In general, the thermocouple output response during the copper sample tests was not as well-behaved as the response of the thermocouples during the aluminum sample tests. In this case, the response of TC S2 was anomalous in that it showed an initial temperature rise just prior to coming into contact with the roll. Secondly, the output of TC S2 was generally erratic. The reason for the relatively poor response of the thermocouples during the copper tests is not known.

CHAPTER 5

HEAT TRANSFER MODEL DEVELOPMENT

5.1 Mathematical Formulation

In order to convert the surface temperature response of the aluminum sample to a HTC, the general heat-conduction equation must be solved subject to initial and boundary conditions. Several assumptions may be made to simplify the governing equation:

1. The process is at steady state, so that at any fixed location in the roll bite the temperature does not change with time;
2. Since, for laboratory rolling, the Peclet number is high, on the order of 100, heat conduction along the length of the sample (y-direction) is assumed to be negligible compared to heat transfer by bulk motion;
3. Heat transfer in the transverse (z) direction is assumed negligible due to the large width-to-thickness ratio;
4. Frictional heat is generated along the arc of contact, and is distributed between the sample and roll according to their respective thermal diffusivities.

The two-dimensional, steady-state governing equation for heat conduction in the sample then can be written as

$$\frac{\partial}{\partial x}\left(k_s \frac{\partial T_s}{\partial x}\right) - v_s \rho_s C_{ps} \frac{\partial T_s}{\partial y} + \dot{Q}_{def} = 0 \tag{5.1}$$

Equation (5.1) can be expressed in a one-dimensional, unsteady-state form by employing the transformation $y = v_S t$, where v_S is the sample velocity, to become

$$\frac{\partial}{\partial x}\left(k_s \frac{\partial T_s}{\partial x}\right) + \dot{Q}_{def} = \rho_s C_{ps} \frac{\partial T_s}{\partial t} \tag{5.2}$$

where t is the time taken for an elemental volume to travel a distance y in the roll bite. Equation (5.2) is solved subject to an initial and two boundary conditions. Initially the temperature of the sample, T_S, is uniform:

$$t = 0, \quad 0 \le x \le \frac{H_i}{2}, \quad T_s = T_s(x,0) \tag{5.3}$$

Assuming symmetrical cooling of the sample about the centreline (x = 0), the boundary condition at this location is

$$t \ge 0, \quad x = 0, \quad -k_s \frac{\partial T_s}{\partial x} = 0 \tag{5.4}$$

The boundary condition at the sample surface ($x = H(t)/2$) can be expressed as

$$t > 0, \quad x = \frac{H(t)}{2}, \quad -k_s \frac{\partial T_s}{\partial x} = h(t)(T_s^{H(t)/2} - T_r^{R_0}) \tag{5.5}$$

where $h(t)$ is the local heat-transfer coefficient at the roll-sample interface and $T_s^{H(t)/2}$ and $T_r^{R_0}$ are the temperatures of the sample and roll surfaces, respectively. The changing sample thickness is $H(t)$.

Since the sample and work rolls are coupled thermally, it is necessary to solve the governing equation of the sample simultaneously with that of the rolls. Neglecting axial heat conduction in the rolls and assuming that circumferential heat conduction is negligible compared to bulk heat flow due to rotation of the rolls, conduction is confined to the radial direction; and the governing heat conduction equation for the roll becomes

$$\frac{1}{r}\frac{\partial}{\partial r}\left(rk_r\frac{\partial T_r}{\partial r}\right)=\rho_r C_{pr}\frac{\partial T_r}{\partial t} \tag{5.6}$$

where t is the time taken for an elemental volume of the roll to rotate through an angle, θ, measured from a reference point.

The temperature increase of the roll due to hot rolling is confined to a surface layer δ. Initially, the temperature of the roll is uniform, that is,

$$t=0,\quad R_0-\delta\le r\le R_0,\quad T_r=T_r(r,0) \tag{5.7}$$

At $R^* = R_0 - \delta$, the boundary condition is

$$t\ge 0,\quad r=R^*,\quad -k_r\frac{\partial T_r}{\partial r}=0 \tag{5.8}$$

At the roll surface ($r = R_0$), the boundary condition is

$$t > 0,\ \ r = R_0,\ \ -k_r \frac{\partial T_r}{\partial r} = h(t)(T_s^{H(t)/2} - T_r^{R_0}) \tag{5.9}$$

5.2 Discretization of the Differential Equations

An implicit finite difference method was used to solve the one-dimensional transient heat transfer equation developed in Section 5.1. The strip and roll were discretized into three types of nodes; surface nodes, interior nodes, and adiabatic nodes, as shown in Figure 5.1. A heat balance was performed on each node to obtain general equations.

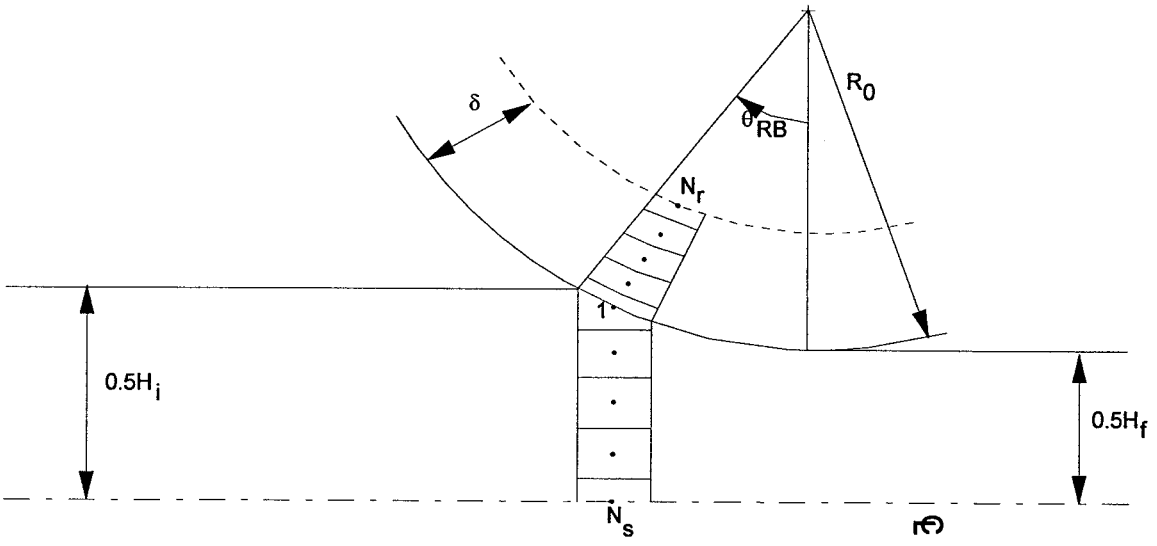

Figure 5.1. Discretization of roll and strip

5.2.1 Nodes in the Strip

At the surface of the strip, heat transfer to the environment is characterized by the heat transfer coefficient $h(t)$. The heat balance on the surface node, Node 1, is then as follows:

$$\left[\frac{2\alpha_s}{\Delta x_1+\Delta x_2}+\frac{h(t)}{k_s\cos\theta}+\frac{\Delta x_1}{2\Delta t}\right]T_1^{j+1}=\frac{2\alpha_s}{\Delta x_1+\Delta x_2}T_2^{j+1}+\frac{h(t)\alpha_s}{k_s\cos\theta}T_h+\frac{\Delta x_1}{2\Delta t}T_1^j \qquad (5.10)$$

where Node 1 is the strip surface node, α_S is the thermal diffusivity of the strip and j is the time step. The heat balance for an interior node i is:

$$\left[\frac{2\alpha_s}{\Delta x_{i+1}+\Delta x_i}+\frac{2\alpha_s}{\Delta x_i+\Delta x_{i-1}}+\frac{\Delta x_i}{\Delta t}\right]T_i^{j+1}=\frac{2\alpha_s}{\Delta x_{i+1}+\Delta x_i}T_{i+1}^{j+1}+\frac{2\alpha_s}{\Delta x_i+\Delta x_{i-1}}T_{i-1}^{j+1}+\frac{\Delta x_i}{\Delta t}T_i^j \qquad (5.11)$$

Finally, the centreline node N_S has an adiabatic side, so the heat balance becomes:

$$\left[\frac{4\alpha_s}{\Delta x_{N_s}+\Delta x_{N_s-1}}+\frac{\Delta x}{\Delta t}\right]T_{N_s}^{j+1}=\frac{4\alpha_s}{\Delta x_{N_s}+\Delta x_{N_s-1}}T_{N_s-1}^{j+1}+\frac{\Delta x_{N_s}}{\Delta t}T_{N_s}^j \qquad (5.12)$$

5.2.2 Nodes in the Roll

The roll node heat balances are similar to the strip heat balances. The heat balance on the surface node of the roll is:

$$\left[\frac{2\alpha_r\left(r_1+\frac{1}{2}\Delta r_1\right)}{\Delta r_1+\Delta r_0}+\frac{h(t)\alpha_r}{k_r}r_0+\frac{r_0^2-\left(r_1+\frac{1}{2}\Delta r_1\right)^2}{2\Delta t}\right]T_0^{j+1}=\frac{2\alpha_r\left(r_1+\frac{1}{2}\Delta r_1\right)}{\Delta r_1+\Delta r_0}T_1^{j+1}+\frac{h(t)\alpha_r}{k_r}r_0T_h+\frac{r_0^2-\left(r_1+\frac{1}{2}\Delta r_1\right)^2}{2\Delta t}T_0^j \tag{5.13}$$

The heat balance for an interior roll node *i* is:

$$\left[\frac{2\alpha\left(r_{i+1}+\frac{1}{2}\Delta r_{i+1}\right)}{\Delta r_{i+1}+\Delta r_i}+\frac{2\alpha\left(r_i+\frac{1}{2}\Delta r_i\right)}{\Delta r_i+\Delta r_{i-1}}+\frac{r_i\Delta r_i}{\Delta t}\right]T_i^{j+1}=\frac{2\alpha\left(r_{i+1}+\frac{1}{2}\Delta r_{i+1}\right)}{\Delta r_{i+1}+\Delta r_i}T_{i+1}^{j+1}+\frac{2\alpha\left(r_i+\frac{1}{2}\Delta r_i\right)}{\Delta r_i+\Delta r_{i-1}}T_{i-1}^{j+1}+\frac{r_i\Delta r_i}{\Delta t}T_i^j \tag{5.14}$$

Finally, the heat balance for the adiabatic node N_r at a depth δ below the roll surface is:

$$\left[\frac{2\alpha_r\left(r_{N_r}+\frac{1}{2}r_{N_r}\right)}{\Delta r_{N_r}+\Delta r_{N_r-1}}+\frac{\left(r_{N_r}+\frac{1}{2}\Delta r_{N_r}\right)^2-r_{N_r}^2}{2\Delta t}\right]T_{N_r}^{j+1}=\frac{2\alpha_r\left(r_{N_r}+\frac{1}{2}r_{N_r}\right)}{\Delta r_{N_r}+\Delta r_{N_r-1}}T_{N_r-1}^{j+1}+\frac{\left(r_{N_r}+\frac{1}{2}\Delta r_{N_r}\right)^2-r_{N_r}^2}{2\Delta t}T_{N_r}^j \tag{5.15}$$

5.2.3 Solving Technique

A Gauss-Siedel iteration method with successive over-relaxation was used in order to solve the nodal equations. Figure 5.2 shows the general technique used to solve for the instantaneous HTC in the roll gap.

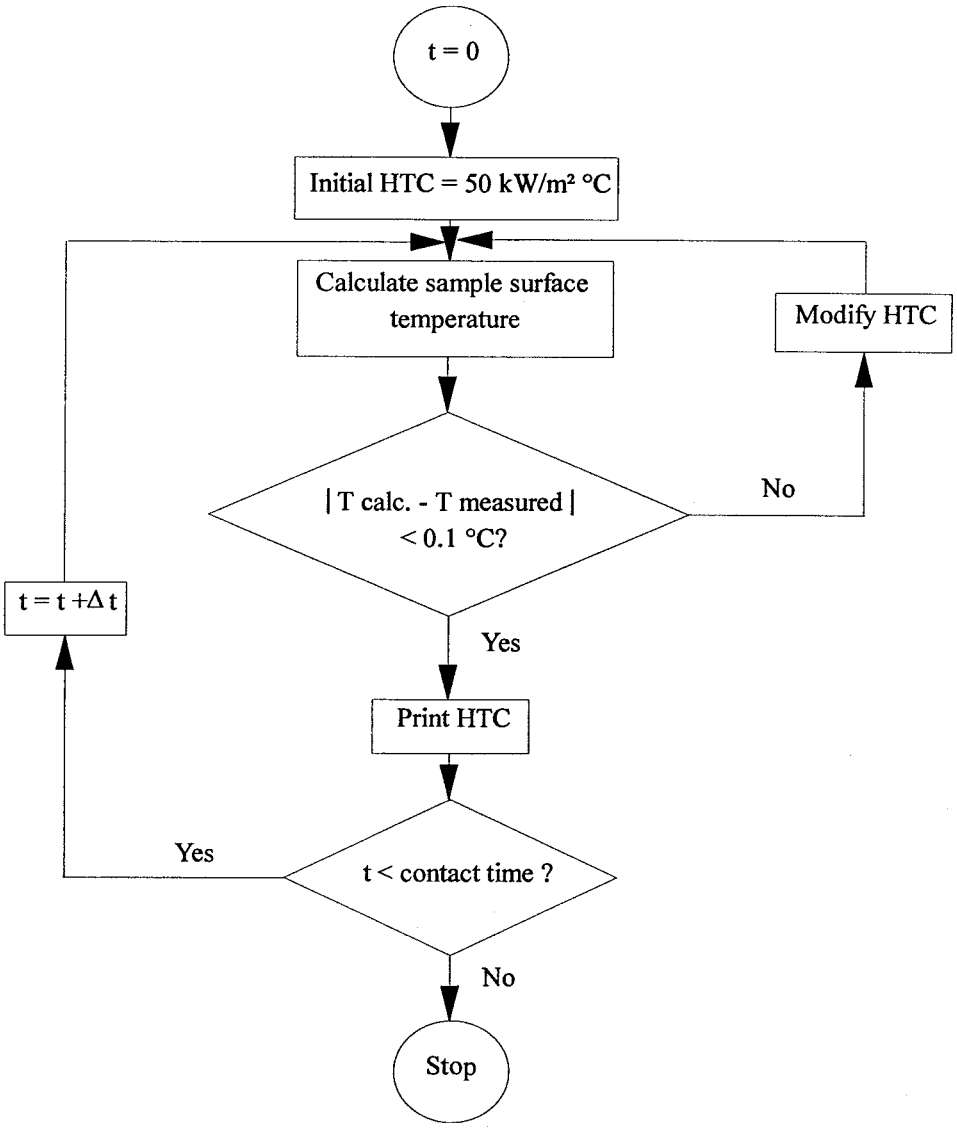

Figure 5.2. Flowchart of HTC-solving algorithm

5.3 Treatment of Heat Generation

5.3.1 Generation and Distribution of Frictional Heat

The frictional heat generation is given by

$$\dot{q}_f = |v_s - v_r| \mu \; P_r \tag{5.16}$$

as formulated by Devadas and Samarasekera [32], in which $|v_s - v_r|$, the relative velocity between the roll and strip, varies continuously along the arc of contact.

Extending the approach of Hatta *et al.* [44], who distributed frictional heat based on rough estimates of the conductivities of the roll and strip, the frictional heat was distributed according to the thermal diffusivity ratio of the strip and roll:

$$\dot{q}_{f,s} = \frac{\alpha_s(T)}{\alpha_s(T)+\alpha_r(T)}\dot{q}_f \tag{5.17}$$

and

$$\dot{q}_{f,r} = \dot{q}_f - \dot{q}_{f,s} \tag{5.18}$$

5.3.2 Bulk Heat due to Deformation

Pavlov's equation [47] calculates the bulk heat of deformation in rolled strip as

$$\Delta T_{def} = \frac{\sigma}{\rho_s C_{ps}} \ln\left(\frac{H_i}{H_f}\right) \tag{5.19}$$

where σ is the temperature-dependent flow-stress of the material being rolled, and H_i and H_f are the entry and exit thicknesses of the strip, respectively. This equation assumes that the plastic deformation is uniform throughout the thickness of the strip. However, this equation also assumes that all the mechanical work is converted into heat, and also only considers the total strain accrued in the strip as a result of deformation. Therefore, the equation was modified to address these deficiencies. The resulting equation is

$$\Delta T_{\text{def}}(t,i) = \eta \frac{\sigma_i\left(T_i, \bar{\dot{\varepsilon}}\right)}{\rho_i C_{p,i}} \ln\left(\frac{H_{i-1}}{H_i}\right) \tag{5.20}$$

where η is the efficiency of the conversion of work to heat, set to 0.95 after Timothy *et al.* [5]. With this form of the equation, for a strip node i at time t, the increase in temperature due to deformation is a function of the strain rate-temperature dependent yield stress σ, as well as the density and heat capacity of the strip at node i, and also of the strain accrued during the time step. Thus, Equation (5.20) takes into account the varying amounts of strain that is accrued by the strip during each time step through the roll gap. Also, the increase in temperature of each node is dependent on the initial temperature of that node. Therefore, the nodes closer to the surface of the strip, being colder than the nodes in the strip's interior, and therefore also having a higher yield stress, increase more in temperature due to the bulk deformation than do the warmer, interior nodes.

5.3.3 Depth of Heat Penetration into the Roll

Due to the extremely short contact time between the strip and roll, the thermal shock experienced by the roll only penetrates to a shallow surface layer of depth δ. Therefore, when modelling the temperature of the roll, it is only necessary to discretize the roll to the depth δ, thus reducing the number of nodes in the roll by a considerable amount and saving computing time. Tseng [48] proposed an equation to calculate the depth of the roll layer; however, the equation was developed for sustained rolling conditions as in an industrial situation. Therefore, this equation calculates a roll surface

layer that is much deeper than is required for the present study, as the test pieces were completely rolled within one roll revolution. Instead, a simple penetration depth was calculated, assuming an infinite HTC (from [52]):

$$\delta_{1\%} = 3.64\sqrt{\alpha_r t_c} \tag{5.21}$$

where $\delta_{1\%}$ is the roll depth at which the temperature changes by one percent of the difference between the initial temperature of the roll and the ambient temperature, α_r is the thermal diffusivity of the roll, and t_c is the contact time. Taking t_c to be 50 milliseconds and α_r to be 1.11×10^{-5} m/s², $\delta_{1\%}$ was calculated to be 2.7 mm. Since Equation (5.21) is strictly valid only for a semi-infinite slab, and taking into consideration the approximate nature of the equation, for the purpose of this study, the thermal layer depth δ was set at 8 mm.

5.4 Conductivities of Materials Used in this Study

This study examined the HTC during rolling for three materials, AA5052, AA5182, and copper. Furthermore, the results of this study were compared against those of Chen [21] for SS304. Finally, it was also necessary to know the thermal properties of the roll as well.

The temperature-dependent thermal conductivity of both AA5052 and AA5182 was obtained from a study by Logunov and Zverev [49]. These researchers reported values for an aluminum alloy known as AMG-3, which contains 3.2-3.8 pct. Mg, and for an aluminum alloy known as AMG-5, which contains 4.8-5.8 pct. Mg. The experimental thermal conductivities obtained in this study compared well with theoretical values.

Both the temperature-dependent heat capacity and thermal conductivity of the copper were obtained from a report by Pehlke *et al.* [50]. These workers have tabulated values of heat capacity and thermal conductivity for copper for temperatures ranging from 273 to 2300 K.

The material of the rolls used in this study was a proprietary Fe-alloy with a chemical composition 1.0 pct. C, 0.32 pct. Mn, 0.25 pct. Si, 1.4 pct. Cr and 0.2 pct. V. Unfortunately, a literature search failed to find any published values of thermal properties for this alloy. AISI 4140, an alloy containing 0.4 pct. C, 1 pct. Cr and 0.2 pct. Mo, has a thermal conductivity of 42.7 W/m °C at 100°C [51]. An alloy containing 0.15 pct. C, 0.57 pct. Mn, 0.26 pct. Si and 0.30 pct. V has a conductivity of 43.1 W/m °C at 100°C [61]. To account for an observed slight lessening of thermal conductivity with increased carbon content [51], the roll conductivity was set at 41.0 W/m °C for the temperature range 25°C - 250°C. Finally, thermal properties for SS304 were obtained from Chen [21].

5.5 Model Verification

5.5.1 Validity of the 1-D Model

A nondimensional analysis was conducted to test the validity of the assumption that heat flow in the length or rolling direction is negligible compared to heat flow in the thickness direction, ie. in the direction perpendicular to the roll-strip interface. The Peclet number, which is the ratio of heat flow due to bulk flow to heat flow due to conduction, defined as

$$Pe = \frac{3\omega R_0 L C_{ps} \rho_s}{k_s} \tag{5.22}$$

where ω is the angular roll speed, R_0 is the roll radius, L is the length of the strip being rolled in the roll bite, and C_{ps} and ρ_s are the heat capacity and density of the strip, respectively, is a useful parameter to evaluate this assumption. A Peclet number on the order of 100 is generally considered to be the value below which heat transfer in the length direction becomes non-negligible as compared to heat transfer in the thickness direction. The result of the Peclet number analysis for the UBC pilot mill is summarized in Table 5.1.

Table 5.1. Peclet Numbers for Various Rolling Speeds and Reductions

Deformation (pct.)	Angular velocity (RPM)	Peclet Number
5	34.3	47
5	68.5	93
10	34.3	66
10	68.5	131
20	34.3	92
20	68.5	185

The table reveals that at lower reductions and rolling speeds the assumption becomes less valid. It was therefore decided, in scheduling the rolling tests, to avoid five percent reductions. Ten percent was set as the minimum reduction, and 34.3 rpm as the minimum rolling speed, to maintain the validity of the 1-D heat transfer model.

5.5.2 Comparison with Analytical Solution

Even though it was impossible to check the complete model against an analytical solution due to the complexity of the coupled roll-strip formulation, the model was modified in order to check the finite-difference solution of the strip and roll separately against analytical solutions.

5.5.2.1 Verification of the Roll Finite-Difference Formulation

The model was modified so that the roll was uncoupled from the strip. The roll, initially at 24°C, was exposed to an environment of 400°C for 294 seconds. Therefore, the Fourier number (*Fo*) for the roll in this situation becomes

$$Fo = \frac{\alpha_r t}{R_0^2} = \frac{(1.7 \cdot 10^{-5} \mathrm{m}^2/\mathrm{s})(294\mathrm{s})}{(0.05\mathrm{m})^2} = 2 \tag{5.23}$$

where α_r is the thermal conductivity of the roll, t is the time, and R_0 is the roll radius. The HTC, h, was set to 1240 W/m² °C, and the roll conductivity was fixed constant at 62 W/m² °C, in order to obtain a Biot (*Bi*) number of 1:

$$Bi = \frac{hR_0}{k_r} = \frac{(1240\mathrm{W}/\mathrm{m}^2\,^\circ\mathrm{C})(0.05\mathrm{m})}{62\mathrm{W}/\mathrm{m}\,^\circ\mathrm{C}} = 1 \tag{5.24}$$

Since *Fo* is greater than 0.2, it is possible to use a single term of the Fourier series solution to obtain an analytical solution of the roll axis temperature after 53 seconds [52]:

$$\theta_c = \frac{T_c - T_h}{T_r - T_h} \cong C_1 \exp\left(-\beta_1^2 Fo\right) \tag{5.25}$$

where T_c is the roll axis temperature, T_h is the ambient temperature, T_r is the initial temperature of the roll, and C_1 and β_1 are constants. However, since the methods for solving for the two constants are very tedious, for the roll a graphical technique was used. The Heissler-Gröber chart is a convenient method of determining the axial temperature of a cylinder for precisely this type of problem. See [52], for example, for a complete description of the H-B charts.

The analytical solution of the axial temperature of the roll, obtained from the H-B chart, was 381°C. The model, employing 200 nodes to discretize the roll, and using 50 time steps, calculated the temperature of the roll axis to be 385°C. The values were judged to be sufficiently close that the finite-difference solution was considered to be verified.

5.5.2.2 Verification of the Strip Finite-Difference Formulation

The strip finite-difference solution was checked against an analytical solution in a manner very similar to the method employed for the roll. The strip, initially at 400°C, was exposed to an ambient temperature of 25°C for 1.331 seconds. For the purpose of comparing the model solution with the analytical solution, the thermal diffusivity α_S of the strip was fixed at 5.689×10^{-5} m^2/s, and the conductivity k_S was fixed at 137 W/m °C. The Fourier number for a strip of thickness $H_i = 8.7$ mm is then

$$Fo = \frac{\alpha_s t}{\left(\frac{H_i}{2}\right)^2} = \frac{(5.689 \cdot 10^{-5} \mathrm{m}^2/\mathrm{s})(1.331\mathrm{s})}{(0.00435\mathrm{m})^2} = 4 \tag{5.26}$$

The HTC was set to 31 264 W/m² °C in order to set the Biot number to 1:

$$Bi = \frac{hL}{k} = \frac{(31264\text{W/m}^2\,^\circ\text{C})(0.00435\text{m})}{136\text{W/m}\,^\circ\text{C}} = 1 \tag{5.27}$$

For this case, the Fourier number is again greater than 0.2, so a single term of the Fourier series solution (Equation (5.24)) is accurate to greater than one percent. Furthermore, for the case of the strip geometry, tables are readily available which tabulate values of C_1 and β_1. From [52.] C_1 is equal to 1.1191 and β_1 is equal to 0.8603. Equation (5.24) is then readily solved to yield a centreline temperature of the strip, 46.7°C. The finite-difference solution, on the other hand, yielded a centreline temperature of 47.4°C. This value was arrived at using 75 nodes to discretize the strip and 1000 time steps. A relatively large number of time steps, compared to the number of time steps used for verifying the roll finite-difference solution, was employed because of the high HTC. Since the difference between the model and analytical solution was less than one degree, the strip finite-difference formulation was considered to be verified.

5.5.3 Convergence of the Model

The implicit finite-difference method does not suffer stability problems as does the explicit finite-difference method. Therefore, one would expect a continual improvement in the numerical solution (that is, the difference between the numerical solution and the true, analytical solution becomes less) as the mesh size and time step is decreased, to the point at which computer round off error becomes significant.

To test the convergence of the model solution, the mesh size and time step was modified for Test AL15, thermocouple S1. The base mesh used by the model is one hundred-fifty nodes to discretize a half-thickness of the strip, two hundred nodes to discretize the surface layer, δ, of the roll, and fifty time steps to advance a slice of the strip through the roll bite. As Figure 5.3 indicates, the HTC through the roll bite was calculated to be essentially the same for all three mesh variations. Even when the mesh was increased to three hundred strip nodes and four hundred roll nodes, and one hundred time steps were used, the calculated HTC changed only slightly. This confirms the stability of the finite-difference model and the convergence of the solution.

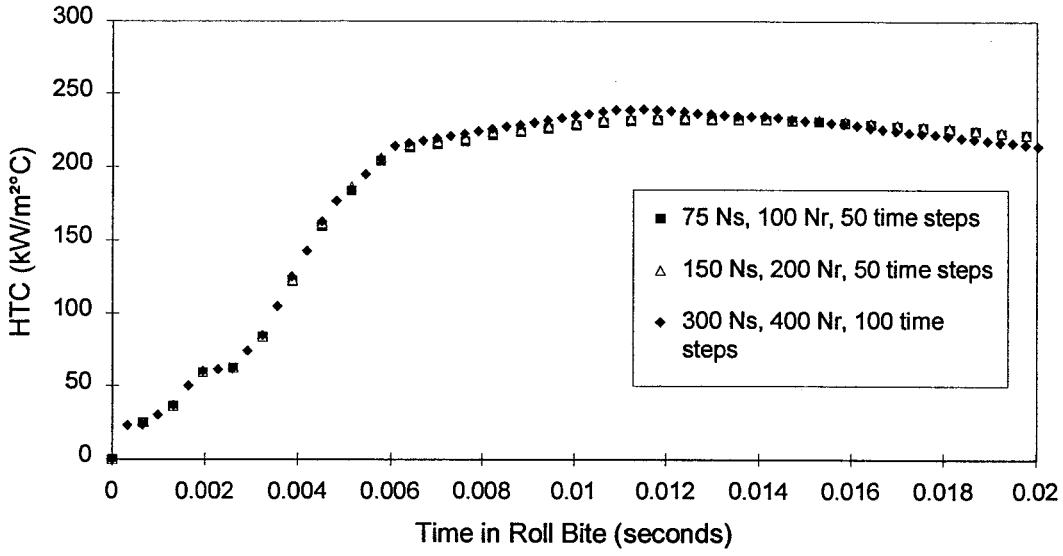

Figure 5.3. Sensitivity of numerical solution to mesh size

CHAPTER 6

ROLL-GAP HEAT-TRANSFER ANALYSIS

6.1 Measurement of Instantaneous Roll-Gap HTC

6.1.1 Aluminum Tests

The finite-difference model developed in Chapter 5 back-calculated the instantaneous HTC as a function of time in the roll gap from the surface temperature measurements. Figures 6.1-6.5 illustrate the calculated HTCs for the tests shown in Figures 4.8-4.12.

According to general rolling theories, the normal pressure acting on the strip should increase from the entry point to a maximum at the neutral point, the angle at which the velocities of the strip and roll are equal. The pressure should then decrease from the neutral point to the exit point. This phenomenon is sometimes referred to as a 'friction hill' [53]. Therefore, the roll-gap HTC, which is expected to be a function of the contact pressure, should follow the same trend; that is, to increase from the initial entry point to a maximum, then to decrease until the exit point is reached. Upon examination of Figures 6.1-6.5, it can be seen that the calculated instantaneous HTCs show too much variability to qualitatively relate the HTC behaviour to a pressure variation within the roll gap.

Often the HTC has been seen to increase again just before exit from the rolls, as seen in Figures 6.2 and 6.3. This could be evidence for a 'double pressure peak' which has been seen by other researchers investigating aluminum rolling [54, 55]. On the other hand, the HTC as calculated by the model becomes unreliable in the latter stages of the roll bite. Figure 6.1, which shows the measured surface temperatures, calculated roll-gap

HTCs, and the calculated roll surface temperature based on the output of TC S1, illustrates this point. As the strip first enters the rolls, the temperature difference between the strip and roll surface is large. However, as the strip proceeds through the roll gap, the strip cools and the roll surface heats up, causing the difference in temperatures between the two surfaces to lessen. In the case of Test AL13, for example (Figure 6.1), the difference in temperatures between the strip temperature and the roll temperature (as calculated from the output of TC S1) becomes very small near the end of the roll bite. The HTC, h, is defined as the heat flux from the strip, $\dot{q}$, divided by the difference in the strip and roll surface temperatures,

$$h = \frac{\dot{q}}{T_s - T_r} \tag{6.1}$$

As T_S - T_r becomes smaller, any error in the calculation of T_r affects the calculated HTC to a larger and larger degree. For example, a ten degree error in the calculation of T_r when the difference in roll and strip surface temperatures is only twenty degrees would cause 100 pct. error in the calculated HTC. Therefore, in the latter part of the roll bite, where the strip and roll surface temperatures are relatively close together, the calculated HTC is subject to large errors. This problem is exacerbated in the case of metals which are rolled at lower temperatures. In the hot rolling of steel, for example, the temperature difference between the strip and roll surfaces remains considerable throughout the roll gap, and therefore any error in the calculation of the roll surface temperature through the use of a heat-transfer model affects the calculated HTC to a lesser extent than in the hot rolling of aluminum.

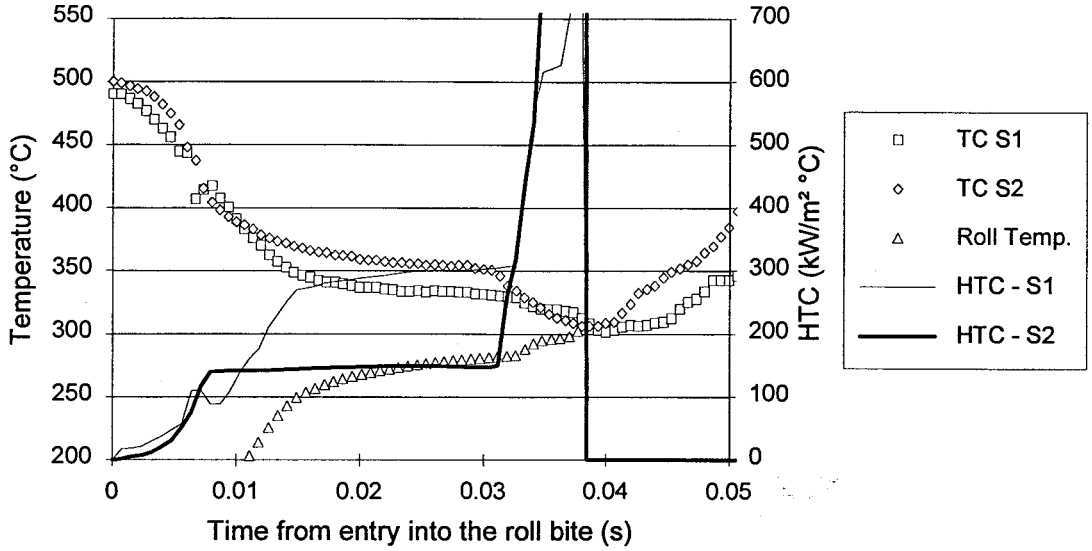

Figure 6.1. Surface temperature and HTC for Test AL13

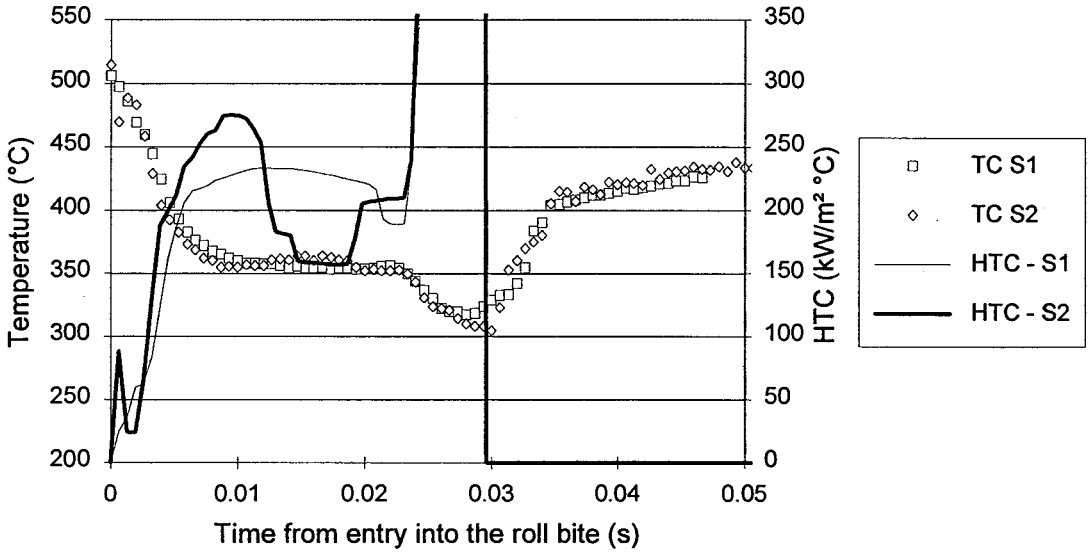

Figure 6.2. Surface temperature and HTC for Test AL15

Figure 6.2 shows the calculated HTC for Test AL15. This test illustrates the high sensitivity of the roll-gap HTC to slight fluctuations in temperature. The two

thermocouple responses during this test were nearly identical. However, at approximately fifteen milliseconds into the roll gap, the surface temperature as recorded by TC S2 increases just slightly -- approximately ten degrees. This small increase in temperature caused the instantaneous HTC to drop from 475 kW/m² °C to 370 kW/m² °C.

The high sensitivity of the roll-gap HTC to small variations in surface temperature arises because of the magnitude of the HTC. A large HTC corresponds to a low resistance to heat flux at the roll-strip interface. Therefore, even small changes in surface temperature would be a result of a large change in the magnitude of the HTC.

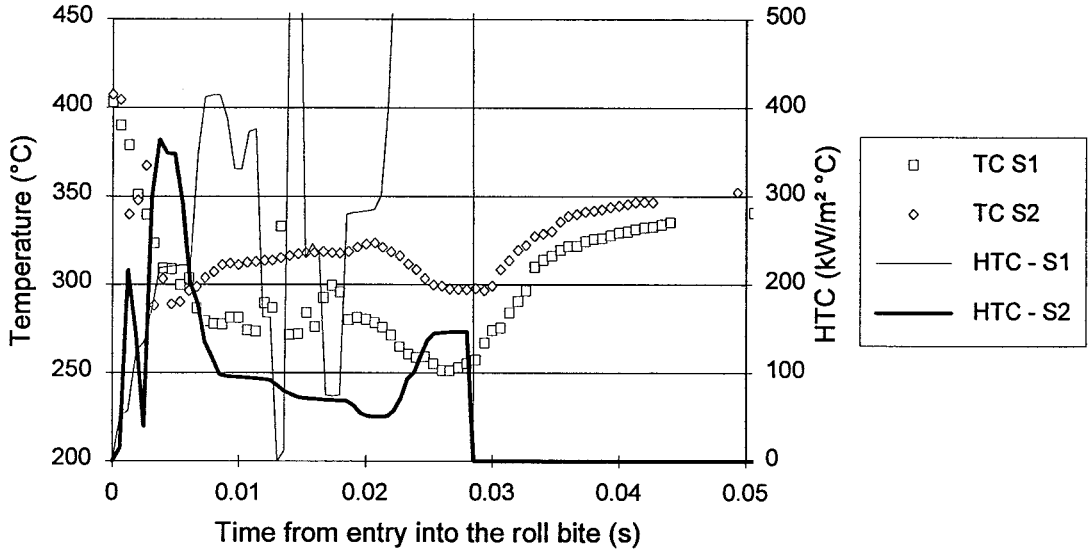

Figure 6.3. Surface temperature and HTC for Test AL21

Figure 6.3 shows the calculated instantaneous HTC for Test AL21. Again, the sensitivity of the calculated HTC to variations in measured surface temperature is seen. For this test, it is apparent that TC S1 failed while in the roll bite for some reason, then recovered as it emerged from the roll bite. On the other hand, TC S2 continued to function satisfactorily throughout the test.

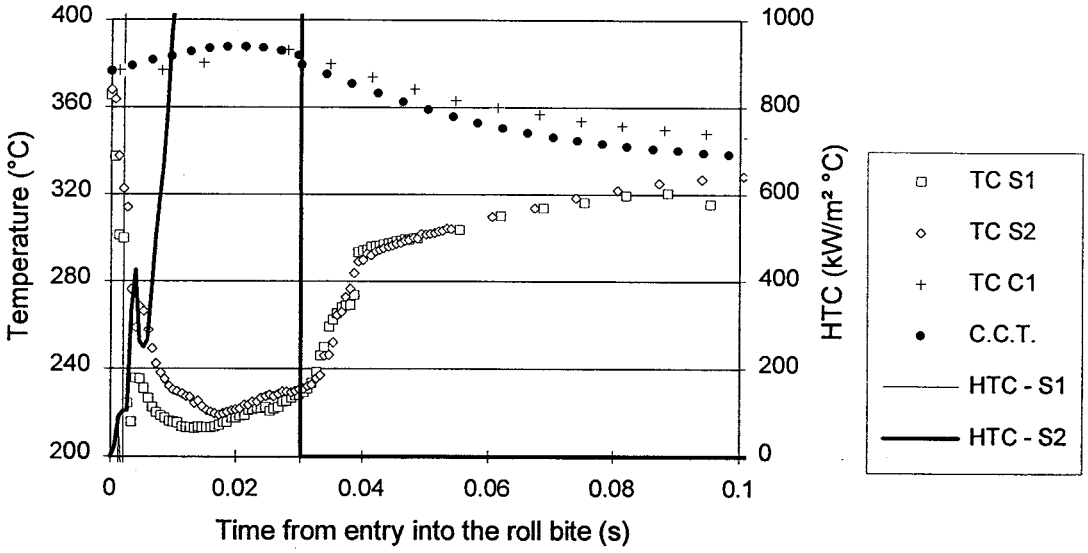

Figure 6.4. Surface temperature and HTC for Test AL24

Figure 6.4 shows, in addition to the measured surface temperatures and the resulting HTCs, the measured centre temperature as recorded by TC C1, and the calculated centre temperature (C.C.T.). In this case, the model had difficulties in calculating the roll-gap HTC for either surface temperature. In both cases, the calculated HTC quickly reaches the cut-off value of the model (arbitrarily set at $1x10^6$ kW/m² °C) at which point contact resistance is essentially zero, and remains there until the end of the roll bite. This indicates that the model was incapable of calculating a HTC that would account for the measured drop in surface temperature of the sample.

Figure 6.4 also shows the measured and calculated temperature of the interior of the sample. The interior temperature of the sample at first rises due to the heat of deformation, then decreases as the heat is conducted to the sample surface. A comparison of the two shows good agreement between the recorded temperature rise of the sample

interior due to the bulk heat of deformation, and the temperature rise as calculated by the model.

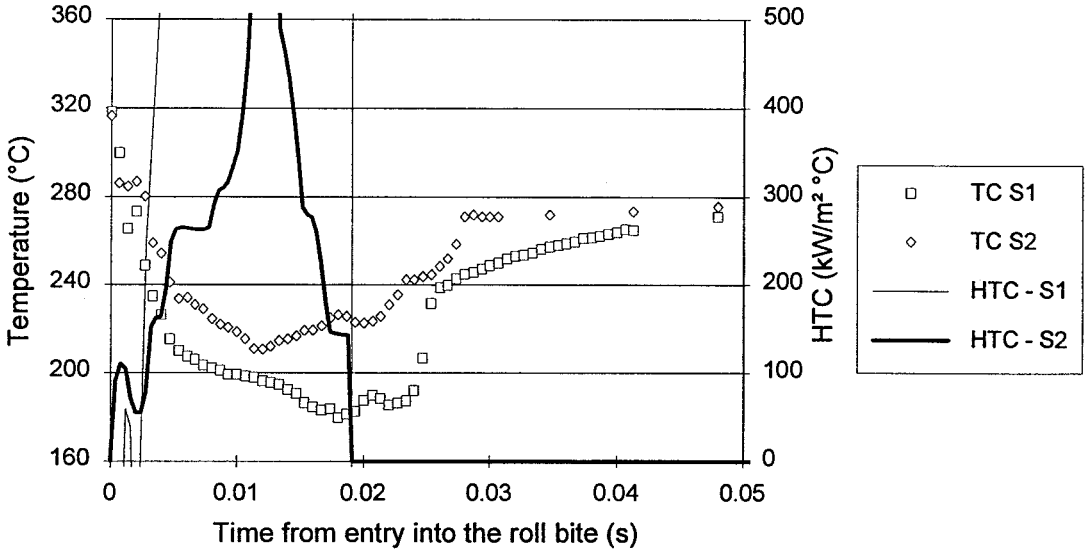

Figure 6.5. Surface temperature and HTC of Test AL31

Figure 6.5 shows the results of Test AL31. In this test, even though both surface thermocouples seemed to be responding properly, there is a large difference in their values throughout the roll gap. This corresponds to a large difference in the calculated HTC from TC S1 and TC S2.

Since there was no means available to measure the normal pressure variation through the roll bite, it was decided to characterize the average HTC as a function of the mean roll pressure. The mean roll pressure P_r was defined as

$$P_r = \frac{F}{W\sqrt{R_0 \Delta H}} \tag{6.2}$$

where F is the total roll load, R_0 is the radius of the roll, and ΔH and W are the difference between the entry and exit thickness, and the width of the sample, respectively. The square root of the product of the roll radius and draft is the projected length of the roll bite. In order to make a comparison between tests meaningful, the time in the roll bite was nondimensionalized as a fraction f of the total time in the roll bite, or $f=t/t_c$. The average HTC was calculated from the instantaneous HTC by employing a simple numerical integration method. Figure 6.6 shows the average HTC at $0.5t_c$ plotted against the mean roll pressure for all aluminum tests performed in this study. Ideally, one would like to show the average HTC for the entire time in the roll bite. However, as stated before, in the latter part of the roll bite, the calculated HTC tended to increase to the model-imposed maximum. Whenever this occurred, the calculated average value over the entire roll bite became meaningless. Therefore, $0.5t_c$ was chosen, because at this point in the roll bite, the calculated HTC for most tests was still relatively well-behaved.

The scatter in the data is seen to be large. The data ranges from 60 to 1200 kW/m^2°C. It is difficult, given the scatter, to establish any trend or dependence of the HTC on the mean roll pressure by considering the average HTC calculated from the response of the surface thermocouples in the roll bite.

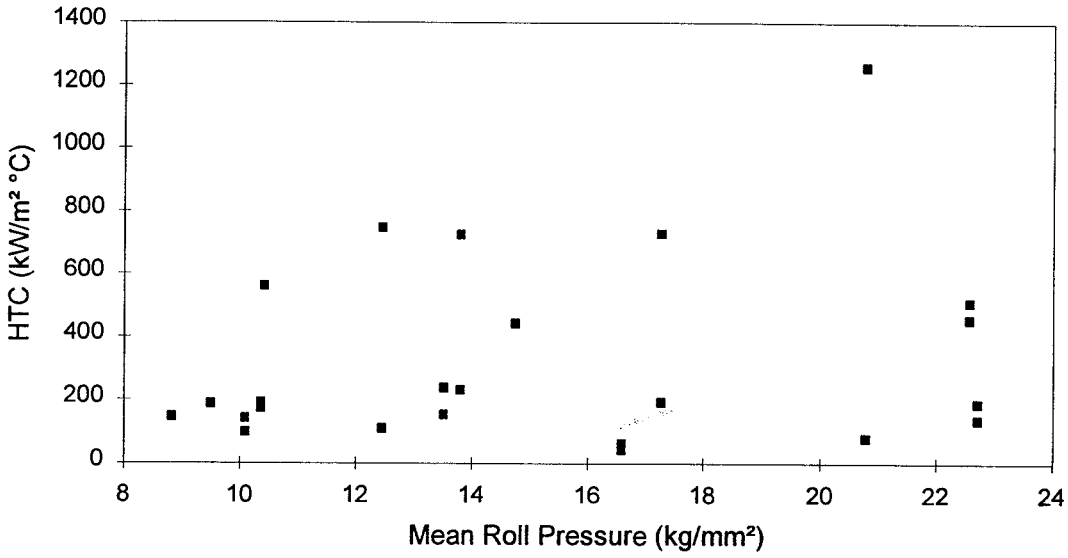

Figure 6.6. Average HTC calculated from surface TCs vs. mean roll pressure

6.1.2 Copper Tests

The model experienced difficulties in calculating the instantaneous HTC versus time in the roll bite for all the copper tests. The calculated HTC in each case quickly reached the cutoff value imposed by the model. These situations were similar to the problem encountered in trying to calculate the HTC for Test AL24 (Figure 6.4). The reason for the problems encountered with the copper rolling tests may be the high thermal conductivity of copper. The Peclet number for the copper rolling tests is on the order of 60 because of the high thermal conductivity of copper. This Peclet number is lower than 100, the value usually considered to be the minimum necessary for conduction along the rolling direction to be considered negligible. In cases where the roll-gap HTC is high, such as in aluminum and copper hot-rolling, even a small amount of conduction along the length direction would increase the HTC calculated by a model that assumes conduction only in the thickness direction.

6.2 HTC Calculated from Initial and Final Sample Temperatures

6.2.1 Aluminum Tests

It was mentioned before (see Section 4.4.1) that within 250 milliseconds of exiting the roll bite, the aluminum samples reattained a homogeneous temperature, which was typically thirty to sixty degrees cooler than the initial bulk temperature. The finite-difference model was modified so that it was capable of guessing an initial roll-gap HTC, predicting a bulk temperature from the initial guess of HTC, and continually modifying the HTC until the predicted and measured final bulk temperatures of the sample agreed to within one degree. This provided an alternative method of determining an average roll-gap HTC. Table 6.1 shows the HTCs calculated by this method for each test.

Table 6.1. HTCs Calculated from Bulk Aluminum Sample Temperatures

Test ID	Mean Roll Pressure (kg/mm^2)	Initial Rolling Temperature (°C)	Temperature After Rolling (°C)	Mean HTC (kW/m^2 °C)
AL12	10.41	513	454	264.5
AL13	10.09	505	424	273.0
AL15	10.35	516	457	258.6
AL16	8.81	510	452	221.3
AL18	13.80	505	450	240.5
AL19	12.45	497	419	276.2
AL21	13.50	415	370	293.3
AL22	9.49	505	447	401.0
AL24	19.89	377	338	378.5
AL27	21.51	321	295	278.4
AL28	22.70	327	295	464.0
AL30	16.46	329	298	273.2
AL31	17.27	323	289	387.5
AL33	14.75	371	333	276.0
AL34	16.59	321	287	424.6
AL37	20.79	321	290	463.0
AL39	22.57	274	267	65.1

Figure 6.7 shows the results of Table 6.1, and compares the HTCs calculated by the difference in bulk temperatures with the HTCs calculated from the surface thermocouple responses. Upon comparing the two different methods of calculating the

roll-gap HTC with the aid of Table 6.2 and Figure 6.8, it is evident that the HTCs calculated from the difference in sample temperatures before and after rolling is the superior method. The data calculated from the bulk sample temperature difference shows considerably less scatter than the data calculated from the surface thermocouple responses (the coefficient of determination for the HTCs calculated from the bulk sample temperatures is seven times as high as for the HTCs calculated from the surface temperature responses). In addition, the regressions of the HTCs calculated from the two different techniques are very similar, which supports the view that both techniques are calculating the same parameter. That is, the sample surface thermocouples are measuring the true surface temperature of the sample, and not some temperature intermediate between the surface temperature of the sample and of the roll. If the surface thermocouples had been measuring a temperature lower than the actual surface temperature, the mean HTC as calculated from the surface thermocouples would have been higher than the mean HTC calculated from the difference in sample temperatures before and after rolling.

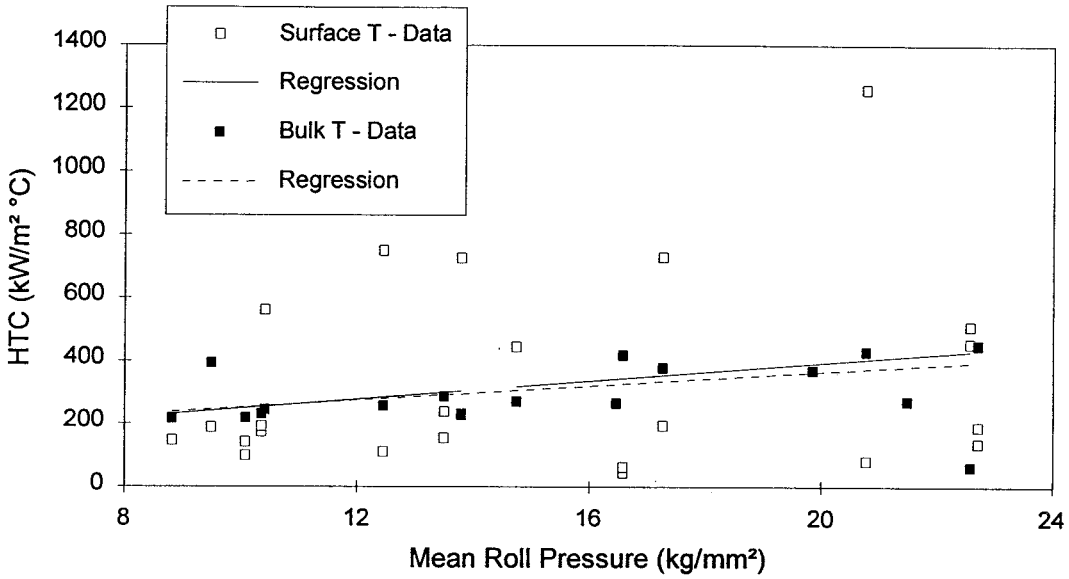

Figure 6.7. Comparison of HTCs calculated from bulk sample temperatures and surface temperatures in the roll bite

Table 6.2. Statistical Comparison of HTCs Calculated from Bulk Sample Temperatures and Surface Temperatures in the Roll Bite

	HTCs from Bulk Sample Temperature	HTCs from Surface Temperature Response
Slope of Linear Regression	11.4	14.6
Coefficient of Determination (r^2)	0.394	0.056
Significance F	0.0009	0.253

Another reason the method of calculating the HTC from the sample bulk temperature is superior to the method of calculating the HTC from the surface temperature response, is that the Significance F -- calculated from an analysis of variance -- is much lower than for the HTCs calculated from the surface temperature response, even though the slope of the linear regression is less. The Significance F is a statistical measure of the hypothesis that the roll-gap HTC increases with pressure, versus the null hypothesis, that the roll-gap HTC does not increase with pressure. In this case, from the HTCs calculated from bulk sample temperatures, the confidence that the HTC rises with pressure is (100 pct.)(1-0.0009)=99.91 pct., versus only 74.7 pct. from the HTCs calculated from the surface temperature response.

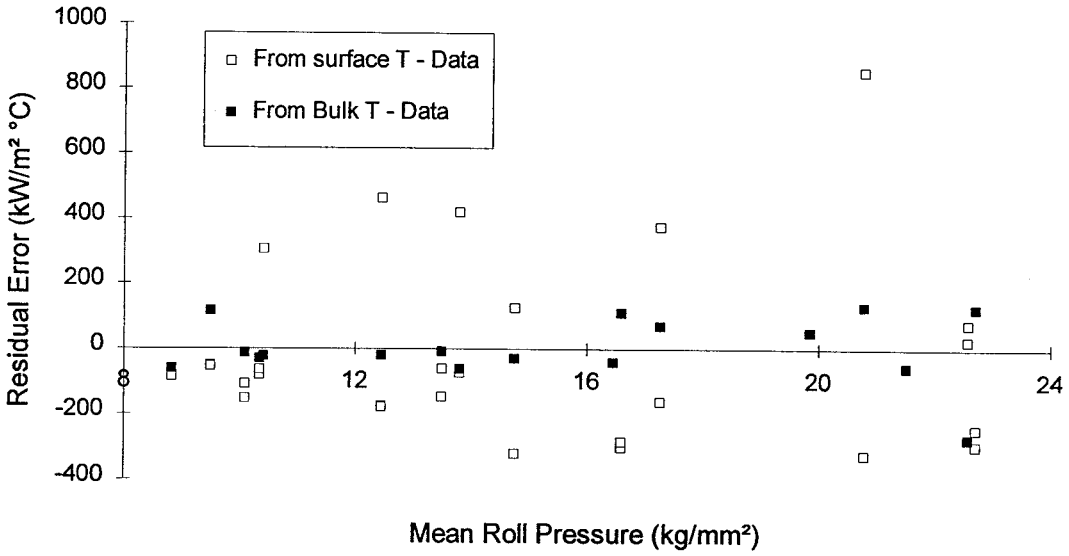

Figure 6.8. Residual Errors from HTC Regression

Figure 6.8 shows the residual errors (defined as the regression value at a pressure subtracted from the data point value) from the linear regressions shown in Figure 6.7. It shows that, for the HTCs calculated from the sample surface temperature responses in the roll gap, not only are the residual errors larger in general, but are not evenly spread out -- relatively few, high-magnitude positive errors cancel out the more numerous, but lower-magnitude, negative errors. The residual errors resulting from the regression of the HTCs calculated from the sample bulk temperatures, on the other hand, are smaller in magnitude, and are distributed more evenly. This indicates that the linear regression is more suited to the bulk sample temperature HTC data than to the sample surface temperature response HTC data.

6.2.2 Copper Tests

Copper has a higher thermal conductivity than aluminum. Therefore, the copper samples after rolling regained a uniform, bulk temperature after rolling more quickly than

the aluminum samples. Consequently, the same technique involving the difference in bulk sample temperature before and after rolling used in calculating a mean HTC through the roll gap for alumimun rolling can be easily utilized in the case of copper rolling as well. The HTCs in the roll gap calculated by this method for the copper rolling samples are tabulated in Table 6.3.

Table 6.3. HTCs Calculated from Bulk Copper Sample Temperatures

Test ID	Mean Roll Pressure (kg/mm^2)	Initial Rolling Temperature (°C)	Temperature After Rolling (°C)	Mean HTC (kW/m^2 °C)
CU4	11.64	574	528	341.2
CU5	11.10	578	523	427.2
CU7	10.44	602	551	347.0
CU8	11.20	523	481	388.2

Despite the fact that the mean roll pressure was quite similar for each copper rolling test, the calculated HTC again shows substantial variation from test to test. Again, this is due to the extreme sensitivity of the HTC to small changes in temperature at high HTC values.

CHAPTER 7

RESULTS AND DISCUSSION

7.1 Effect of Rolling Parameters on the HTC

Figure 7.1 shows selected HTCs calculated from the sample bulk temperatures versus rolling pressure for the two aluminum alloys, AA5052 and AA5182, examined in this study. HTCs were chosen only from tests that were conducted at 20 pct. deformation at 68.5 rpm using Lubricant 'A', so that the effect of alloy type was isolated.

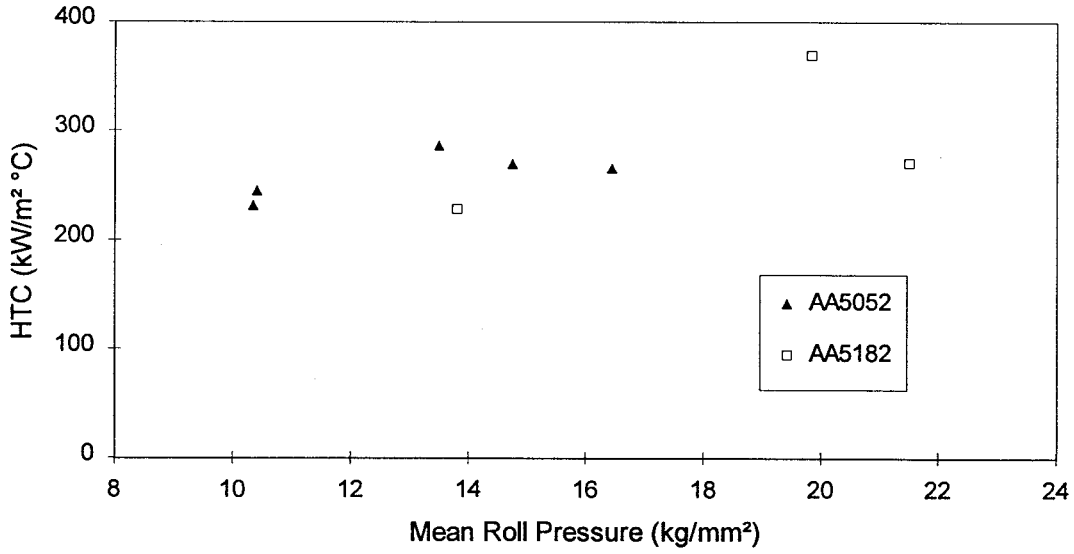

Figure 7.1. Effect of alloy type on the HTC

According to the theory (see Section 7.3), there should be a difference in alloy behaviour because of the difference in thermal conductivities, as well as the difference in

flow stress behaviour between the two alloys. Since AA5052 has a slightly higher thermal conductivity than AA5182 (an average of 152 W/m °C for AA5052 versus 136 W/m°C for AA5182), one would expect to see a marginally higher HTC vs. rolling pressure for the AA5052. In order to test whether or not this effect is statistically observable, the following approach was taken. Firstly, a line of regression was calculated from the AA5052 HTC data. Secondly, residual errors for both AA5052 and AA5182 were calculated from the regression analysis of the AA5052 data, Figure 7.2. Finally, a confidence interval for the difference of the means of the residual errors of the AA5052 and AA5182 HTC data was calculated.

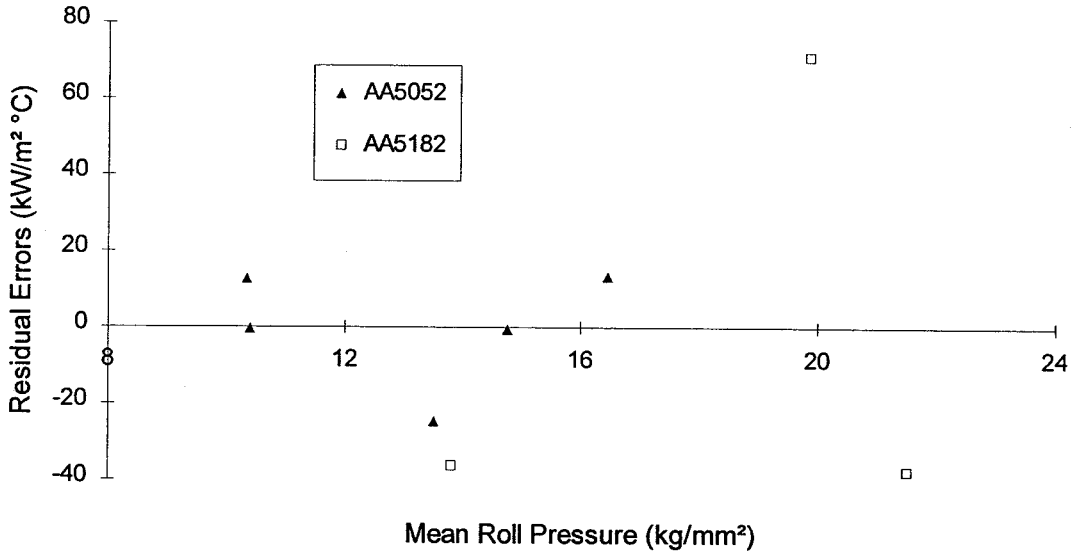

Figure 7.2. Residual errors in comparison of AA5052 vs. AA5182

The confidence interval of the difference between two means determines a range that the difference between the means of two population samples lies within at a certain level of confidence. In this case, the mean of the residuals of the AA5052 data points is zero. However, the mean of the AA5182 data points is not zero, because these data

points were not included in the regression. If the mean of the AA5182 residual errors is significantly different than zero, then it is reasonable to conclude that the roll-gap HTC is affected by alloy type. Hogg and Ledolter [58] provide an equation for the confidence interval for the difference of two means, used for situations where the variance is unknown and the sample sizes are small:

$$\mu_1 - \mu_2 \pm t\left(\frac{\alpha_c}{2}; r = n_1 + n_2 - 2\right) S_p \sqrt{\frac{1}{n_1} + \frac{1}{n_2}} \tag{7.1}$$

where μ_1 and μ_2 are the means of the two populations, n_1 and n_2 are the sizes of the two populations, t is the Student t-distribution at a confidence level α_c and having r degrees of freedom, and S_p, called the pooled variance, combines the variance estimates from the two samples in proportion to their degrees of freedom:

$$S_p = \sqrt{\frac{(n_1 - 1)S_1^2 + (n_2 - 1)S_2^2}{n_1 + n_2 - 2}} \tag{7.2}$$

where S_1 and S_2 are the variances of the two samples.

When applied to a graph of residual errors, the confidence interval of the difference of the two means establishes whether or not there is a statistically significant deviation of data values of one group from the line of regression calculated from the other data group.

Table 7.1 shows the results of the confidence interval tests at the 90 pct. confidence level that were performed on the residual errors shown in Figure 7.2. It also shows the results of the same tests for comparisons of rolling speed, lubrication type and the effect of re-rolling.

Table 7.1. Statistical Significance of Effect of Rolling Parameters on the HTC

Effect of:	Group 1	Group 2	$\mu_1-\mu_2 \pm 90\%$C.I.
Alloy type	AA5052	AA5182	0.9 ± 40.0
Re-rolling	20 pct.	10 pct.	-69.4 ± 65.5
Rolling speed	68.5 rpm	34.3 rpm	86.5 ± 79.4
Lubrication type	'A'	'B'	-52.8 ± 67.9

The results of the confidence interval test reveal that there is no statistical basis for concluding that the type of alloy has an effect on the roll-gap HTC behaviour. The difference in means between the residual errors of the HTCs of the two alloys lies well within the 90 pct. confidence interval. Another way to consider the result of the confidence interval would be to consider the set [$\mu_1-\mu_2$ - 90 pct. C.I., $\mu_1-\mu_2$ + 90 pct. C.I.], and if zero is contained in the set, there is no evidence at the 90 pct. confidence level that the means of the residual errors of the two alloy types are different.

In a similar fashion, the effect of re-rolling, roll speed and lubrication type was determined by the use of a residual error plot and the confidence interval test, and the results are shown in Table 7.1. In each case, the tests chosen for comparison were selected so that no parameter was varied except for the one being tested.

A small enhancement of the HTC behaviour of the aluminum samples rolled to 10 pct. might be expected as compared to the aluminum samples rolled to 20 pct. if surface roughness has an effect on the HTC, since the samples rolled to 10 pct. deformation had all been previously rolled. This could have had the effect of smoothening the sample surface, so that in the second (10 pct.) deformation, a greater metal-metal contact would

exist between the roll and the sample, and therefore the HTC would be increased. The confidence interval test performed on two data sets isolating the effect of re-rolling the samples on the HTC show that the mean of the residuals for the 10 pct. tests is negative (which implies that the HTCs of the 10 pct. reduction tests are higher than the 20 pct. HTCs) and lies slightly outside the confidence interval. Thus, there is some evidence to support the conclusion that the initial surface roughness has a small effect on the roll-gap HTC. However, the surface roughness of the samples or roll was not characterized in this study, so the effect can not be quantified.

The confidence interval test performed on the data comparing the tests conducted at 34.3 rpm and the tests conducted at 68.5 rpm shows that the HTCs for the 34.3 rpm tests are slightly lower than the HTCs of the 68.5 rpm tests. This effect was unexpected and is difficult to explain. It may be that, since at lower rolling speeds the Peclet number is lower, some conduction may be taking place in the rolling direction. If this were the case, the sample surface would be slightly warmed by heat transferring from the entry direction of the sample to the exit sample, thus decreasing the apparent roll-gap HTC. In this case, however, the effect is only a minor one, and the one-dimensional approach is still adequate even for the 38.3 rpm tests.

The confidence interval tests performed for the comparison of the two lubricants show that the difference of the means of the HTCs obtained using Lubricant 'A' and Lubricant 'B' lies within the 90 pct. confidence interval. Thus, there is no evidence to indicate that the use of Lubricant 'B', the less-viscous lubricant of the two, enhances the roll-gap HTC. This corroborates the findings of at least two other studies. Chen *et al.* [3] concluded that, for the hot rolling of aluminum, the roll-gap HTC was independent of the presence or absence of lubrication. Furthermore, Williamson and Hunt [57] presented

evidence that the trapping of lubrication does not affect asperity behaviour, which in turn implies that the presence of a lubricant should have no effect on the contact HTC.

7.2 Friction in the Roll Bite

Even though the validity of the use of a constant coefficient of friction throughout the roll bite has been questioned (see Section 2.1.1), it is a simple way to include the effect of friction in the roll bite and easy to incorporate into the heat-transfer model. The coefficient of friction can be calculated by a variety of methods, but for the present study the following equation (from Schey [59]) is useful:

$$\mu \geq \sqrt{\frac{\Delta H}{R_0}} \tag{7.3}$$

where μ is the coefficient of friction, ΔH is the draft and R_0 is the roll radius. From the fact that 20 pct. reductions were achieved in this study with 8.7 mm thick specimens, it follows that the coefficient of friction was at least 0.19. A value somewhat higher than this, 0.3, was assigned to the model for all tests. This value is also the same that was used by Chen *et al.* [42].

In order to evaluate the effect this assumption had on the calculated HTC, the coefficient of friction was varied for two aluminum tests, AL15 and AL37. Table 7.1 shows the sensitivity of the calculated HTC on the coefficient of friction.

Table 7.2. Effect of Friction on the HTC

Friction Coefficient	HTC (kW/m² °C) Test AL15	Test AL37
0.1	230	429
0.3	231	429
0.5	231	429

It is evident, upon examination of Table 7.2, that the choice of the coefficient of friction has an insignificant effect on the calculated HTC. It is possible that, whenever HTCs are very high, such as in aluminum and copper rolling, the quench of the surface of the material being rolled is so severe that the heat flux at the interface generated due to friction is insignificant as compared to the heat flux at the interface that is due to the high HTC.

7.3 Comparison of the Roll-Gap HTC with Earlier Values for Aluminum Rolling

Previous estimates of the roll-gap HTC for aluminum rolling are an order of magnitude less than the values determined in this study. One of the deficiencies of the previous works has been the lack of consideration paid to the roll-gap HTC as a function of the rolling pressure. This may help explain why figures reported for laboratory rolling experiments have usually been an order of magnitude less than those reported for actual mill conditions. For example, Lenard and Pietzryck [6] reported values of 4.8 W/m² °C for the hot rolling of steel on a laboratory scale rolling mill at a rolling speed of only 4.0 rpm. These workers went on to point out that successful modelling of temperature profiles of steel strip rolled on production mills requires the use of a HTC in the range of 23.3 to 81.0 kW/m² °C. These researchers did not attempt to explain the discrepancy

between the laboratory- and production-scale HTCs. However, it is probable that the pressures experienced by the steel strip under production conditions are much greater than under laboratory scale predictions. This would result in a larger true area of contact between the roll and steel strip under production conditions, and hence a higher HTC.

Another defiency of previous work has been the lack of consideration paid to the experimental setup. Chen *et al.* [3] reported roll-gap HTCs of between 10 and 60 kW/m^2 °C. These workers observed the HTC to continually increase almost linearly in the roll gap to a maximum at the exit point. A comparison of three different reductions revealed no change in the magnitude of the HTC. It is believed that the results by these workers are consistent with temperatures measured by thermocouples with response times that are slow compared to the time the samples spent in the roll gap. These workers reported using 1.0 mm diameter intrinsic surface thermocouples in their study; it is believed that this type of thermocouple would not have a sufficient response time. If this were the case, then as long as the actual decrease in temperature at the sample surface as it entered the roll bite was quicker than the response time of the thermocouples, the thermocouples would continually cool throughout the roll bite in an attempt to 'catch up' with the actual sample surface temperature. Therefore, no effect of pressure on the HTC would be observed, because the thermocouples would already be cooling at their maximum rates.

In the Appendix an equation (Equation A.9) has been developed that, given the measured bulk temperature of an aluminum sample before and after rolling, calculates a 'minimum value' HTC. By assuming that the roll and sample surface temperatures remain fixed while in the roll gap, Equation (A.9) calculates the lowest theoretically possible roll-gap HTC that can account for the temperature drop of the sample due to heat loss to the rolls. When Equation (A.9) is applied to data from this study, it calculates minimum value HTCs that are on the order of one-fifth to one-eighth the HTCs calculated

by the finite-difference model (see Appendix for a sample calculation). In other words, Equation (A.9) has been found to calculate roll-gap HTCs that are five to eight times lower than the true HTCs measured in this study. The reason for the discrepancy between the values calculated by the finite-difference model and Equation (A.9) is that the difference in the roll and sample temperatures in the roll gap does not remain at its initial value, but decreases continuously as the roll surface heats up and the sample surface cools. Thus, given a specific heat flux, the calculated HTC increases in order to compensate for the lower driving force for the flow of heat.

In a rolling test of AA5083 Timothy *et al.* [5] reported a HTC of 15 kW/m² °C. In comparison, the minimum HTC as calculated by Equation (A.9) using the data provided by these workers is 14.2 kW/m² °C. The similarity of the estimate provided by Timothy *et al.* [5] and the lowest possible HTC suggests that the estimate by these workers is much too low.

Pietrzyk and Lenard [6] reported HTCs between 18.5 and 21.5 kW/m² °C in warm rolling of commercial pure aluminum. The HTC as calculated by Equation (A.9), on the other hand, is 18.4 kW/m² °C (see Appendix for sample calculation). Again, the fact that the roll-gap HTC reported by these workers is similar to the minimum HTC suggests that the value reported is too low. Since the calculation by Pietrzyk and Lenard of the roll-gap HTC was performed using Equation (2.1), which is an equation similar in form to Equation (A.9), and the HTC calculated by Pietrzyk and Lenard [6] and by Equation (A.9) are very similar, the possibility arises that these workers, due to the slow response time of their surface thermocouple [36], overestimated the value for $\Delta T_{r\text{-}s}$, the average difference in temperature between the roll and sample surface in the roll bite. If this were the case, then their value for $\Delta T_{r\text{-}s}$ would be similar to the term T_s - T_r used in Equation

(A.9), and they would in fact have calculated a value close to the minimum-value solution.

7.4 Generalized Correlation for the HTC

The theoretical treatments of the dependence of the HTC on contact pressure discussed in Chapter 2 have two major flaws that have to be overcome before any successful application of the theoretical equations to rolling. First of all, the equations have generally been validated for low apparent pressure-to-microhardness (P_a/H) ratios (0.01 to 0.1) -- their applicability to high (P_a/H) ratios that occur in bulk forming processes such as hot rolling (0.2 - 0.3 and perhaps higher) has not been proven. Secondly, the fact that a material's surface microhardness is temperature-dependent, and therefore is dependent on the HTC, has not been taken into account. Thus, an explicit formulation of the HTC is not possible.

7.4.1 Underlying Assumptions

7.4.1.1 Dependence of the HTC on Pressure and Surface Hardness

In developing an equation for the prediction of the HTC in rolling, the following line of reasoning was taken. Firstly, both surfaces, that of the roll and of the workpiece, have an initial surface roughness profile. For any commercial rolling operation, the roughness of the workpiece can be assumed to be greater than the roughness of the roll; therefore, the workpiece surface becomes smoother as a result of the rolling operation. Some evidence of this phenomenon has been presented by Chen [21]. It is a difficult matter, then, to incorporate the roughness of the workpiece as part of a HTC-prediction equation because the workpiece profile changes significantly throughout the roll bite.

Therefore, it was chosen to include surface roughness parameters of the workpiece into the HTC-prediction equation as a general constant.

Secondly, when the hot workpiece first comes into contact with the roll, as metal-metal contact is established at the asperity tips, there is an immediate quench of the workpiece surface. The greater the extent of metal-metal contact, the higher the resulting HTC and the quicker the quench. However, the lowering of the workpiece surface temperature leads to hardening of the workpiece asperities. The plastic deformation of asperities effectively ceases when the material surface becomes hard enough and metal-metal contact extensive enough that the true pressure acting on the surface of the workpiece -- the roll force divided by the true area of metal-metal contact -- becomes equal to the surface flow stress of the workpiece material. Therefore, the HTC is dependent not only on the pressure being applied to the two surfaces in contact, but also on the surface hardness of the material.

7.4.1.2 The Dependence of the HTC on the Conductivity of the Workpiece and Tool

Conductivity must also be a factor in determining the behaviour of the roll-gap HTC. The thermal conductivity affects the HTC in two ways. Firstly, it plays a role in determining the temperature-dependent yield stress of the asperities. At an applied apparent pressure, the higher the conductivity of the sample, the quicker the heat extracted from the sample surface is replaced from the sample interior. Therefore, the surface temperature of the sample quenches slower than if the sample had a lower conductivity. The HTC thus tends to increase, since because the surface temperature of the sample remains higher, the surface of the sample stays softer. Thus, the surface asperities would deform more at an applied pressure, and therefore, the HTC would be expected to be enhanced with increased sample conductivities.

Secondly, at the points of direct metal-metal contact between two materials, the conductivity of each material determines the relative flow of heat from one material to the other. Therefore, the HTC is expected to be proportional to an effective conductivity, which is a function of the conductivities of the two materials, at the points of contact between the surfaces of the two materials. Superficially, it might seem that the effective conductivity, k_{eff}, might be expressed as the sum of the conductivities of the two contacting materials, as shown in Equation (7.4a). However, a more appropriate parameter is the 'harmonic' conductivity of the two materials, which is the inverse of the sum of the inverses of the conductivities of both materials, as shown in Equation (7.4b).

$$k_{\text{eff}} = k_1 + k_2 \tag{7.4a}$$

$$\frac{1}{k_{\text{eff}}} = \frac{1}{k_1} + \frac{1}{k_2} \tag{7.4b}$$

A full proof of the applicability of Equation (7.4b) in an HTC-prediction equation is provided by Cooper *et al.* [13]; however, the reason why the harmonic thermal conductivity and not the average thermal conductivity should be included in the HTC-prediction equation can be demonstrated with the aid of Figure 7.3.

Figure 7.3 shows the temperature profile between two materials of differing thermal conductivities, $k_1 > k_2$, in direct contact with each other at the meeting point of two opposing asperites. Since at the contact plane of the two asperities there is no interfacial gap between Material 1 and Material 2, the temperatures of the two materials at the contact plane are the same, T_0. The term ΔT_c is the macroscopic difference in temperature between the surface temperatures of Material 1 and Material 2, and ΔT_1 and

ΔT_2 are the components of ΔT_c due to the conductivity of Material 1 and Material 2, respectively. Because Material 1 has a higher conductivity than Material 2, ΔT_1 is less than ΔT_2.

Now, two limiting cases can be examined; firstly, the case where k_1 approaches infinity, and secondly, the case where k_2 approaches zero. In the first case, as k_1 approaches infinity, ΔT_1 approaches zero. The macroscopic-temperature gap ΔT_c, and by inference, the HTC, is then entirely a function of the conductivity of Material 2, k_2. The effective thermal conductivity, k_{eff}, is then equal to k_2, as calculated correctly by Equation (7.4b); whereas in Equation (7.4a), k_{eff} is calculated to be infinity. In the second case, as k_2 approaches zero, the plane of contact becomes an insulated boundary, and the temperature gradient becomes zero at the plane of contact. Since there is no temperature gradient, there is no flow of heat across the plane of contact and the effective conductivity becomes zero. Again, Equation (7.4b) calculates this result correctly, whereas Equation (7.4) calculates k_{eff} to be equal to k_1.

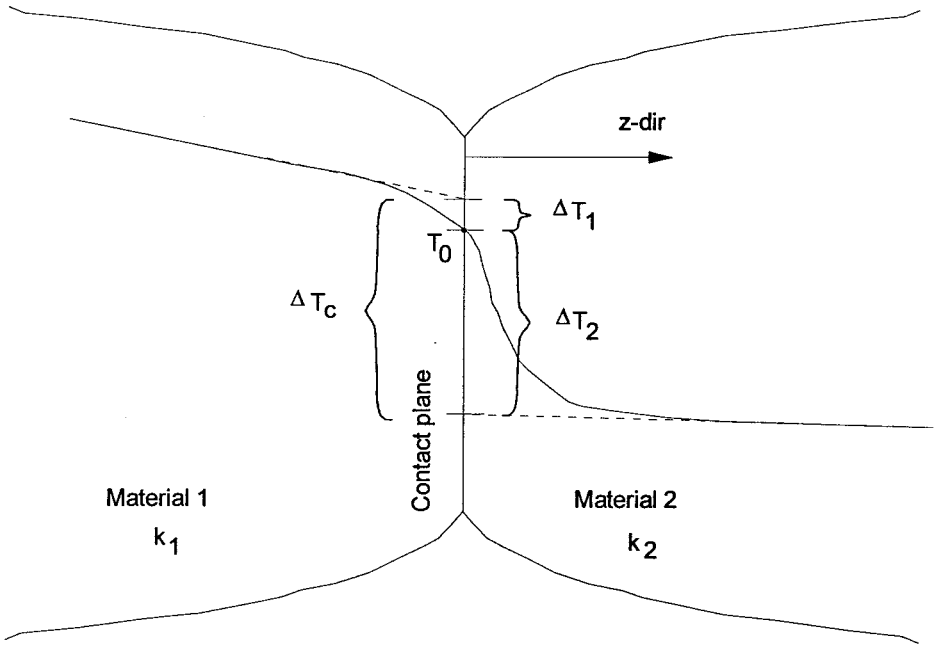

Figure 7.3. Temperature gradients between two asperities in contact

7.4.2 Quantification of the Dependence of the HTC on Pressure and Conductivity

7.4.2.1 Formulation of the General Equation

Reflecting this approach, an equation of the general form, patterned after Cooper *et al.* [13], is formulated as:

$$h = Ck\left(\frac{1}{1-A_c}-1\right)^n \tag{7.5}$$

where C is a general constant that replaces the surface roughness terms that are found in the equation of Cooper *et al.* [13]. The term k is defined as

$$k = \frac{k_t k_{wp}}{k_t + k_{wp}} \tag{7.6}$$

which is similar in form to Equation (2.5) and is equivalent to Equation (7.4b). Finally, the term $\left(\frac{1}{1-A_c}-1\right)^n$ characterizes a family of equations that approaches 0 as A_c (the real contact area = A_r/A_a) approaches 0, and approaches infinity as A_c approaches 1.

Employing the relation of contact area to normal load proposed by Pullen and Williamson [56] (shown in a slightly different form than in Equation (2.2)),

$$A_c = \frac{P_a}{H + P_a} \tag{7.7}$$

where P_a is the apparent pressure (the force acting over the total area), and substituting this relation into Equation (7.5) yields

$$h = Ck\left(\frac{P_a}{H}\right)^n \tag{7.8}$$

where C is a general constant with units m^{-1}. The roll-gap HTC is now characterized as a function of the applied pressure and the surface hardness of the material being deformed. Equation (7.8) is, in effect, a generalized version of the equation proposed by Cooper *et al.* [13]. In local indentation tests, it has been found that full plastic deformation at the surface occurs when the applied pressure is approximately three times the yield stress [17, 57]. Therefore, the surface hardness H is calculated as:

$$H = 3Y_0 \tag{7.9}$$

where Y_0 is the bulk yield stress of the material being deformed. By incorporating the temperature-strain rate dependent nature of the yield stress at the sample surface,

$$Y_0 = \sigma\left(T_{\text{surface}}, \dot{\varepsilon}\right) \tag{7.10}$$

and substituting Equation (7.9) and (7.10) into Equation (7.8), the following equation is obtained:

$$h = Ck\left(\frac{P_a}{3\sigma\left(T_{\text{surface}}, \dot{\varepsilon}\right)}\right)^n \tag{7.11}$$

Equation (7.11) is inherently an implicit equation, because the roll-gap HTC is characterized as a function of the surface temperature of the workpiece, which in turn is dependent on the HTC.

7.4.2.2 Modification of the Equation for Rolling Conditions

Equation (7.11) describes the relationship between the HTC and apparent pressure between two surfaces in metal-metal contact. However, this surface hardness-yield stress relation has not been verified for the case of rolling. In addition, Equation (7.8) contains the general constant, C, which replaces any surface roughness parameters and can also take into account any constant multiple of the yield stress; in this case the sample hardness is simply taken to be the flow stress at the sample surface:

$$H = \sigma\left(T_{\text{surface}}, \dot{\varepsilon}\right) \tag{7.12}$$

where σ is the flow stress in free tension, T_{surface} is the surface temperature of the sample, and $\dot{\varepsilon}$ is the strain rate at the sample surface.

In the case of hot rolling, because of the large temperature gradient that exists between the surface of the sample and the sample interior while the sample is in the roll bite, the strain rate at the sample surface is not accurately known. Therefore, a mean strain rate, $\bar{\dot{\varepsilon}}$, is used:

$$\bar{\dot{\varepsilon}} = \frac{\bar{\varepsilon}}{t_c} \tag{7.13}$$

where t_c is the contact time and $\bar{\varepsilon}$, the mean strain of the sample caused by the rolling operation, is defined as:

$$\bar{\varepsilon} = \frac{2}{\sqrt{3}} \ln\left(\frac{H_i}{H_f}\right) \tag{7.14}$$

where H_i and H_f are the entry and exit thicknesses of the sample, respectively.

By substituting Equation (7.12) into Equation (7.8), and Equation (7.14) and (7.13) into (7.12), Equation (7.11) is thus modified for the rolling case:

$$h = Ck\left(\frac{P_r}{\sigma\left(T_{surface}, \bar{\dot{\varepsilon}}\right)}\right)^n \tag{7.15}$$

where P_r is defined in Equation (6.2).

7.4.3 Numerical Solving Technique

The program that was used to calculate the HTC in the roll gap based on the sample surface temperature was modified to predict the roll-gap HTC, employing an iterative technique, as shown in Figure 7.4.

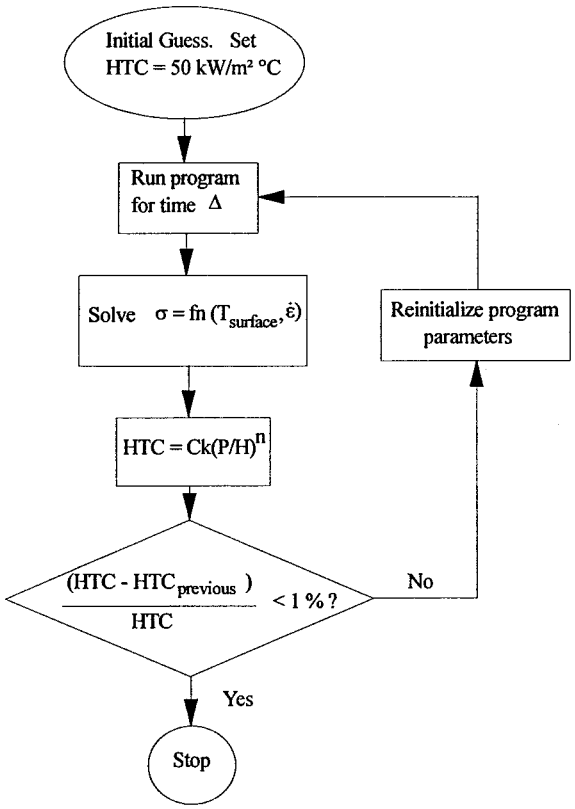

Figure 7.4. Flowchart of algorithm used to predict the roll-gap HTC

In order to determine values for the equation parameters C and n, the equation was fit to the experimental data obtained by Chen [21] for stainless steel rolling tests. There were two reasons that the stainless steel data, rather than the data for aluminum alloy obtained in the present study, were used. Firstly, the data from Chen [21] exhibits less scatter than the data obtained in this study. Therefore, the coefficients for the equation could be determined from the stainless steel data with more precision. Secondly, the pressure range was greater in the study by Chen [21] than in the present study. Thus, fitting the equation parameters to the stainless steel data enables the equation to be applied to the aluminum and copper rolling experiments in this study without need for extrapolation.

7.5 Prediction of Roll-Gap HTCs Using the Developed Equation

It was found that for $\Delta = 0.015$ seconds, $C = 15\ 800\ m^{-1}$ and $n = 1.4$, Equation (7.15) provided predictions of the HTC that fitted the line of regression through the observed steel rolling data. Using the same parameters, the equation was then applied to selected aluminum rolling tests and to all the copper rolling tests. Figure 7.5 shows that the roll-gap HTCs predicted by Equation (7.15) for aluminum hot rolling lie in the midrange of the experimental data, while the predicted HTCs for copper rolling lie at the upper range of the experimental data.

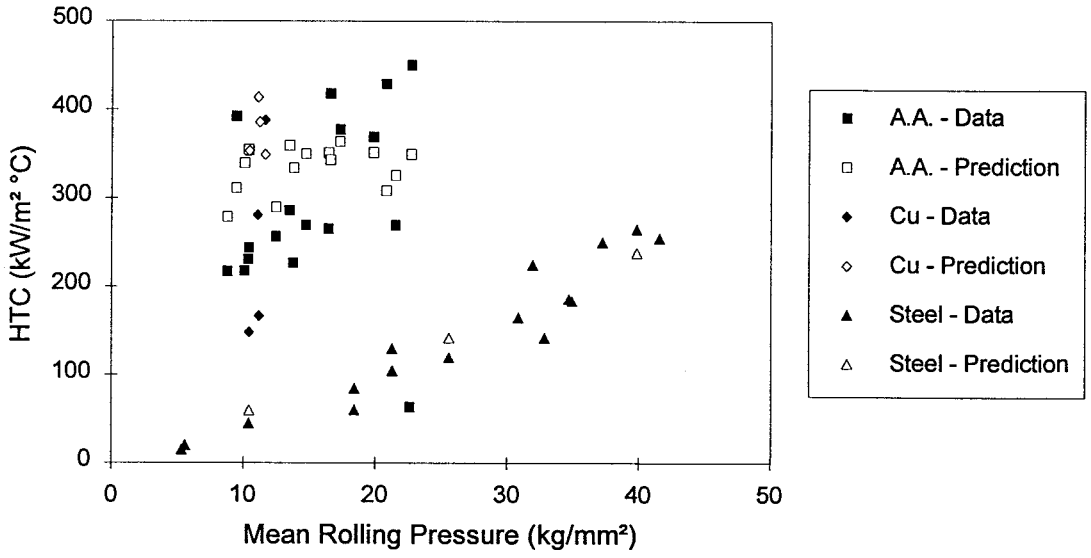

Figure 7.5. Comparison of experimental and predicted HTCs

7.5.1 Suitability of Conductivity and *n* as Equation Parameters

Even though all the HTC-prediction equations in the literature include thermal conductivity as a parameter [13, 15, 16, 17, 20], one might expect the thermal diffusivity

to be a more appropriate parameter to include because of the transient nature of the problem. However, the flow of heat is only transient at the macroscopic level.

Upon examining only two asperities in contact with each other (referring once again to Figure 7.3 where Material 1 is the sample material and Material 2 is the roll material), there is no resistance to heat flow from one asperity to the other at the plane of contact between the two asperities. When the two asperities first contact each other, immediately the temperature at the plane of contact becomes T_0, which is determined by (from [60])

$$T_0 = T_{s,init} - (T_{r,init} - T_{s,init}) \frac{\rho_s C_{ps}}{\rho_s C_{ps} + \rho_r C_{pr}} \tag{7.16}$$

where $T_{r,init}$ and $T_{s,init}$ are the initial temperatures of the roll and sample, respectively, ρ_r and ρ_s are the densities of the roll and sample, respectively, and C_{pr} and C_{ps} are the specific heats of the roll and sample, respectively.

Treating each asperity as a control volume, and assuming that for the short contact time T_0 remains constant and the interior temperatures of the roll and sample remain largely unaffected, any inflow of heat into an asperity through the contact plane must be balanced by a corresponding outflow (and vice-versa). Therefore, considering each asperity contact plane individually, the heat flow from a sample asperity to a roll asperity is a steady-state and not a transient event. The mathematical problem is then described by the general equation

$$\nabla^2 T = 0 \tag{7.17}$$

or, considering heat flow to be one-dimensional only, and defining the z-direction as perpendicular to the contact plane, with z=0 at the contact plane,

$$\frac{\partial}{\partial z}\left(k\frac{\partial T}{\partial z}\right)=\rho C_p\frac{\partial T}{\partial t}=0 \tag{7.18}$$

It can be seen that, since the right-hand side of Equation (7.18) is equal to zero, the thermal conductivity, and not the thermal diffusivity, becomes the relevant thermophysical material property.

In order to verify experimentally the validity of the preceeding argument, the predictive ability of Equation (7.15) was compared with that of two modified equations,

$$h=C\alpha_{\text{eff}}\left(\frac{P_r}{H}\right)^n \tag{7.19a}$$

and

$$h=C\left(\frac{P_r}{H}\right)^n \tag{7.19b}$$

where H is defined in Equation (7.12), and α_{eff} is defined as

$$\frac{1}{\alpha_{\text{eff}}}=\frac{1}{\alpha_r}+\frac{1}{\alpha_s} \tag{7.20}$$

to determine whether the thermal conductivities or the thermal diffusivities of the roll and sample were more appropriate equation parameters, or if a parameter involving material thermal properties was required at all.

Each equation had the parameter C adjusted to predict the HTC values for stainless steel rolling tests, as determined by Chen [21]. Table 7.3 shows the resulting value of C for each equation.

Table 7.3. Value of C for Equation 7.15, 7.19a and 7.19b

Equation	Value of C
$h = Ck(P_r/H)^{1.4}$	15 800 (m^{-1})
$h = C\alpha_{eff}(P_r/H)^{1.4}$	$9.7x10^{10}$ (J/m^4 °C)
$h = C(P_r/H)^{1.4}$	$2.54x10^5$ (W/m^2 °C)

The equations were then applied to predict the HTC for aluminum and copper rolling tests. Figure 7.6 shows that the equation using α_{eff} as the relevant material thermal property (Equation 7.19a), overpredicts the HTC for aluminum rolling, while the equation that doesn't incorporate any thermal property parameter (Equation (7.19b)), underpredicts the HTC for aluminum rolling. This provides experimental confirmation that the harmonic conductivity is a more appropriate parameter to include in Equation (7.8) than the thermal diffusivity.

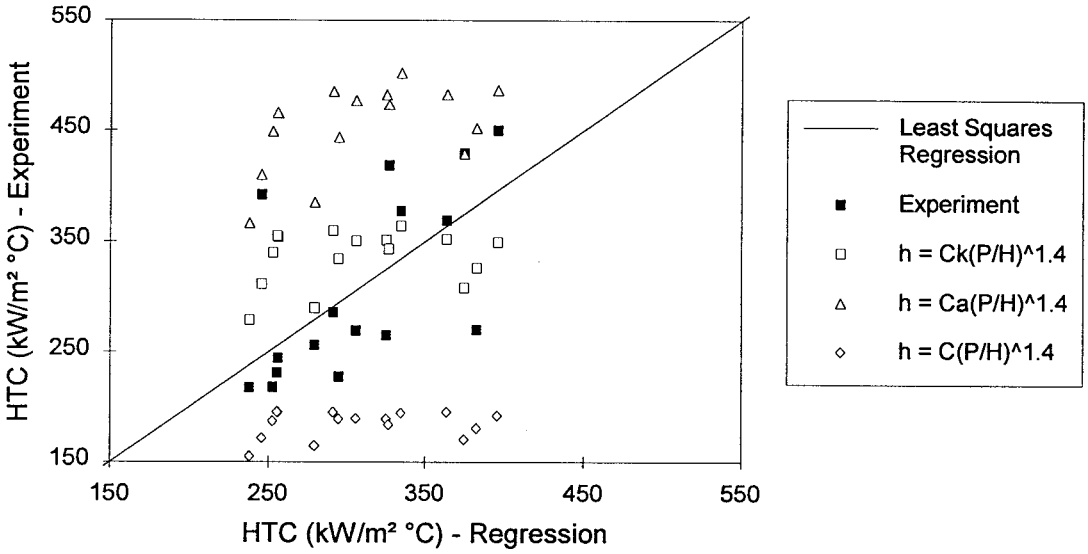

Figure 7.6. Comparison of predictive capabilities of Eq. 7.15, 7.19a and 7.19b

Figure 7.7 presents the logarithm of the HTC-harmonic conductivity ratio plotted against the logarithm of the rolling pressure-surface flow stress ratio. The dotted line represents the relationship between the HTC-harmonic conductivity and pressure-surface hardness ratios as characterized in Equation (7.15), using n=1.4 and C=15 800 m^{-1}. The solid line represents the line of best fit through the data, and the shaded lines represent the +/- 95 pct. confidence intervals for the line of best fit. The slope of the line of best fit through the data is 0.92, which is close to the values for n proposed by other investigators [13, 20, 21]. However, due to the scatter of the data, at the 95 pct. confidence level the true slope of the regressed line (and therefore the value of n) lies somewhere between 0.44 to 1.4. The value used for n in this study, 1.4, thus lies on the extreme edge of the confidence interval of the data.

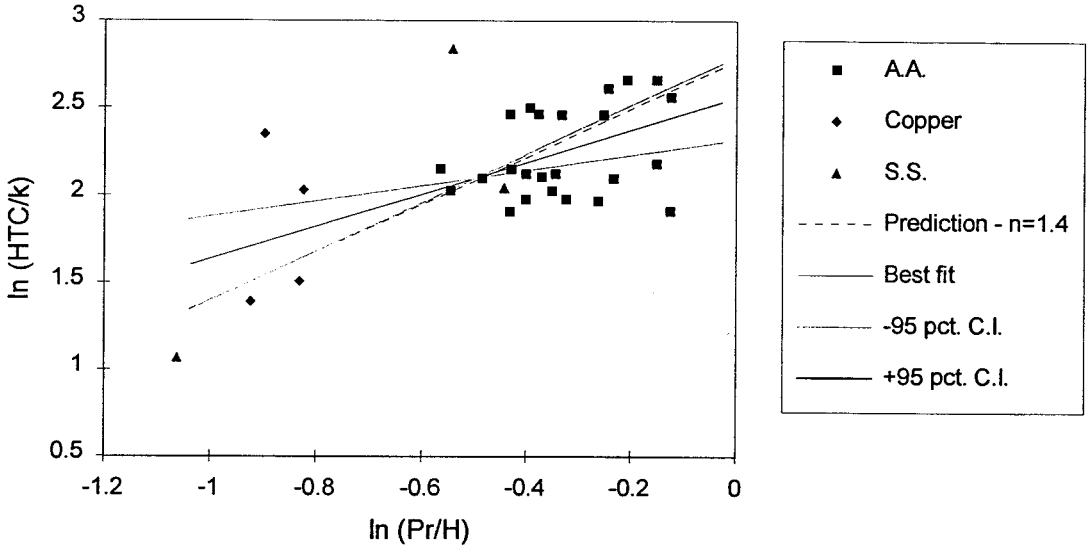

Figure 7.7. Check of applicability of Equation 7.15

7.5.2 Effect of Δ on Equation Parameters

A difficulty in using Equation (7.15) involves the choice of Δ, the length of time in the roll bite, to use as the point at which the workpiece surface flow stress is calculated from the surface temperature. Obviously, as Δ is changed, the surface temperature of the workpiece changes as well. This leads to the conclusion that the parameters C and n of Equation (7.15) are not unique, but rather are dependent on the choice of Δ.

To determine whether the choice of Δ affects the prediction capabilities of Equation (7.15), three different times, Δ=0.005, 0.010, and 0.015 seconds were chosen for comparison. Table 7.4 shows the values of the parameters C and n for the different values of Δ. It was found that the choice of Δ changes the values of C and n necessary to calibrate the equation to predict the HTC values for the stainless steel data.

Table 7.4. Effect of Δ on Parameters of Equation (7.15)

Δ (s)	C (m^{-1})	n
0.005	24 500	2.2
0.010	19 600	1.7
0.015	15 800	1.4

Even though n appears to decrease as Δ increases, its value at Δ=0.015 s is still significantly higher than the values proposed by Cooper *et al.* [13] (0.985), Song and Yovanovich [20] (0.97) or Chen [21] (1.0). Equations (7.15) was then applied to predicting the HTC for the aluminum rolling tests using the three different values of Δ, C and n shown in Table 7.4; the results are presented in Figure 7.8. In addition, the comparison of the mean of the residual errors of the predicted HTCs versus the regression through the experimental data (the same technique as developed in Section 7.1) is presented and compared to the 95 pct. confidence interval of the experimental data in Table 7.5. It can be seen that only the roll-gap HTCs calculated using the equation parameters Δ=0.015 s, n=1.4 and C=15 800 m^{-1} adequately predict the experimental HTCs of the aluminum rolling tests.

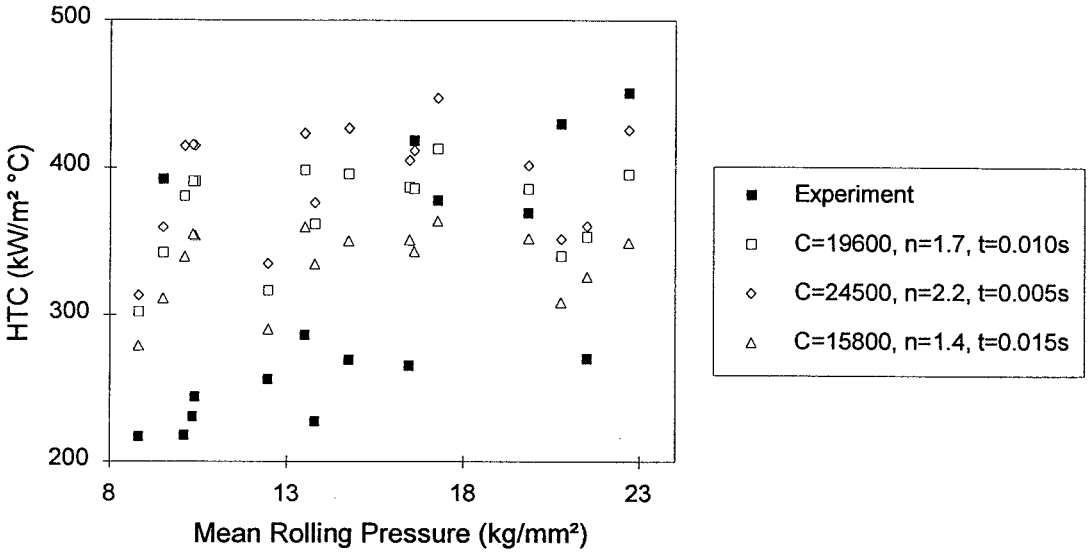

Figure 7.8. Effect of Δ on predictive capability of Equation 7.15

Table 7.5. Statistical Effect of Δ on Predictive Capability of Equation 7.15

Equation Parameters			$\mu_{predict.}$-$\mu_{exp.}$ ± 95%C.I.
Δ (s)	n	C (m^{-1})	
0.05	2.2	24 500	85.0 ± 35.6
0.10	1.7	19 600	63.5 ± 35.6
0.15	1.4	15 800	27.9 ± 35.6

7.5.3 Significance of the General Constant *C* in the HTC-Prediction Equation

Equation (7.8) may also be expressed in a dimensionless form:

$$\frac{hC'}{k} = \left(\frac{P_a}{H}\right)^n \tag{7.21}$$

where C' is equal to C^{-1}, and therefore has units of length (m). The left-hand side of Equation (7.21) has the same form as both the Nusselt and Biot numbers. However, the Nusselt number is usually defined as the ratio of convection heat transfer to fluid convection heat transfer; C' refers to a fluid layer width and k is the conductivity of the fluid [52]. This definition of the left-hand side of Equation (7.21) is clearly inappropriate. Instead, considering it as a form of Biot number may be more suitable. The term k would then be the conductivity of the solid, and C' would refer to a characteristic length, in this case a roughness parameter.

Therefore, by utilizing Equation (7.15) to predict roll-gap HTCs for aluminum and copper rolling tests, employing the value of C developed from steel rolling data, the implicit assumption involved is that the initial roughness parameters of the samples of the different rolling materials are the same, or unimportant. However, it is been established that there is statistical evidence that re-rolling enhances the roll-gap HTC (see Table 7.1) in the hot rolling of the aluminum samples. Figure 7.9 shows the logarithm of the HTC-harmonic conductivity ratio plotted against the logarithm of the rolling pressure-surface hardness ratio for the aluminum tests, comparing the roll-gap HTCs measured from the first and second passes. By once again employing the statistical technique developed in Section 7.1, and taking a regression line through the first pass (20 pct. reduction) data and comparing the means of the residual errors of the first pass and second pass data, it was found that the 95 pct. confidence interval of the difference of the means of the residual errors of the first and second pass data is 0.166, whereas the mean of the residuals errors of the second pass is 0.239. Therefore, the difference of the means of the residual errors was within the interval 0.239 +/- 0.166 at the 95 pct. confidence level. Since zero is not part of the interval, this suggests that because of the first rolling pass, the surfaces of the

aluminum samples were smoothened, causing the roll-gap HTCs to be enhanced during the second pass. This HTC-enhancement can be characterized in Equation (7.8) and (7.15) by employing a larger value of C, or in Equation (7.21) by employing a lower value of C', which implies a connection between the general parameter C or C' and the initial surface roughness of the sample being rolled.

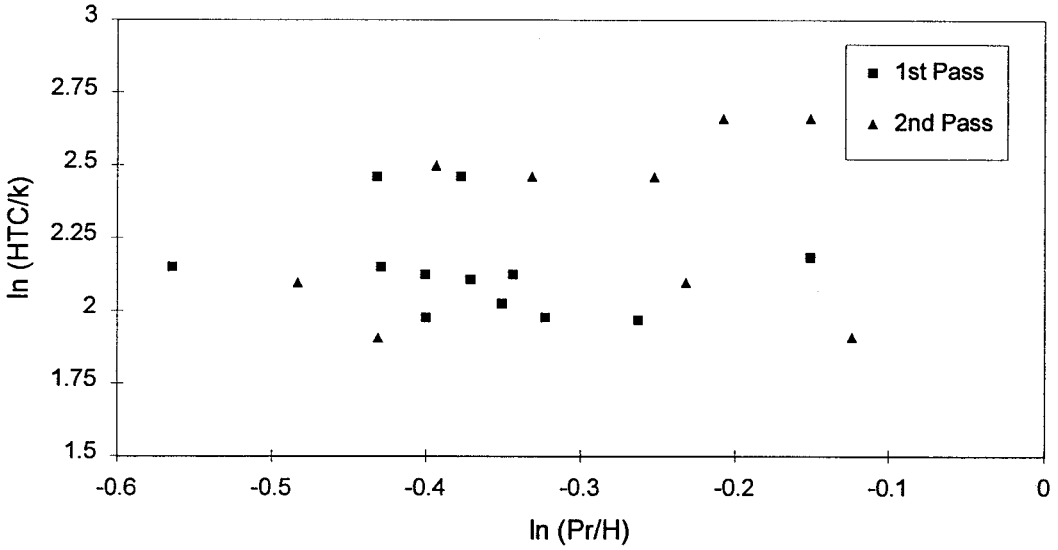

Figure 7.9. Effect of re-rolling on roll-gap HTCs

7.6 Maximum Theoretical HTC

When deforming an unsupported material, it is obvious that the applied pressure cannot exceed the yield stress of the material being deformed. Therefore, the pressure-surface flow stress ratio cannot exceed unity, and therefore a theoretical maximum roll-gap HTC is obtained:

$$h \leq Ck \tag{7.21a}$$

or, expressed in a dimensionless form,

$$\frac{hC'}{k} \leq 1 \tag{7.21b}$$

where k is calculated from Equation (7.6).

Table 7.6 shows the calculated maximum theoretical roll-gap HTC for each of the four materials studied, using the value of C (15 800 m^{-1}) developed from the data from Chen [21].

Table 7.6. Theoretical Maximum Roll-Gap HTCs

Material	k (W/m °C)	Max. HTC (kW/m² °C)
AA5052	32.3	510
AA5182	31.5	498
Copper	37.0	585
Stainless steel	15.5	245

From Figure 7.5, it is seen that none of the measured copper and aluminum roll-gap HTCs exceed the theoretical maximum HTCs shown in Table 7.6. One data point from the steel series of tests exceeds 245 kW/m² °C, but not by an amount that exceeds the error limit at that level of HTC (see next section).

7.7 Error in HTC Measurement due to Temperature Measurement Error

The scatter of data for the hot rolling of aluminum has been seen to be considerable. However, this is expected due to the magnitude of the HTCs that were measured in this study. As explained earlier (see Section 6.1), at large values of the HTC, the HTC measured from the surface thermocouple responses is highly sensitive to small fluctuations in surface temperature. Similarly, the HTC measured from the bulk sample temperatures before and after rollling also becomes increasingly sensitive to small errors in temperature measurement. As an example of the increase in uncertainty in roll-gap HTC measurement at larger HTCs, consider Figure 7.10. Using Test AL24 as a base, HTCs were calculated based on hypothetical roll-gap exit temperatures. The roll-gap entry temperature for Test AL24 was 376.7 °C, and the true roll-gap exit temperature was 338 °C. The finite-difference model calculated roll-gap HTCs based on hypothetical roll-gap exit temperatures in the range 334 °C - 370 °C.

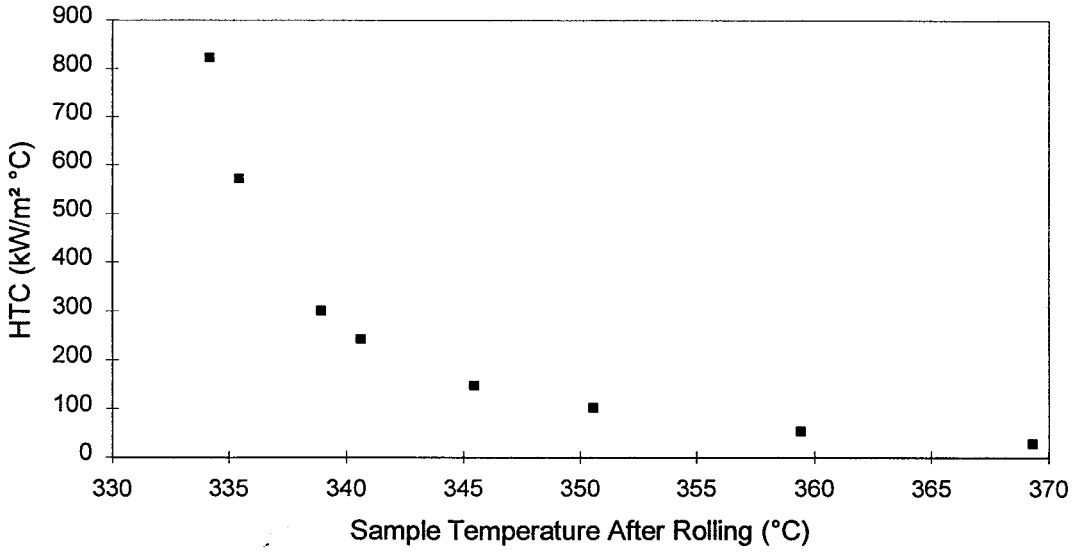

Figure 7.10. Sensitivity of the HTC to the roll-gap exit temperature

Figure 7.10 shows that the roll-gap HTC exponentially approaches infinity as the hypothetical roll-gap exit temperature decreases. From this graph, error estimates of calculated roll-gap HTC values can be established. Figure 7.11 shows the level of error expected at different levels of the calculated roll-gap HTC, assuming that the post-rolling bulk sample temperatures measured by the thermocouples were accurate to within ± 1 or 2 °C of the true sample temperatures.

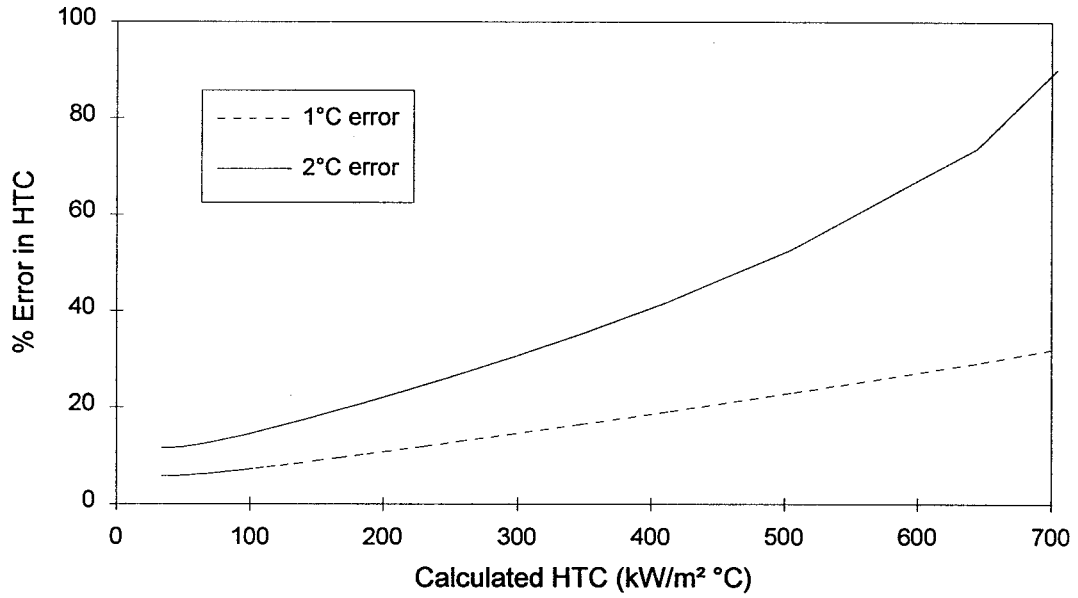

Figure 7.11. Error estimates of the HTC

Figure 7.11 shows that the order of the error increases very rapidly as the HTC approaches higher values. In the present study, HTCs in the range of 200 - 450 kW/m² °C were measured. Assuming errors of temperature measurement in the range of 1 to 2 °C, pct. errors in HTC measurement range from 10 - 20 pct. at the lower HTC level to up to 15 - 40 pct. at the upper HTC level. Due to the fact that the HTCs measured by Chen

[21] ranged from 10 - 250 kW/m² °C, the errors associated with the measured HTCs were much less, and therefore less scatter was exhibited.

However, keeping in mind that the ultimate aim of measuring the roll-gap HTC is to predict the strip temperature, the large scatter in the measured HTC is not very significant. At such large HTCs as were measured in this study, the calculated strip temperature is not very sensitive to large variations in the HTC. At larger HTCs, the resistance to heat flow due to the contact resistance at the strip-roll interface becomes only a small proportion of the total resistance to heat flow. For example, at a roll-gap HTC of 200 kW/m² °C, the resistance to heat flow due to conduction through the aluminum sample and through the roll layer, δ, is five and thirty times greater, respectively, than that due to contact resistance at the roll-sample interface. In fact, another interpretation of Figure 7.11 is considering it a graph of acceptable error in the assumed roll-gap HTC if a 1°C or 2°C error in strip temperature prediction is acceptable. Then it is easily seen that as the roll-gap HTC increases, a larger percentage error in the reported roll-gap HTC becomes acceptable.

7.8 HTC Measurement Error due to Roll Conductivity Error

Because the chief resistance to heat flow is the roll, the calculated HTC is sensitive to the choice of roll conductivity. Figure 7.12 shows the effect of changing the value for roll conductivity, as assumed by the model on the average HTC calculated from the surface thermocouple responses. By using a value for roll conductivity that is considered high by 50 pct. (62 W/m°C), the calculated HTC has dropped by a factor of approximately two, but their is no appreciable effect on the sensitivity of the HTC to roll pressure.

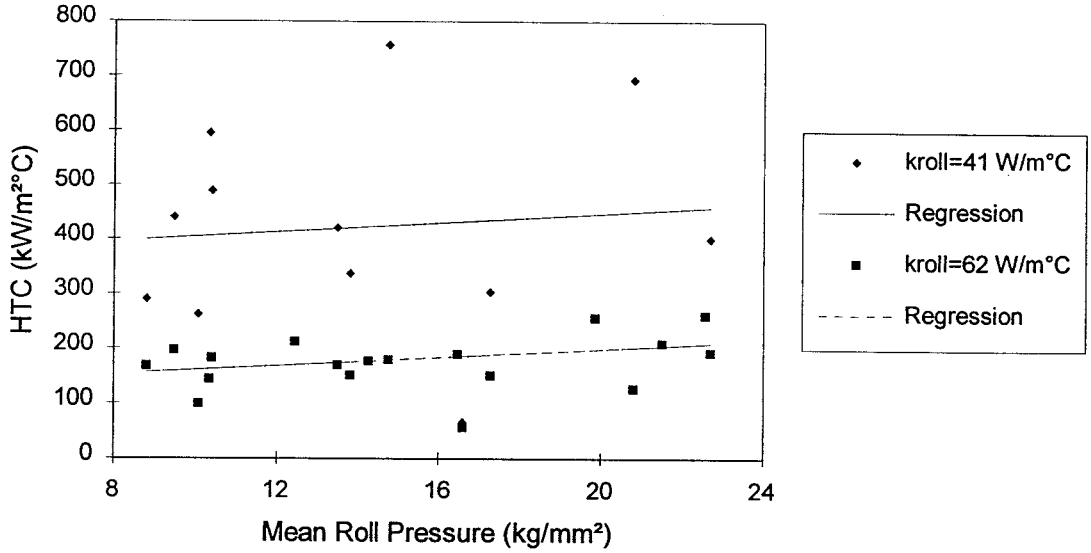

Figure 7.12. Effect of changing the model roll conductivity assumption on the calculated HTC

The reason for the decrease in calculated HTC is that, at higher roll conductivities, heat that transfers from the sample surface to the roll surface is extracted away from the roll surface into the roll interior quicker than at lower roll conductivities. Therefore, the roll surface temperature, as calculated by the model, remains cooler. Thus, the average difference in roll and sample surface temperatures throughout the roll gap remains greater, which has the effect of reducing the calculated roll-gap HTC. It is felt that, based on the conductivities for various steels with similar compositions to the roll alloy used in this study (see Section 5.4), that the roll thermal conductivity value (41.0 W/m °C) is accurate to within 2 W/m °C. Based on Figure 7.12, the corresponding effect on calculated HTC values is about 7.5 pct. Thus, the uncertainty introduced into the HTC measurement due to uncertainty in the value of roll conductivity is relatively small as compared to the error introduced into the HTC due to uncertainties in temperature measurement.

7.9 The Effect of the Heat-Transfer Coefficient on the Sample Temperature Profile in the Roll Gap

Figures 7.13 and 7.14 show the effect the HTC has on the temperature profile of the workpiece. Figure 7.13 shows the calculated temperature profile for a sample, initially at a temperature of 377°C, rolled to 20 pct. deformation with an HTC of 378 kW/m² °C. At this HTC, the sample surface cools from the initial temperature to less than 254°C within the first 10 pct. of the roll bite length and then remains at almost a constant temperature through the remainder of the roll bite. In the interior of the sample, the temperature has increased due to the heat of deformation.

Figure 7.14 shows the calculated temperature profile for a sample with an assumed HTC of 37.8 kW/m² °C, which is ten times less than the HTC assumed in Figure 7.13. As compared to Figure 7.13, the surface temperature in Figure 7.14 cools much more gradually through the length of the roll bite. Also, the interior zone of the sample, which was heated to above the initial rolling temperature due to the heat of deformation, is enlarged because of the reduced temperature gradient.

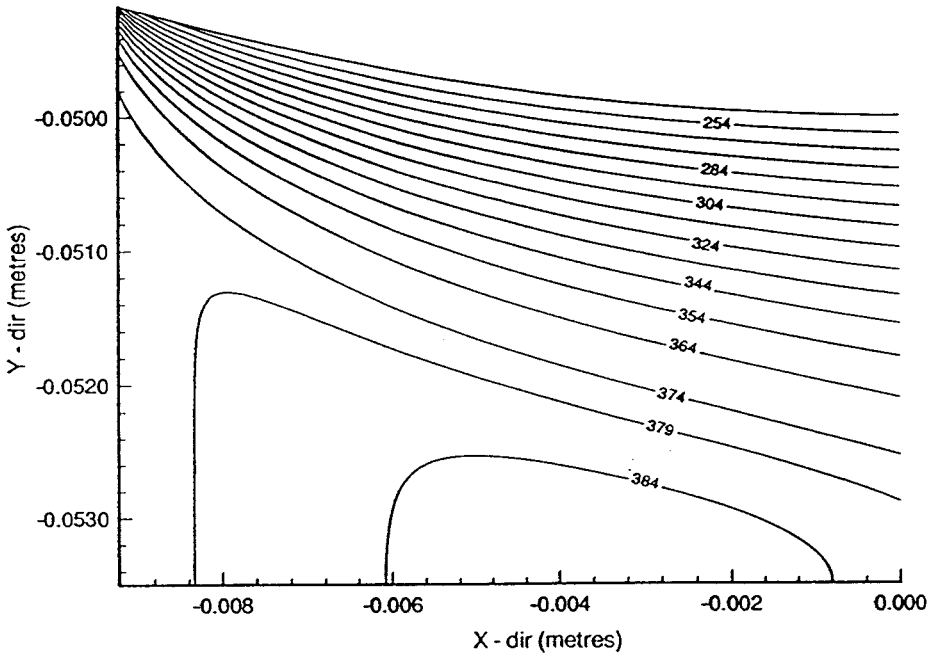

Figure 7.13. Sample temperature profile for an HTC of 378.5 kW/m² °C

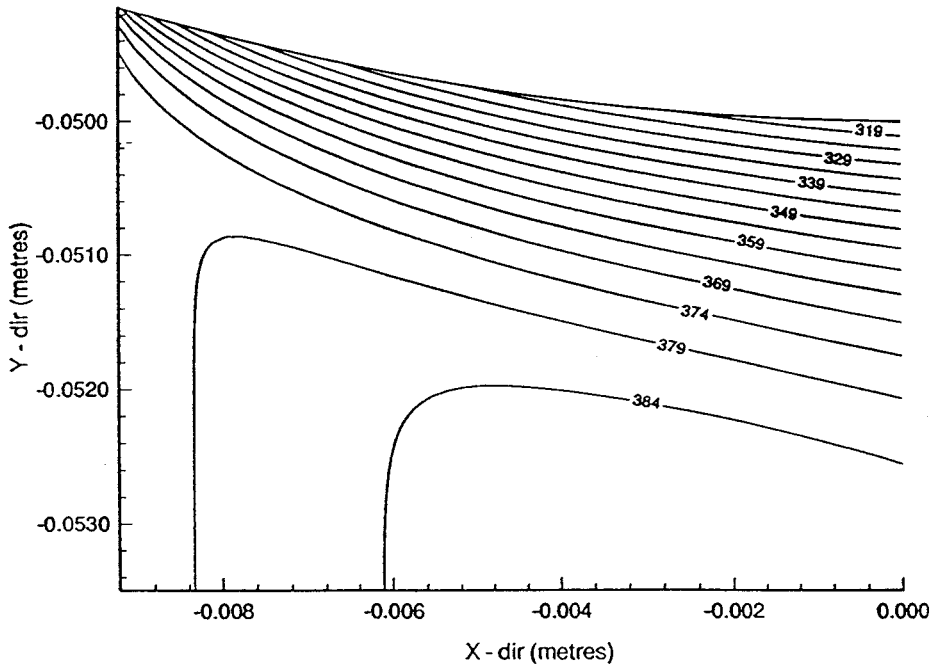

Figure 7.14. Sample temperature profile for an HTC of 37.8 kW/m² °C

CHAPTER 8

SUMMARY AND CONCLUSION

8.1 Summary of Results

The roll-gap HTC has been found to be a function of the harmonic conductivity of the roll and the material being rolled, the ratio of the mean rolling pressure to the surface flow stress being rolled, and the surface roughness. This equation is expressed in the form

$$h = Ck\left(\frac{P_r}{\sigma\left(T_{surface}, \bar{\dot{\varepsilon}}\right)}\right)^n \tag{8.1}$$

where C is a parameter probably related to initial surface roughness, k is the harmonic conductivity of the roll and sample, P_r is the applied roll pressure acting on a sample and $\sigma\left(T_{surface}, \bar{\dot{\varepsilon}}\right)$ is the flow stress of a sample at the roll-sample interface. The physical mechanism relating the dependence of the HTC to rolling pressure is the deformation of asperities at the workpiece surface. As pressure increases, the asperities of the workpiece deform, thus increasing direct metal-metal contact at the interface of the roll and workpiece. Since the main flow of heat from the workpiece to the roll is through the

points of metal-metal contact, as the area of metal-metal contact increases, contact resistance to heat flow decreases and the HTC increases.

The roll-gap HTC of samples which had been previously rolled has been shown to be higher than samples which had not been previously rolled. This is possibly due to the surface of the samples being smoothened by the first pass through the rolling mill, thus increasing metal-metal contact between the sample and roll during the second pass.

Furthermore, it was found that the choice of lubricant did not have a statistically observable effect on the behaviour of the roll-gap HTC. In addition, the HTCs calculated from the bulk temperature of the samples before and after rolling proved superior to those calculated from the surface thermocouple responses, because the scatter of the data was reduced.

The HTCs obtained in this study are about an order of magnitude greater than those reported in previous studies of aluminum rolling. The usefulness of the earlier studies has been limited because of inadequate consideration of measurement techniques, faulty methods of analysis, and difficulties in translating laboratory test results to an industrial scale due to a lack of understanding of the importance of rolling pressure in characterizing the HTC.

8.2 Recommendations for Further Study

The attempt to relate the roll-gap HTC to rolling and material parameters has been hampered by the large amount of scatter in the measured data. It has been shown that the scatter in the measured HTCs is due, to a large extent, to the magnitude of the HTC. Therefore, a further series of rolling experiments involving lower HTCs would lessen the errors involved in the measurement of the HTC, thus allowing for a more precise comparison of experimental and theoretical values.

In addition, it has been suggested in this study that the initial surface roughness of the samples has an effect on the roll-gap HTC. It was not possible to quantify this effect, however, because the surface profiles of the samples were not recorded. A series of tests involving samples of differing roughnesses would help clarify the relationship between the value C in Equation (8.1) and the roughness parameters.

8.3 Concluding Remarks

Sellars writes,

> "Use of a computer model with 'typical' values of [roll-gap HTC] ... provides a more reliable way of determining temperatures than attempting to measure them directly." [30]

This statement is paradoxical, because the determination of these 'typical' values of the HTC requires reliable strip temperature measuring techniques! Furthermore, these 'typical' values of the roll-gap HTC could only be obtained by experiments that had to be performed for each different rolling operation. It is hoped that the information presented in this study will provide a more rational basis for determining roll-gap HTCs for rolling operations than has previously been available.

BIBLIOGRAPHY

[1.] P. J. S. Brooks, "Advances in Hot Rolling Technology", Aluminum Technology '86, T. Sheppard, Ed., The Institute of Metals, 1986

[2.] I. V. Samarasekera, "The Importance of Characterizing Heat Transfer in Hot Rolling of Steel Strip", Proceedings of the International Symposium on Mathematical Modelling of Hot Rolling of Steel, Aug. 1990, 148-167

[3.] B. K. Chen, P. F. Thomson and S. K. Choi, "Temperature Distribution in the Roll-Gap during Hot Flat Rolling", Journal of Materials Processing Technology, Vol. 30, 1992, 115-130

[4.] S. L. Semiatin, E. W. Collings, V. E. Wood and T. Altan, "Determination of the Interface Heat Transfer Coefficient for Non-Isothermal Bulk-Forming Processes", Journal of Engineering for Industry, Feb. 1987, Vol. 109, 49-57

[5.] S. P. Timothy, H. L. Yiu, J. M. Fine and R. A. Ricks, "Simulation of Single Pass of Hot Rolling Deformation of Aluminium Alloy by Plane Strain Compression", Materials Science and Technology, Mar. 1991, Vol. 7, 195-201

[6.] M. Pietrzyk and J. G. Lenard, "A Study of Boundary Conditions in Hot/Cold Flat Rolling", Second International Conference on Computational Plasticity, D. R. J. Owen, E. Hinton and E. Oñate, Eds., Barcelona, Spain, 1989, 947-958

[7.] K. T. Lang, "Lubrication and Thermal Effects in Metal Processing",

[8.] I. Yarita, "Problems of Friction, Lubrication, and Materials for Rolls in the Rolling Technology", Transactions ISIJ, Vol. 24, 1984, 1014-1035

[9.] C. L. Wandrei, "Review of Hot Rolling Lubricant Technology for Steel", ASLE Special Publication SP-17, 1984

[10.] W. R. D. Wilson and S. Sheu, "Real Area of Contact and Boundary Friction in Metal Forming", International Journal of Mechanical Science, Vol. 30, No. 7, 1988, 475-489

[11.] M. P. F. Sutcliffe, "Surface Asperity Deformation in Metal Forming Processes", International Journal of Mechanical Science, Vol. 30, No. 11, 1988, 847-868

[12.] N. Bay, "Friction Stress and Normal Stress in Bulk Metal-Forming Operations", Journal of Mechanical Working Technology, Vol. 14, 1987, 203-223

[13.] M. G. Cooper, B. B. Mikic and M. M. Yovanovich, "Thermal Contact Resistance", International Journal of Heat and Mass Transfer, Vol. 12, 1969, 279-300

[14.] J. V. Beck, "Determination of Optimum, Transient Experiments for Thermal Contact Resistance", International Journal of Heat and Mass Transfer, Vol. 12, 1969, 621-633

[15.] B. B. Mikic, "Thermal Constriction Resistance due to Non-Uniform Surface Conditions; Contact Resistance at Non-Uniform Interface Pressure", International Journal of Heat and Mass Transfer, Vol. 13, 1970, 1497-1500

[16.] H. Fenech, J. J. Henry and W. M. Rohsenow, "Thermal Contact Resistance", in 'Developments in Heat Transfer', W. M. Rohsenow, Ed., The M.I.T. Press, Cambridge, Massachusetts, 1964

[17.] B. B. Mikic, "Thermal Contact Conductance; Theoretical Considerations", International Journal of Heat and Mass Transfer, Vol. 17, 1974, 205-214

[18.] C. Devadas, I. V. Samarasekera and E. B. Hawbolt, "The Thermal and Metallurgical State of Steel Strip during Hot Rolling: Part I. Characterization of Heat Transfer", Metallurgical Transactions A, Vol. 22A, Feb. 1991, 307-319

[19.] W. C. Chen, I. V. Samarasekera and E. B. Hawbolt, "Characterization of the Thermal Field during Rolling of Microalloyed Steels", 33rd MWSP Conference Proceedings, Vol. XXIX, ISS-AIME, 1992, 349-357

[20.] S. Song and M. M. Yovanovich, "Relative Contact Pressure: Dependence on Surface Roughness and Vickers Microhardness", Journal of Thermophysics, Vol. 2, No. 1, Jan. 1988, 43-47

[21.] W. C. Chen, "Thermomechanical Phenomena during Rough Rolling of Steel Slab", M.A.Sc. Thesis, The University of British Columbia, 1991

[22.] B. F. Bradley, W. A. Cockett and D. A. Peel, "Transient Temperature Behaviour of Aluminium during Rolling and Extrusion", Iron and Steel Institute International Conference on Mathematical Models in Metallurgical Process Development, London, Feb. 1969, 79-92

[23.] R. E. Smelser and E. G. Thompson, "Validation of Flow Formulation for Process Modelling", Advances in Inelastic Analysis, Winter Annual Meeting of the ASME, Boston, Massachusetts, 1987, 273-282

[24.] W. R. D. Wilson, C. T. Chang and C. Y. Sa, "Interface Temperatures in Cold Rolling", Journal of Materials Shaping Technology, Vol. 6, 1989, 229-240

[25.] G. D. Lahoti, S. N. Shah and T. Altan, "Computer-Aided Analysis of the Deformations and Temperatures in Strip Rolling", Journal of Engineering for Industry, Vol . 100, May 1978, 159-166

[26.] J. G. Lenard and M. Pietrzyk, "The Predictive Capabilities of a Thermal Model of Flat Rolling", Steel Research, Vol. 60, No. 9, 1989, 403-406

[27.] A. A. Tseng, "A Numerical Heat Transfer Analysis of Strip Rolling", Transactions of the ASME: Journal of Heat Transfer, Vol. 106, Aug. 1984, 512-517

[28.] J. Pavlossoglou, "Mathematical Model of the Thermal Field in Continuous Hot Rolling of Strip and Simulation of the Process", Arch. Eisenhuttenwes., Vol. 52, No. 4, 1981, 153-158

[29.] A. Laasroui and J. J. Jonas, "Prediction of Temperature Distribution, Flow Stress and Microstructure during the Multipass Hot Rolling of Steel Plate and Strip", ISIJ International, Vol. 31, No. 1, 1991, 95-105

[30.] C. M. Sellars, "Computer Modelling of Hot-Working Processes", Materials Science and Technology, Vol. 1, Apr. 1985, 325-332

[31.] A. A. Tseng, S. X. Tong, S. H. Maslen and J. J. Mills, "Thermal Behavior of Aluminum Rolling", Transactions of the ASME: Journal of Heat Transfer, Vol. 112, May 1990, 301-308

[32.] C. Devadas and I. V. Samarasekera, "Heat Transfer during Hot Rolling of Steel Strip", Ironmaking and Steelmaking, Vol. 13, No. 6, 1986, 311-322

[33.] T. Sheppard and D. S. Wright, "Structural and Temperature Variations during Rolling of Aluminium Slabs", Metals Technology, July 1980, 274-281

[34.] P. R. Dawson, "A Model for the Hot or Warm Forming of Metals with Special Use of Deformation Mechanism Maps", International Journal of Mechanical Sciences, Vol. 26, No. 4, 1984, 227-244

[35.] J. W. Kannel and T. A. Dow, "The Evolution of Surface Pressure and Temperature Measurement Techniques for Use in the Study of Lubrication in Metal Rolling", Transactions of the ASME: Journal of Lubrication Technology, Oct. 1974, 611-616

[36.] A. N. Karagiozis and J. G. Lenard, "Temperature Distribution in a Slab During Hot Rolling", Transactions of the ASME: Journal of Engineering Materials and Technology, Vol. 110, Jan. 1988, 17-21

[37.] S. I. Steindl and W. B. Rice, "Measurement of Temperature in the Roll Gap during Cold Rolling", Annals of the CIRP, Vol. 22, No. 1, 1973, 89-90

[38.] M. Pietrzyk, J. G. Lenard and A. C. M. Sousas, "A Study of Temperature Distribution in Strips during Cold Rolling", Heat and Technology, Vol. 7, No. 2, 1989, 12-25

[39.] J. Jeswiet and W. B. Rice, "Measurement of Strip Temperature in the Roll Gap during Cold Rolling", Annals of the CIRP, Vol. 24, No. 1, 1975, 153-156

[40.] Manual on the Use of Thermocouples in Temperature Measurement, ASTM Committee E-20 on Temperature Measurement and Subcommittee E20.04 on Thermocouples, ASTM, 1981

[41.] N. P. Bailey, "The Measurement of Surface Temperatures, Accuracies Obtainable with Thermocouples", Mechanical Engineering, Vol. 54, Aug. 1932, 553-556

[42.] B. K. Chen, P. F. Thomson and S. K. Choi, "Computer Modelling of Microstructure during Hot Flat Rolling of Aluminum", Materials Science and Technology, Vol. 8, No. 1, Jan. 1992, 72-77

[43.] A. T. Male, "The Relative Validity of the Concepts of Coefficient of Friction and Interface Friction Shear Factor for Use in Metal Deformation Studies", ASLE Transactions, Vol. 16, No. 3, 177-184

[44.] N. Hatta, J. Kokado, H. Nishimura and K. Nishimura, "Analysis of Slab Temperature Change and Rolling Mill Line Length in Quasi Continuous Hot Strip M:ill Equipped with Two Roughing Mills and Six Finishing Mills", Journal of the Japan Society for Technology of Plasticity, Vol. 21, 1980, 230-236

[45.] C. H. J. Davies, I. S. Geltser, E. B. Hawbolt, J. K. Brimacombe and I. V. Samarasekera, "Modelling the Hot Deformation of 6061/Alumina Composites", Symposium on Light Metals Processing and Applications, CIM Conference of Metallurgists, 1993, Quebec City

[46.] J. G. Beese, "Ratio of Lateral Strain to Thickness Strain during Hot Rolling of Steel Slabs", Journal of the Iron and Steel Institute, June 1972, 433-436

[47.] Z. Wusatowski, 'Fundamentals of Rolling', 1969, Oxford, Pergamon Press

[48.] A. A. Tseng, "Roll cooling and Its Relationship to the Roll Life", Metallurgical Transactions A, Vol. 20A, Nov., 1938-2305

[49.] A. V. Logunov and A. F. Zverov, "Investigating the Thermal Conductivity and Electrical Resistance of Aluminum and a Group of Aluminum Alloys", Journal of Engineering Physics, Vol. 15, No. 1, 1256-1260

[50.] R. D. Pehlke, A. Jeyarajan and H. Wada, "Summary of Thermal Properties for Casting Alloys and Mold Materials", University of Michigan, Dec. 1982, NSR/NEA-82028

[51.] Metals Handbook, Desk Edition, H. E. Boyer and T. L. Gall, Eds., ASM, 1985

[52.] F. M. White, 'Heat and Mass Transfer', 1988, Addison-Wesley

[53.] E. Orowan, "A Simple Method of Calculating Roll Pressure and Power Consumption in Hot Flat Rolling", Special Reports: Iron and Steel Institute, First Report of the Rolling Mill Research Committee, Sec. V, 1946, 124-126

[54.] F. A. R. Al-Salehi, T. C. Firbank and P. R. Lancaster, "An Experimental Determination of the Roll Pressure Distributions in Cold Rolling", International Journal of Mechanical Science, Vol. 15, 1973, 693-710

[55.] L. Lai-Seng and J. G. Lenard, "Study of Friction in Cold Strip Rolling", Journal of Engineering Materials and Technology, Vol. 106, April 1984, 139-146

[56.] J. Pullen and J. B. P. Williamson, "On the Plastic Contact of Rough Surfaces", Proceedings of the Royal Society of London, Vol. 327A, 1972, 159-173

[57.] J. B. P. Williamson and R. T. Hunt, "Asperity Persistence and the Real Area of Contact Between Rough Surfaces", Proceedings of the Royal Society of London, Vol. 327A, 1972, 147-157

[58.] R. V. Hogg and J. Ledolter, 'Engineering Statistics', MacMillan Publishing Co., 1987

[59.] J. A. Schey, 'Metal Deformation Processes: Friction and Lubrication', Marcel Dekker Inc., 1970

[60.] E. Osinski, "Hot Rolling - Coefficient of Heat Transfer between Rolls and Strip", Internal Report, Nov. 1993

[61.] 'Handbook of Thermophysical Properties of Solid Materials', MacMillan Co., 1961

APPENDIX A

Determination of Minimum HTC

It is possible to calculate, without need of an iterative solution, a minimum solution for the HTC. This is accomplished by using the assumption that, while in the roll bite, the surface temperature of the roll and strip do not change from their initial temperatures. The roll-gap HTC then simply becomes

$$h = \frac{\dot{Q}/A_c}{T_s - T_r} \tag{A.1}$$

where $\dot{Q}/A_c$ is the average heat flux in W/m², and T_S and T_r is the surface temperature of the strip and roll, respectively, throughout the roll gap. These temperatures are set to the initial bulk temperature of the strip and roll. The heat flux is equivalent to the net energy lost by the sample, ΔE, while in the roll bite, divided by the contact time, t_c:

$$\dot{Q} = \frac{\Delta E_s}{t_c} \tag{A.2}$$

The energy loss is related to the temperature drop, ΔT_S, of the sample through the volume V_S, the density ρ_S, and the heat capacity C_{pS}, of the sample:

$$\Delta E_s = \rho_s C_{ps} V_s \Delta T_s \tag{A.3}$$

The volume V_S is taken to be a half-volume of the sample in the roll bite. Furthermore, it is approximated to be the product of the sample width, the contact length, and the average of the entry and exit thickness:

$$V_s = \frac{1}{4} W \sqrt{R_0 \Delta H} (H_i + H_f) \tag{A.4}$$

where W is the width of the sample, R_0 the radius of the roll and ΔH the draft. The square root term is the projected length of the contact arc. In addition, H_i is the entry thickness of the sample, and H_f is the exit or final thickness of the sample.

The area of the sample in contact with the roll is characterized as

$$A_c = W \sqrt{R_0 \Delta H} \tag{A.5}$$

Substituting Equation (A.4) into Equation (A.3), (A.3) into (A.2), and (A.2) and (A.5) into Equation (A.1), the following equation is obtained:

$$h = \frac{\rho_s C_{ps} (H_i + H_f) \Delta T}{4 t_c (T_s - T_r)} \tag{A.6}$$

The term ΔT has to include not only the initial and final temperature of the strip, T_i and T_f, but the heat of deformation ΔT_{def} as well:

$$\Delta T = T_i - T_f + \Delta T_{def} \tag{A.7}$$

Finally, the contact time, t_c, can be calculated as:

$$t_c = \frac{\cos^{-1}\left[\dfrac{R_0 - \frac{1}{2}(H_i - H_f)}{R_0}\right]}{\frac{2\pi}{60}N} \tag{A.8}$$

where N is the angular velocity of the roll in rpm.

Substituting Equation (A.7) and (A.8) into (A.6), the equation for a lower-bound roll-gap HTC is obtained:

$$h = \frac{\pi \rho_s C_{ps} N (H_i + H_f)(T_i - T_f + \Delta T_{def})}{120 \cos^{-1}\left[\dfrac{R_0 - \frac{1}{2}(H_i - H_f)}{R_0}\right](T_s - T_r)} \tag{A.9}$$

Applying this equation to Test AL24, for example, yields:

$$h = \frac{\pi(2636\text{kg/m}^3)(900\text{J/kg°C})(68.5\text{rpm})(0.0087\text{m} + 0.00695\text{m})(377°\text{C} - 338°\text{C} + 10°\text{C})}{120\cos^{-1}\left[\dfrac{0.05\text{m} - \frac{1}{2}(0.0087\text{m} - 0.00695\text{m})}{0.05\text{m}}\right](377°\text{C} - 24°\text{C})} = 49300\text{W/m}^2\text{°C}$$

The estimate of the HTC from Equation (A.9) for Test AL24 is 49.3 kW/m² °C, as compared to 378.5 kW/m² °C, as calculated in Section 6.2.1. The HTC as calculated by Equation (A.9) is thus eight times lower than that calculated by the finite-difference program. The discrepancy is due to the assumption that the roll and sample remain at their initial temperature, whereas in fact the temperature differential decreases with increasing time in the roll gap.

When Equation (A.9) is applied to the data supplied by Timothy *et al.* [5], the following HTC is obtained:

$$h = \frac{\pi(2660\text{kg/m}^3)(1120\text{J/kg°C})(10\text{rpm})(0.03\text{m}+0.0159\text{m})(460°\text{C}-430°\text{C}+18°\text{C})}{120\cos^{-1}\left[\dfrac{0.184\text{m}-\frac{1}{2}(0.03\text{m}-0.0159\text{m})}{0.0184\text{m}}\right](460°\text{C}-24°\text{C})} = 14200\text{W/m}^2\text{°C}$$

And similarly, the calculation for the test performed by Pietrzyk and Lenard [6] yields

$$h = \frac{\pi(2700\text{kg/m}^3)(900\text{J/kg°C})(7.3\text{rpm})(0.013\text{m}+0.0106\text{m})(210°\text{C}-175°\text{C}+8°\text{C})}{120\cos^{-1}\left[\dfrac{0.127\text{m}-\frac{1}{2}(0.013\text{m}-0.0106\text{m})}{0.127\text{m}}\right](210°\text{C}-24°\text{C})} = 18400\text{W/m}^2\text{°C}$$